

RIJKSUNIVERSITEIT GRONINGEN

Interactions between *Emiliana huxleyi* and
the dissolved inorganic carbon system

Proefschrift

ter verkrijging van het doctoraat
in de Wiskunde en Natuurwetenschappen
aan de Rijksuniversiteit Groningen
op gezag van de
Rector Magnificus, dr. D. F. J. Bosscher,
in het openbaar te verdedigen
op maandag 25 september 2000
om 14.15 uur

door

Erik Theodoor Buitenhuis,
geboren op 10 september 1967 te Rotterdam.

2

Promotor: Prof. dr. ir. H. J. W. de Baar

Beoordelingscommissie: Prof. dr. J. T. M. Elzenga
Prof. dr. P. Westbroek
Prof. dr. D. A. Wolf-Gladrow

In memory of my best friend and mother,
Wil Buitenhuis van Veen
(1937-2000)

Colophon

The research for this thesis was carried out at the Netherlands Institute for Sea Research (NIOZ) in the departments Biological Oceanography and Marine Chemistry & Geology, P.O. box 59, 1790 AB Texel, The Netherlands. The research was funded by the Dutch Science Foundation (NWO) as project Global Change 9.1b 'The partial pressure of CO₂ in seawater as a control on marine biological productivity and calcification'.

Cover design: Jan & Erik Buitenhuis.

Feedback to Erik Buitenhuis: martinburo@email.com

Contents

Statements	6
A thesis is not written by just one person.....	7
A story	8
Chapter 1: Synthesis	9
Chapter 2: Photosynthesis and calcification by <i>Emiliana huxleyi</i> (prymnesiophyceae) as a function of inorganic carbon species Erik T. Buitenhuis, Hein J. W. de Baar, Marcel J.W. Veldhuis (1999) <i>Journal of phycology</i> 35 949-959.....	29
Chapter 3: Zn ²⁺ -HCO ₃ ⁻ colimitation of <i>Emiliana huxleyi</i> (prymnesiophyceae) Erik T. Buitenhuis, Klaas R. Timmermans, Hein J. W. de Baar Submitted to journal of phycology	42
Chapter 4: Trends in inorganic and organic carbon in a bloom of <i>Emiliana huxleyi</i> in the North Sea Erik Buitenhuis, Judith van Bleijswijk, Dorothee Bakker, Marcel Veldhuis (1996) <i>Marine ecology progress series</i> 143 271-282.....	50
Chapter 5: Blooms of <i>Emiliana huxleyi</i> are sinks of atmospheric carbon dioxide; a field and mesocosm study derived simulation Erik T. Buitenhuis, Paul van der Wal, Hein J. W. de Baar Submitted to Global biogeochemical cycles	64
References	79
Biography Cesare Emiliani	86
Biography Thomas Henry Huxley	88
Samenvatting.....	91

Statements

1. If you think that the whole is greater than the sum of the parts then you have overlooked some parts (page 7).
2. By a rough estimate, *Emiliana huxleyi* precipitates 1.4 ‰ of the oceanic CaCO₃ production, and is therefore probably not the most productive CaCO₃ precipitating organism on earth (pro: chapter 1, contra: Westbroek et al. 1985).
3. There is no missing sink (chapter 1).
4. Doubling of the atmospheric CO₂ (at constant alkalinity) decreases the atmospheric CO₂ sink of a bloom of *E. huxleyi* by 1% (chapter 1).
5. *E. huxleyi* blooms reduce the atmospheric CO₂ concentration more than blooms of algae that are solely made of organic material (pro: chapter 5; contra: Robertson 1994).
6. It is possible to reduce our standard of living without reducing our quality of life, and it is necessary to do so in order not to compromise the quality of life of future generations.
7. If we tend to associate what we enjoy with what is bad for us then there is something wrong with our educational system.

A thesis is not written by just one person

When I was about 12 years old, we brought a cassette player during the summer holidays, and as far as I can remember only one cassette: 'The concert in Central Park' by Simon & Garfunkel, which contains the following acknowledgement: 'I would like to thank the police department, and the fire department, and the park's commissioner, and Ed Koch. And particularly, you know, people who never get recognised for doing ... for doing good deeds for the city are donating half of the proceeds that they are making tonight. The guys who sell and lose joints are giving the city half of their income tonight.' Subsequently, I have been very uncomfortable with acknowledgements. There is also a practical reason for me not to prepare a list of everybody who has helped me to do my PhD: if I tried to make the list exhaustive it would be so long that nobody would read it, and still I could not hope to make it complete; conversely, I can think of no criteria to select the people who have been most important.

Well, that is the theory and it sounds all right to me, but it doesn't work ... I enjoyed sharing rooms with Marcel Veldhuis, Judith van Bleijswijk, Paul van der Wal, Rob Kempers, Willem Stolte, Anna Noordeloos and Corina Brussaard. Hein de Baar is my promoting professor. That should explain his central importance to the work that lies before you, and if it doesn't, nothing I can say will make it any clearer. Nelleke Schogt and Klaas Timmermans freely provided me with laboratory space, which was much appreciated. Rob Kempers, Erika Koning, Martin Laan, Herman Boekel, Edwin Keijzer, Edwin de Jong, Ruud Groenewegen, Jeroen de Jong, Patrick Laan and Josje Snoek gave excellent technical assistance. And then there's at least another page worth of people who helped with intellectual, moral and/or technical support.

A story

Emiliana huxleyi is a unicellular marine alga that likes carbon so much that it fixes it in two forms, organic and inorganic. At first sight the inorganic part looks rather beautiful both when seen under an electron microscope (Figure 1.4) and when seen from space (Figures 2.1b and 1.6). But when looked at from a chemical perspective, it turns out that it is just one component (CaCO_3), precipitated in a single crystal form (calcite). The converse is true for the organic part. At first sight it is just the preparation of more alga by that same alga. This is called growth. But this organic part is prepared by a complicated recipe, the basic manipulations of which are shared by all life on earth. The general outline of these manipulations are known and involve such almost mundane processes like DNA replication, RNA transcription, protein translation, electron transfer and ion transport. The total result of all this is rather startling. Although it does not follow that the whole is greater than the sum of the parts, the observation of what all this moving around and recombination of physical particles can accomplish in terms of living organisms makes one rather more cautious in any subsequent inference of logical conclusions from observable facts (statement 1).

Chapter 1 : Synthesis

Outline

This thesis deals with the interactions between *Emiliana huxleyi* and dissolved inorganic carbon in seawater. This interaction is separately dealt with for the two directions: The influence of the dissolved inorganic carbon system on *E. huxleyi* (chapters 1.4, 2 & 3), and the influence of *E. huxleyi* on the dissolved inorganic carbon system (chapters 1.5, 4 & 5). In the first section it is shown that the growth rate of *E. huxleyi* is close to the maximum growth rate under typical oceanic conditions of dissolved inorganic carbon (Figure 2.7). Therefore, no feedback between the two directions of interaction is to be expected, and thus there is no third section to deal with this feedback, just as in the model there is no influence of dissolved inorganic carbon on growth rate (chapter 5). Chapter 2 deals with the influence of the different species of the dissolved inorganic carbon (DIC) system on the rates of carbon fixation in particulate organic carbon (POC) and calcite (CaCO_3) by *E. huxleyi*. Chapter 3 deals with the influence of zinc limitation on the use of DIC. Chapter 4 presents the influence of *E. huxleyi* on the DIC system in a phytoplankton bloom in the North Sea in 1993. Chapter 5 presents the influence of *E. huxleyi* on the DIC system using a numerical model of a bloom of *E. huxleyi*. At the end of these two sections some recommendations are given for extending the research in the direction that has been followed in this thesis (at the end of the discussion in chapter 3 and the summary in chapter 5). In order to place these detailed studies in the wider context of the global carbon cycle this chapter starts with three sections on the global carbon cycle (chapter 1.1), the marine carbon cycle (chapter 1.2) and intracellular processes (chapter 1.3). The first section proceeds from the largest pool of carbon on the earth (solid carbonates in the sediments) to the smallest (biomass in the sea), and the second section illustrates how part of this minute pool of biomass in the ocean, the calcifying planktonic algae, are responsible for producing $\frac{3}{4}$ of the pool of carbonates (calcite) by slow accumulation over geological timescales. Since it is impossible to give a full description of the research that has been conducted on all of the topics that are briefly addressed here, each subsection ends with some references for further reading.

1.1 The global carbon cycle

‘The virtues of carbon dioxide are in inverse ratio to the sinister reputation which “a little knowledge” and a narrow homocentric point of view have given it’ (Chamberlin 1898).

After hydrogen and oxygen, carbon is the most abundant atom in living organisms. Figure 1.1 gives an estimate of the reservoirs of carbon on the earth. Over the second half of the 20th century, a major scientific effort has focused on the global carbon cycle, especially on the more active reservoirs, which are also the smaller reservoirs. While this effort is by no means completed, with the increase in knowledge additional areas for future study have been identified, which may gain in importance in future research. Three areas come to mind:

- 1) The importance of the biosphere not only in performing chemical reactions which are predicted by chemical equilibria (such as the precipitation of CaCO_3), but also of redirecting biogeochemical cycles (such as the production of all the oxygen in the atmosphere from an initially reducing atmosphere) and to make use of this catastrophe (Westbroek 1991),
- 2) The feedbacks that result from the coupling of the biogeochemical cycles of the various chemical elements that have thus far mostly been studied separately (as noted in several chapters of Butcher et al. 1992),
- 3) Now that the larger fluxes among the smaller reservoirs become more and more accurately known, it is to be expected that the small fluxes that only become important by accumulating over geological time scales, and that can depart further from steady state assumptions on short time scales, will probably receive more attention.

(Further reading, Bolin et al. 1979).

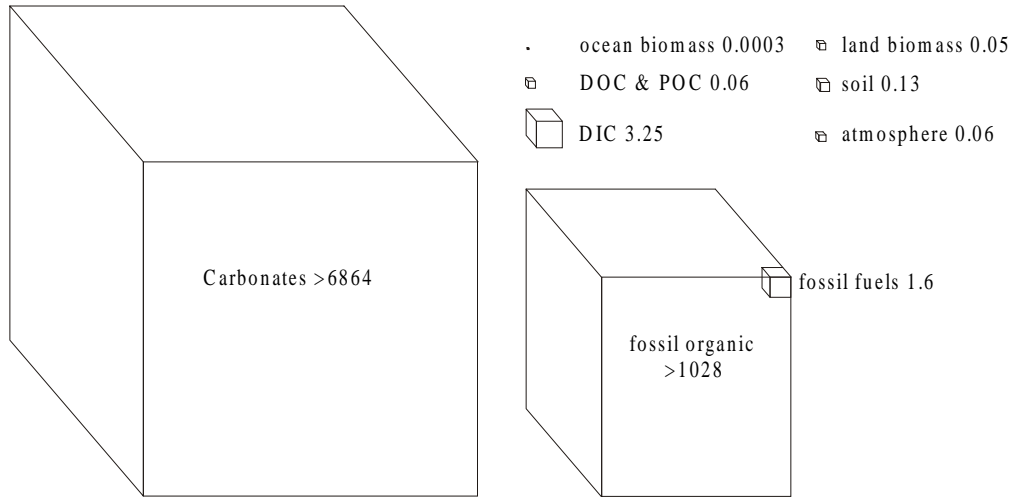
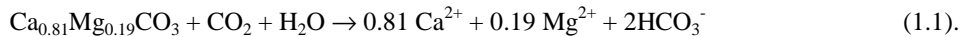


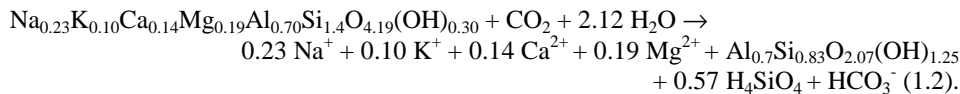
Figure 1.1 Reservoirs of carbon on the earth in 1018 mol C (adapted from Figure 1 in McConnaughey 1994, data from Hay 1985 (carbonates & fossil organic), IPCC 1990 (DIC, soil, atmosphere, DOC & biomasses), Table 1.1 (fossil fuels)), for flux magnitudes see Figure 0.2 on page 92.

The global carbonate cycle

The major processes in the global carbonate cycle are weathering (= corrosion), precipitation, sedimentation and dissolution. The two major processes of weathering on land that consume atmospheric CO_2 are weathering of carbonates and of silicates. The gross reaction of weathering of carbonates proceeds according to the reaction:



The fractional contributions for calcium and magnesium indicate that the two main carbonates calcite (CaCO_3) and dolomite ($\text{CaMg}(\text{CO}_3)_2$) are weathered in a ratio of about 3:1. The gross reaction of weathering of silicates proceeds according to the reaction:



This involves the weathering of a mixture of feldspars. These two types of weathering proceed at approximately equal rates (Morse & Mackenzie 1990), and the weathering of organic carbon (the reverse of reaction 1.5) also proceeds at a comparable rate (Butcher et al. 1992). This means that of the dissolved inorganic carbon in rivers about $\frac{1}{3}$ comes from the atmosphere, $\frac{1}{3}$ comes from the weathering of organic carbon, and the remaining $\frac{1}{3}$ comes from carbonates.

The products of these weathering reactions are transported to the ocean by rivers, and constitute the input for the ocean carbonate budget in Figure 1.2. In the ocean carbonates are precipitated by marine organisms: several sorts of animals: corals, foraminifera and pteropods, and a group of plants: the coccolithophorid algae, of which *Emiliania huxleyi* is a member. These algae are eaten by zooplankton (small animals) and their fecal pellets (faeces) sink to the ocean floor, this is called sedimentation. Some of the carbonates dissolve in the upper ocean.

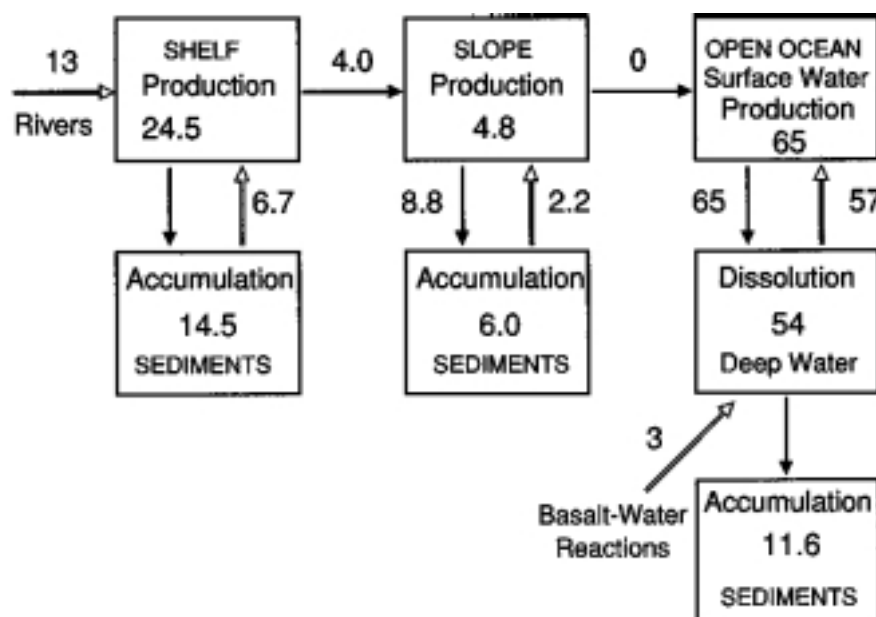


Figure 1.2 The global carbonate cycle. All fluxes in $10^{12} \text{ mol} \cdot \text{year}^{-1}$ (Figure 12 in Wollast 1994).

Because the upper ocean is supersaturated with calcite, it is generally assumed that this dissolution is caused by acid production by marine organisms in microenvironments within the diffusive boundary layer around particles (see chapter 4), although sufficient proof for this assumption is lacking. In the deep ocean the water is undersaturated with respect to calcite and here the carbonate is dissolved by chemical dissolution. Although the shelf seas represent only a small part of the ocean by surface area (7%, Menard & Smith 1966), the amount of carbonates that are stored in the sediments there is highest (45% of total in Figure 1.2), because production per surface area is higher than in the open ocean (26% of total in Figure 1.2), and the continental shelf lies well above the depth where carbonates dissolve.

According to the budget in Figure 1.2, the total export of carbonates by sedimentation ($33.1 \cdot 10^{12} \text{ mol} \cdot \text{y}^{-1} = 66.2 \cdot 10^{12} \text{ equivalent} \cdot \text{y}^{-1}$)* is higher than the import by the rivers ($13 \cdot 10^{12} \text{ mol} \cdot \text{y}^{-1} = 26 \cdot 10^{12} \text{ equivalent} \cdot \text{y}^{-1}$). Although it is generally thought that export is higher than import during interglacials, the difference must be much smaller, because at this rate the ocean would be devoid of alkalinity (alkalinity is explained in 'Inorganic carbon speciation in sea water') in 10^5 years. The river fluxes reported by Morse & Mackenzie (1990, their table 9.7) suggest that the import by rivers in Figure 1.2 represents only the particulate flux of $13.9 \cdot 10^{12} \text{ mol CO}_3^{2-} \cdot \text{y}^{-1}$, and not the dissolved flux of $32.4 \text{ mol HCO}_3^- \cdot \text{y}^{-1}$. Together these would bring the import of alkalinity to $60.2 \cdot 10^{12} \text{ equivalent} \cdot \text{y}^{-1} (= 2 * 13.9 + 32.4, \text{ with the factor 2 due to the 2 negative charges of } \text{CO}_3^{2-})$, which is a much closer correspondence between export from and import into the ocean. The higher export during interglacials is compensated by higher import

* Recently, alkalinity has been expressed in mol rather than equivalent (e.g. Milliman et al. 1999). I think this only adds to the risk of confusion, which already exists, because the carbonate / alkalinity budget is sometimes expressed as concentration (mol) and sometimes as alkalinity (equivalent). For instance, when particulate river transport is expressed as carbonate (CO_3^{2-}) and dissolved river transport is expressed as bicarbonate (HCO_3^-), with $1 \text{ mol CO}_3^{2-} = 2 \text{ equivalent CO}_3^{2-}$, and $1 \text{ mol HCO}_3^- = 1 \text{ equivalent HCO}_3^-$.

during glacial periods, when the sea level is some 100 meters lower, so that more land is exposed and the weathering rate is higher. Over long periods of time the imports must equal the exports, for otherwise the carbonate concentration in the ocean would keep changing, while the available evidence shows that this is not the case (Sigman et al. 1998). There is a feedback mechanism that maintains this balance: if sedimentation exceeds weathering the carbonate concentration decreases and the depth at which carbonates are saturated becomes shallower. Carbonates between the old saturation depth and the new saturation depth then dissolve, which acts as an additional import until a new steady state is generated.

In the ocean most of the carbonate is precipitated by marine organisms (Morse & Mackenzie 1990), and during the last decades the perceived importance of chemical (abiotic) precipitation has been decreasing (Westbroek 1991). Marine organisms precipitate either calcite (e.g. coccolithophorids and foraminifera) or aragonite (e.g. pteropods and corals) (Morse & Mackenzie 1990). Since aragonite is less stable than calcite, aragonite is more easily dissolved in the water column or in the top of the sediment. If it survives, then most of it is converted to calcite within the sediment. Calcite generally contains between 0 and 15 % Mg^{2+} (mol/mol). Since a mixture of low magnesium calcite (< 1%) and dolomite ($\text{CaMg}(\text{CO}_3)_2$) is more stable than high magnesium calcite, dolomite is formed within the sediment, but it has also been precipitated directly from seawater (Morse & Mackenzie 1990). The average Ca /Mg ratio of continental carbonate rocks is about 5:1 (Ronov 1980 as quoted in Morse & Mackenzie 1990), which corresponds to a calcite /dolomite ratio of about 4:1.

The contribution of coccolithophorids to the CaCO_3 flux at 1000 m. depth has been estimated to be $12 \pm 6\%$ (Broerse 2000, Table 7.1). The fractional contribution of coccolithophorids to oceanic CaCO_3 production may be even lower, since benthic foraminifera produce high magnesium calcite and pteropods and corals produce aragonite, both of which are more soluble than the low magnesium calcite that is produced by coccolithophorids (Morse & Mackenzie 1990). Dissolution of CaCO_3 above the lysocline (which lies at ~4 km. depth for calcite) has only recently been recognized as an important process (chapter 4, and references in Milliman et al. 1999). This also implies that dissolution of the more soluble high magnesium calcite and aragonite (the lysocline for the latter lies at ~1 km. depth) may be important, even if most of the production of these forms of CaCO_3 is by shallow-living benthic organisms. The total bloom productivity of coccolithophorids can be estimated to be $1.3 \cdot 10^{11} \text{ mol} \cdot \text{y}^{-1}$, by multiplying the average calcification rate in the 1993 *E. huxleyi* bloom in the North Sea of $3 \text{ mmol} \cdot \text{m}^{-2} \cdot \text{d}^{-1}$ (Wal et al. 1995) with the surface area of coccolithophorids which is visible on satellite images of $1.4 \cdot 10^6 \text{ km}^2 \cdot \text{y}^{-1}$ (Brown & Yoder 1994) and an average bloom duration of 30 days. This coccolithophorid bloom productivity estimate is 1.4 ‰ of the total CaCO_3 production in Figure 1.2. This contrasts rather markedly with the statement of Westbroek et al. (1985) that '*E. huxleyi* is the most productive lime-secreting species on earth' (statement 2) (further reading: Milliman et al. 1999).

The organic carbon cycle

The amount of fossil organic carbon that is formed is of the same order of magnitude as the amount of calcite. However, there is a much greater variation in estimated rates of preservation, possibly due to the following reasons:

- 1) At present fossil fuels are burned between 100 and 1000 times faster than the preservation of fossil organic carbon, so that it is impossible to measure the non-human degradation rate (this is usually called the pre-industrial degradation rate),
- 2) There is a much bigger difference between production and fossilisation of organic carbon (100 to 1000-fold) than between production and fossilisation of carbonates (3 to 7-fold), so that it is more difficult to estimate how much is preserved on the basis of how much arrives on the ocean floor,

Table 1.1 Fossil fuel reserves (data for 1993)

	Identified [10 ²¹ J]*	undiscovered [10 ²¹ J]*	10 ⁻⁶ mol·J ⁻¹ +	10 ¹⁸ mol C
Conventional oil	6.3	2.69	1.66	0.015
Conventional gas	5.48	6.27	1.27	0.015
Coal	21.915	239.59	2.11	0.553
non-conventional oil	10.795		1.66	0.018
non-conventional gas		815.5	1.27	1.038
Total [10 ¹⁸ mol C]	0.082	1.557		1.638

* 'Voorraden en prijzen van fossiele brandstoffen' ECN, Petten, The Netherlands

+ pers. comm. P. Lako (ECN)

- 3) There is a wide variety of organic molecules, that all have different biodegradabilities. Only the least biodegradable organic molecules get preserved in the sediment. By contrast, only two carbonates are produced to any significant extent: calcite and aragonite, of which aragonite is either dissolved or transformed into calcite, while some calcite is transformed into dolomite (see 'The global carbonate cycle').

The present estimate of the fossil fuel reserves is subject of considerable debate, because only 5% of the estimated reserves have been identified (Table 1.1). At the current rate of production of fossil fuels the identified reserves alone will last us 150 years. However, the production rate is increasing, while the production capacity is decreasing. Therefore, it is predicted that the demand will exceed the production capacity at around 2015 (<http://www.dieoff.org>)(further reading: Kump & Arthur 1999).

The dissolved inorganic carbon cycle

In Table 1.2 it can be seen that the ocean is a sink for anthropogenic CO₂. There are two mechanisms that are responsible for this sink. There is a physical carbon pump and a biological one. The physical carbon pump is composed of two components. The faster component transports water along isopycnals (water of equal density) in the upper ocean (to maximum depths of 1 km at 30°N) between approximately 40°N and 40°S. This has an exchange time of about 130 years. The slow component encompasses the slow turnover of all ocean waters, and has been nick-named the conveyor belt (Broecker & Peng 1982, Figure 1.3). The conveyor belt runs as follows: surface water sinks in the Antarctic (~40°S) and in the North Atlantic (~40°N). The deep water in the North Atlantic flows south to Antarctica and mixes with the Antarctic deep water, which flows north into the South Atlantic and east in the Southern Ocean. This mix flows north into the Indian and Pacific Oceans. The water rises again (this is called upwelling)

Table 1.2 Global anthropogenic carbon budget, average for 1980-1989 in 10¹⁴ mol·year⁻¹ (IPCC 1996).

CO₂ sources	
Fossil fuel combustion and cement production	4.6 ± 0.4
Changes in tropical land use	1.3 ± 0.8
Partitioning amongst reservoirs	
Storage in the atmosphere	-2.7 ± 0.2
Ocean uptake	-1.7 ± 0.7
Northern Hemisphere forest regrowth	-0.4 ± 0.4
Total	1.1 ± 1.3*

* Estimated effects of nitrogen fertilisation (-0.4 ± 0.8·10¹⁴ mol·year⁻¹) and CO₂ fertilisation and climatic effects (0 to -1.7·10¹⁴ mol·year⁻¹) have not been included.

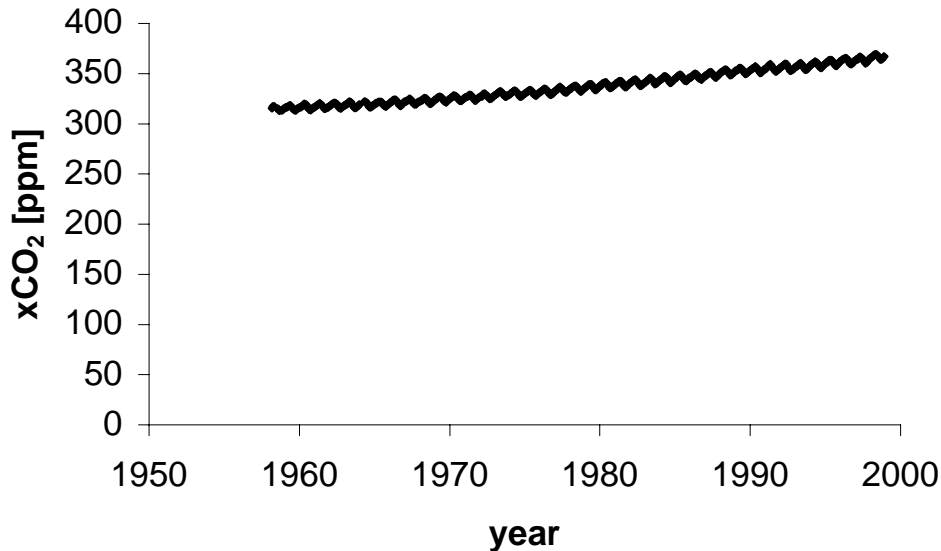


Figure 1.3 Schematic representation of ocean currents: the global conveyor belt. Solid lines represent deep water flow, dashed lines represent surface water flow, filled circles represent upwelling regions and open circles represent regions of deep water formation (Figure 1-13 in Broecker & Peng 1982).

in the Equatorial Pacific and in the Southern Ocean (~60°S). The conveyor belt completes its journey by surface flows between Asia and Australia to the southern tip of Africa and then north-west into the Atlantic and also south of South America into the Atlantic (Semtner & Chervin 1992, see also Broecker 1991). Surface water is 15°C on average, and cools before it sinks (cold water is heavier) and becomes deep water, which is around 4°C. This cooling increases the solubility of CO₂, and therefore the temperate regions where the water is cooled are sinks for atmospheric CO₂, while the water that wells up is warmed so that the Equatorial Pacific is a source for atmospheric CO₂. Because the atmospheric CO₂ is on the increase (Figure 1.4), the sink of newly formed deep water can be calculated to be bigger than the source of deep water that was formed before the industrial revolution. This net sink constitutes the physical carbon pump. The rate at which this conveyor belt runs has been estimated by comparing the average concentration of ¹⁴C (which is formed in the atmosphere) in the surface ocean with the average concentration of ¹⁴C in the deep sea, which is lower because the concentration of ¹⁴C decreases by radioactive decay (see chapter 5 in Broecker & Peng 1982 for details). The average age of deep water is about 1000 years. Because the surface ocean is made up of only the upper 200 m and the other 3600 m is the deep ocean, surface currents are much faster than the deep currents. It only takes a few years for surface water to circle the ocean basins such as the North Atlantic.

The biological pump is fuelled by algae growing on sunlight and using inorganic carbon (CO₂ and/or HCO₃⁻). Part of this carbon is replenished from the atmosphere by air-sea gas exchange. This is the first step in the biological carbon pump. The second step is in particulate form by sinking particles from the upper ocean to the deep sea. Since algae are mostly very small and therefore sink very slowly most of the particle flux is in the form of fecal pellets of zooplankton and marine snow (particles that have been formed by aggregation of smaller particles of which it is usually hard to recognise the origin). In the deep ocean most of the material is broken down by bacteria and animals into inorganic carbon again to enter into the

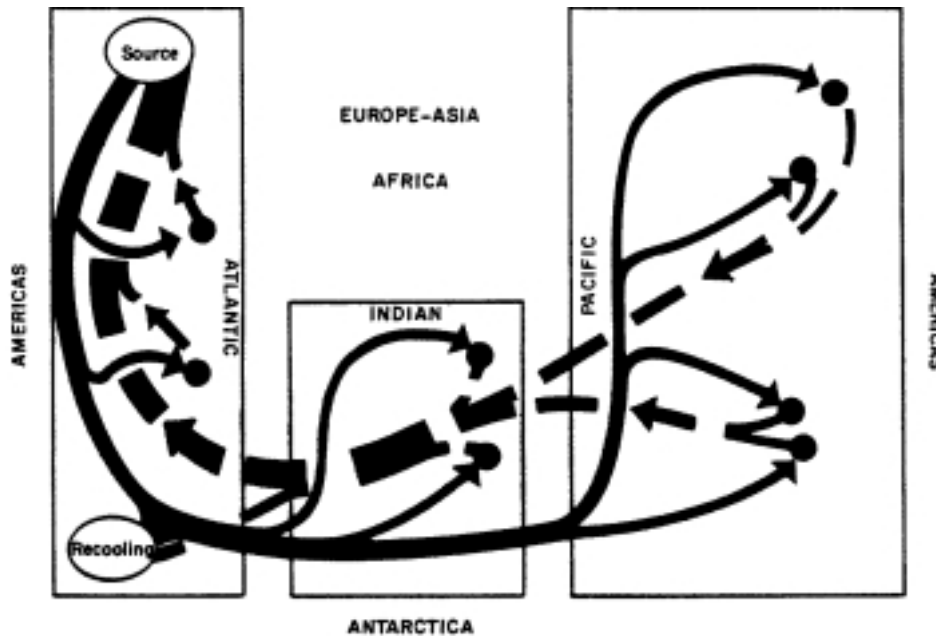


Figure 1.4 CO₂ concentration in the atmosphere, sampled on Mauna Loa, Hawaii, USA. Data from <http://cdiac.esd.ornl.gov/ftp/maunaloa-co2>, see also Keeling et al. (1996).

conveyor belt. Only a small portion escapes this respiration and ends up at the bottom of the ocean, where again most is broken down by benthic organisms, and a minute fraction is buried in the sediments. Over the last $3.6 \cdot 10^9$ years, this burial (and to a smaller extent also sediment formation on land) has given rise to the fossil organic carbon, and over the last $5.3 \cdot 10^8$ years the larger amount of fossil carbonates has been formed. Since the physical pump, and maybe also the biological pump transport more carbon downward than is transported upward during times that the atmospheric CO₂ is on the rise the oceans act as a buffer for atmospheric CO₂ over time-scales shorter than 1000 years (see 'Ocean uptake' in Table 1.2)(further reading, Broecker & Peng 1982, Bakker 1998).

Organic carbon in the biosphere

Apart from the fossil organic carbon, organic carbon is stored in biomass, in soils on land and as dissolved organic carbon in the ocean. The cycling of organic carbon on land is quite different from that in the sea. On land the average lifetime of biomass is about 5 years, while in the sea it is in the order of 1 month. Therefore, although the productivity on land is only about 3 times as much as in the sea (IPCC 1990), the amount of biomass on land is about 200 times as large as in the sea (Figure 1.1). Soil organic carbon acts as a temporary reservoir of carbon, with a lifetime of about 30 years (IPCC 1990), but there is no significant fossil carbon formation on land nowadays (Bolin et al. 1979). Any organic carbon of terrestrial origin that gets incorporated into the sediment does so by being transported to the sea by rivers and sedimenting on the sea floor. Most of the organic carbon pool in the ocean is refractory dissolved organic carbon, which has a lifetime of about 9000 years (Clercq 1997)(further reading: Clercq 1997, Wiebinga 1999).

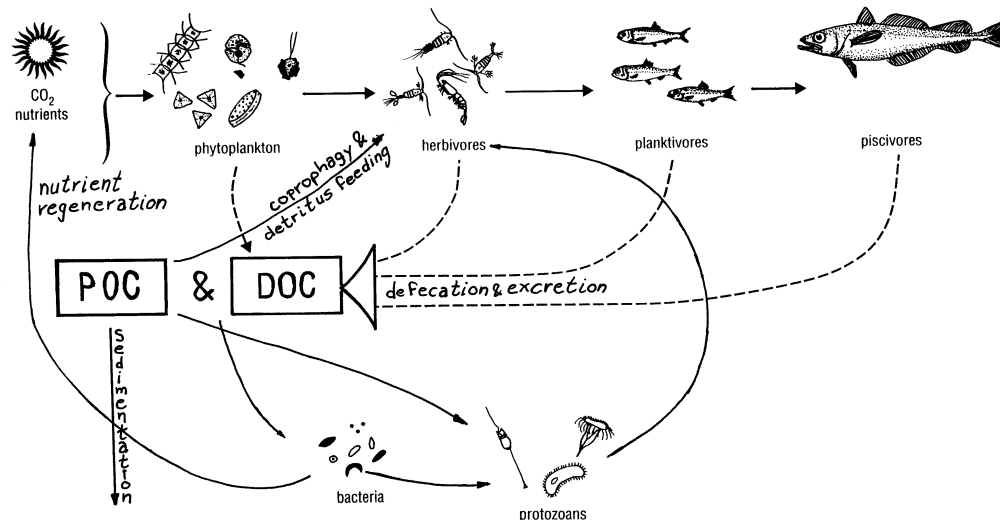


Figure 1.5 Cycles of material through the food web (adapted from Figure 5.7 in Lalli & Parsons 1993). On top the classical foodchain from the primary producers (phytoplankton) to the toppedators (*Homo sapiens*, not indicated). Below, the microbial loop which both degrades and repackages the dissolved and particulate organic carbon (POC & DOC) from the classical food chain.

Anthropogenic changes in the global carbon cycle

'The scientists who extrapolate trends agree to a large extent, but that doesn't mean that they are right' (Verkoren (2000) suggesting a parallel between the mistaken demographic predictions of the 1960s and demographic predictions of today; my translation).

The research that is described here falls within the NWO-project Global Change (Verstoring van Aardsystemen). Global change is first of all change in elemental cycles on the earth due to human activities. While the absolute anthropogenic impact on the global carbon cycle is larger than of any other element, the impact on several metals, sulfur and nitrogen is much larger relative to their natural cycles (Butcher et al. 1992) However, because this thesis is about an alga and carbon, for the purposes of this thesis global change is most readily apparent from the rise in the atmospheric concentration of carbon dioxide (CO_2 ; Figure 1.4). This rise can be readily attributed to the burning of fossil fuels and the production of cement, which have been on the increase since around 1780. In addition, due to the cutting of forests and the conversion of grassland into agricultural land, the amount of carbon in terrestrial biomass and soils has been decreasing. In this way, an estimated total of 34.5 Pmol have been emitted up to 1995. The increase in atmospheric CO_2 has been estimated at 12.9 Pmol (Pilson 1998). In order to trace where the remaining 21.6 Pmol carbon has gone, a global carbon budget has been derived (Table 1.2). As can be seen the uncertainty on these data is rather large, which is not surprising since it must integrate every process on the planet that involves carbon. Since the loss to and gain from space is negligible, the added total of sources and sinks should not be significantly different from zero, and it isn't. Thus, there is no missing sink (statement 3).

1.2 Marine biology and chemistry

Food web and elemental cycles

The study of the marine food web started from the perspective of fisheries (Mills, 1989). As a consequence of this the food web was first studied as a linear progression from algae via zooplankton to zoonekton (plankton being non-motile organisms and those that swim more

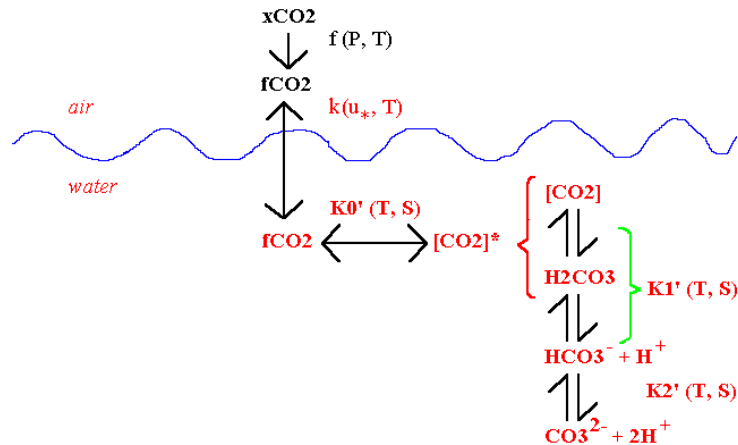


Figure 1.6 Speciation of the dissolved inorganic carbon system. $x\text{CO}_2$ is the mixing ratio of CO_2 in air, this ratio can be measured by infrared absorption. Multiplying $x\text{CO}_2$ by the pressure (P) gives the partial pressure ($p\text{CO}_2$, not indicated) and by correcting for the non-ideal gas behaviour the fugacity ($f\text{CO}_2$) is obtained (Weiss 1974). The concentration of CO_2^* is often expressed as the fugacity in equilibrium with this concentration, the equilibrium concentration is given by the apparent solubility constant K_0' . If CO_2^* in the sea is not in equilibrium with $f\text{CO}_2$ in the air then diffusion will start to equilibrate these two at a rate that is a function of the concentration difference and the gas transfer velocity k , which is a function of wind speed u^* and temperature T . The equilibrium between CO_2^* , bicarbonate (HCO_3^-) and carbonate (CO_3^{2-}) is governed by the apparent first and second dissociation constants of carbonic acid K_1' and K_2' , which are functions of temperature and salinity S .

slowly than ocean currents, and nekton being able to move independent of ocean currents), which is therefore called the classical food chain (Figure 1.5). When staining techniques were developed that made it possible to count bacteria, the important role of bacteria in recycling the material from dead organisms and excreted material (both particulate and dissolved) was discovered, and the concept of the microbial loop was introduced (Azam et al. 1983). Part of this dead material is degraded to nutrients and part is converted to biomass. The bacterial biomass is then eaten by microzooplankton, and the latter are eaten by mesozooplankton, thus reintroducing material that has been 'lost' from the classical food chain. The total picture of this then is that at the base of the marine food chain are the alga that use the energy from the sun to produce organic matter, and this material feeds the whole community of heterotrophic organisms, with each organism feeding preferentially on live organisms, and during food shortage on degraded material as well (Figure 1.5). For a different representation of the same food chain from the perspective of carbon flow see Figure 5.1 (further reading: Lalli & Parsons 1993, Berger et al. 1989).

Inorganic carbon speciation in sea water

Figure 1.6 shows a schematic representation of the chemical speciation of carbon dioxide (CO_2). CO_2 is not a particularly soluble gas: at 10°C about as much CO_2 can be dissolved in 1 L. water as in 1 L. air. Once dissolved, however, CO_2 is hydrated to form carbonic acid (H_2CO_3), which splits of 1 or 2 protons, to give bicarbonate (HCO_3^-) and carbonate (CO_3^{2-}). Sea-water in equilibrium with the atmosphere contains about 2 mM of dissolved inorganic

Table 1.3 The DIC system: dissociation constants and definitions.

K_0'	$=$	$\frac{f\text{CO}_2}{[\text{CO}_2]^*}$
K_1'	$=$	$\frac{[\text{H}^+][\text{HCO}_3^-]}{[\text{CO}_2]^*}$
K_2'	$=$	$\frac{[\text{H}^+][\text{CO}_3^{2-}]}{[\text{HCO}_3^-]}$
DIC	$=$	$[\text{HCO}_3^-] + [\text{CO}_3^{2-}] + [\text{CO}_2]^*$
Alkalinity	$=$	$[\text{HCO}_3^-] + 2*[\text{CO}_3^{2-}] + [\text{B}(\text{OH})_4^-] + [\text{SiO}(\text{OH})_3^-] + [\text{OH}^-] + [\text{HPO}_4^{2-}] + 2*[\text{PO}_4^{3-}] + [\text{NH}_3] + [\text{HS}^-] + 2*[\text{S}^{2-}] - [\text{H}^+] - [\text{HSO}_4^-] - [\text{HF}] - [\text{H}_3\text{PO}_4]$

carbon (DIC), which is the sum of CO_2 , H_2CO_3 , HCO_3^- and CO_3^{2-} . Of this 2 mM less than 1% is CO_2 , ~0.002% H_2CO_3 , ~90% HCO_3^- and ~9% CO_3^{2-} . Because of the very low concentration of H_2CO_3 , this is usually included with CO_2 , which is then written as CO_2^* (or often simply as CO_2). The dissociation constants that define the equilibrium ratios between the inorganic carbon species are defined in Table 1.3.

DIC, which is the sum of all dissolved inorganic carbon species, keeps track of the mass balance. Alkalinity keeps track of the charge balance, and is measured in equivalents (that is, the charge or valency of an ion multiplied by its concentration). Alkalinity is the difference between the fully dissociated cations and the fully dissociated anions. This difference is balanced by the dissociation of weak acids, 97% of which is the dissociation of carbonic acid. Thus, alkalinity can be simplified to:

$$\text{carbonate alkalinity} = [\text{HCO}_3^-] + 2*[\text{CO}_3^{2-}] \quad (1.3).$$

When discussing biological processes these two parameters (DIC and alkalinity) are very useful. For instance, when considering the production of organic carbon by plants that use inorganic carbon it does not matter in the bulk solution whether they take up CO_2 or HCO_3^- , which is often a matter of debate. (There is a difference in the diffusive boundary layer around the cell (Wolf-Gladrow & Riebesell 1997).) If cells take up HCO_3^- they take up DIC and a negative charge (= alkalinity). The charge balance of a cell is under tight control, and to compensate for the negative charge the cells have two options. Non-calcifying cells take up H^+ or excrete OH^- . This compensates for the alkalinity taken up with HCO_3^- (Table 1.3), and the net effect is the same as for CO_2 uptake: DIC decreases and alkalinity is not affected. Calcifying algae compensate for the negative charge by taking up Ca^{2+} and precipitating this as calcite:



which is the reverse of the weathering reaction 1.1 of carbonate rocks that is mentioned in ‘The global carbonate cycle’ (chapter 1.1). Thus, calcification decreases alkalinity twice as much as DIC, and increases the concentration of CO_2 , even though DIC decreases. This CO_2 is normally used in photosynthesis:



with $(\text{CH}_2\text{O})_{\text{org}}$, the formula for carbohydrate, as a simplified representation of organic matter. If

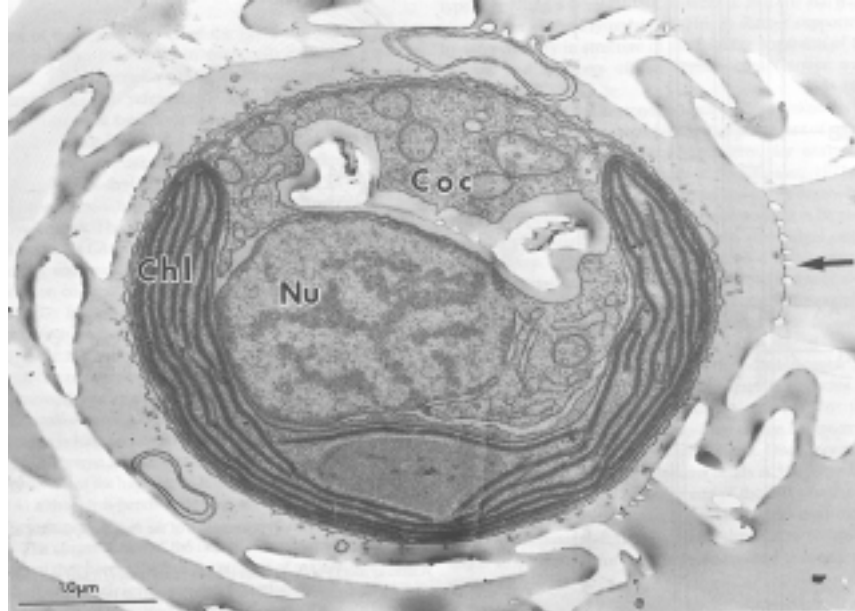


Figure 1.7 Transmission electron micrograph of *Emiliana huxleyi*. White areas are formed by dissolution of the extracellular and intracellular (Coc) coccoliths during sample preparation. The chloroplast (Chl) and nucleus (Nu) are indicated (Figure 9 in Pienaar 1994).

calcification and photosynthesis are performed in a ratio of 1:1 the overall reaction then becomes:



In chapter 2 it is shown that *E. huxleyi* uses both HCO_3^- and CO_2 , thus performing a mixture of reactions 1.5 and 1.6. DIC and alkalinity are also the more useful parameters when discussing physical processes. Since the mass and charge balances must also apply when two different water masses are mixed, the DIC and alkalinity can be directly calculated from the respective contributions of the two water masses to the mixture. The same is not true for the other concentrations in the DIC system, because HCO_3^- , CO_3^{2-} , CO_2 and pH depend in a non-linear way on DIC, alkalinity, temperature and salinity. In order to make DIC and alkalinity independent of temperature, salinity and pressure they are expressed in units per kg, because a kg is always a kg, whereas a cold, saline litre of water in the deep ocean weighs more than a warm, fresh litre of water at the surface.

The intricacies of inorganic carbon speciation can become quite complicated, and for a theoretical understanding I would recommend Zeebe & Wolf-Gladrow (in prep.). However, when considering combinations of organic carbon production, calcification and organic nitrogen production (for the latter, see chapters 2, 4 and 5), it proved to be more informative to do some calculations, for which a freeware program is available by Lewis & Wallace (<http://cdiac.esd.ornl.gov/oceans/co2rprt.html>) (further reading: Stoll 1994).

Coccolithophorids

There are several families of algae that produce coccoliths, which are collectively known

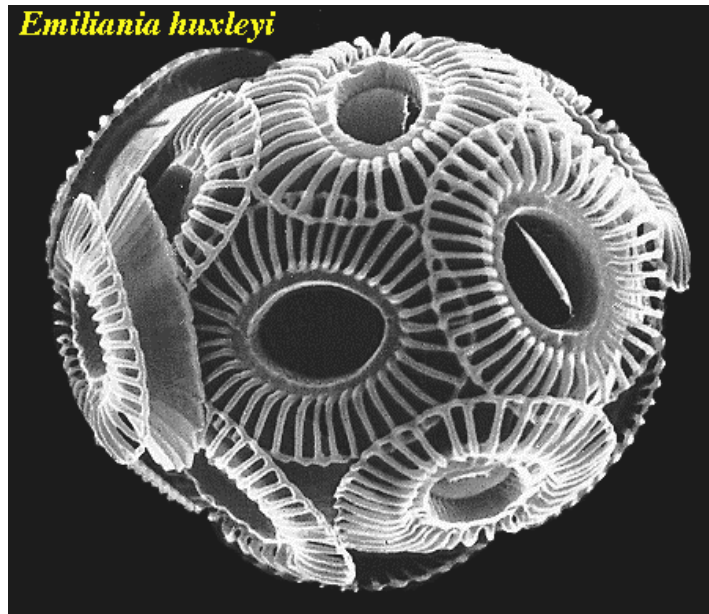


Figure 1.8 Scanning electron micrograph of *Emiliana huxleyi*.

as the coccolithophorids. Coccoliths are platelets of CaCO_3 , which are precipitated as calcite crystals. The calcite is precipitated intracellularly in specialised vesicles that are connected with the Golgi apparatus (Figure 1.7). After completion the coccoliths are extruded, but are retained in a sphere of interlinked coccoliths on the outside of the cell (the coccosphere, Figure 1.8). The shape of these coccoliths is very distinctive and allows the identification of different species, and even of different morphotypes within the same species (Young & Westbroek 1991). Coccolithophorids first appeared in the sedimentary record about 230 million years ago. They were especially abundant during the late Cretaceous (around 80 million years ago) and formed a layer of chalk on what was the sea bottom at that time. This layer of chalk covers most of north-west Europe, among other regions (Young et al. 1994). The white cliffs of Dover are the best-known example. Coccolithophorids form massive blooms which cover a total area of $1.4 \cdot 10^6 \text{ km}^2$ on average each year (Figure 1.9).

Young (1994) divides the coccolithophorids into four groups according to ecological and morphological criteria (Figure 1.10):

- 1) Placolith bearing r-selected (MacArthur & Wilson 1967) opportunist species adapted to exploit variable eutrophic conditions. These are highly productive species found in upwelling areas, coastal seas and in the temperate regions.
- 2) Umbelliform K-selected (MacArthur & Wilson 1967) affinity specialised species adapted to steady oligotrophic conditions. These are low productive species found in the upper 100 m of the subtropical ocean gyres (10-30° latitude).
- 3) Floriform deep dwelling species, low light adapted, and highly productive; possibly r-selected.
- 4) Motile species with a widespread biogeography and relatively low abundance. These are possibly K-selected storage specialists that exploit high nutrient patches by being motile.

In the same paper (Young 1994) a compilation is given of possible functions of coccolith production (Figure 1.11). It is relatively straightforward to test the applicability of these functions by comparing calcified to non-calcified species, but it has proven very difficult to undertake the ecologically more interesting task of predicting the relative success of species on

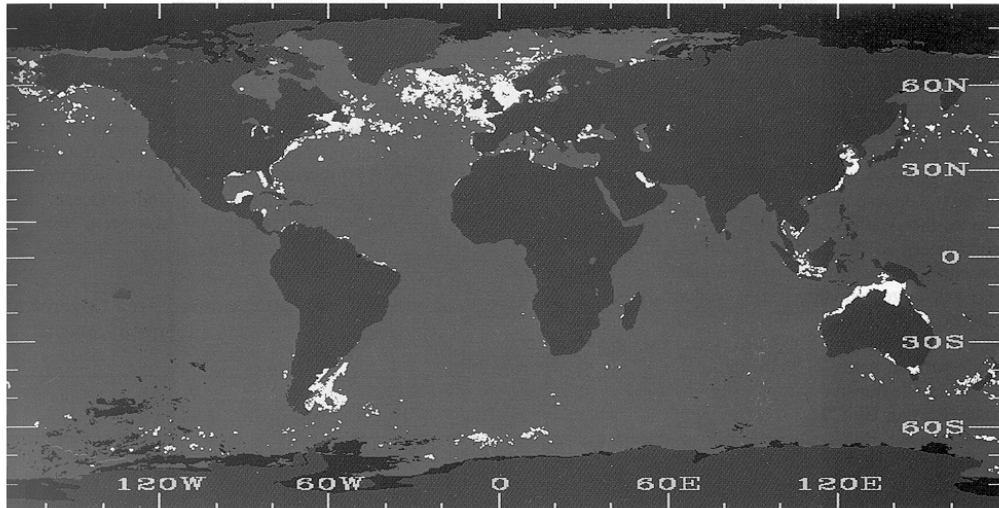


Figure 1.9 Composite satellite image of all the coccolithophore blooms (in white) between November 1978 and June 1986, taken by the Coastal Zone Color Scanner (Plate 1 in Brown & Yoder 1994).

the basis of such studies. In chapter 2 it is shown that the tight coupling between calcification and photosynthesis rates is consistent with function 2a: the biochemical convenience of using HCO_3^- with only a small increase in the seawater pH (Figure 1.11). In this respect it is relevant to note that function 2a is the only function that depends on the process of coccolith formation while the other functions depend on the possession of a coccosphere around the cell, and that *E. huxleyi* is the only coccolithophore that continues producing coccoliths even when the cell has a complete coccosphere. (This results in either more than one layer of coccoliths around the cell

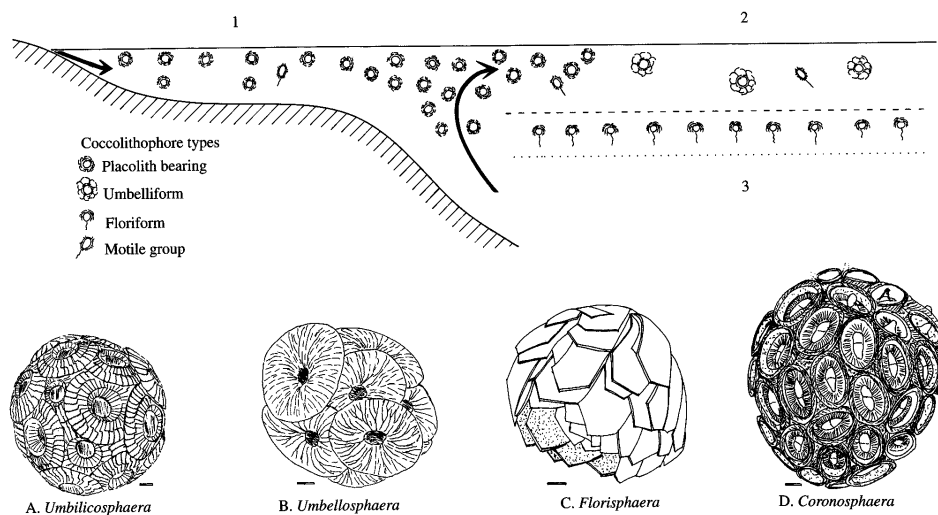


Figure 1.10 Ecological distribution of coccolithophore types. Cartoon to illustrate the three communities discussed in the text: 1. Placolith dominated, 2. Umbelliform dominated, 3. Floriform dominated, 4. Motile species (dispersed). Arrows indicate nutrient flux (Figure 6 in Young 1994).

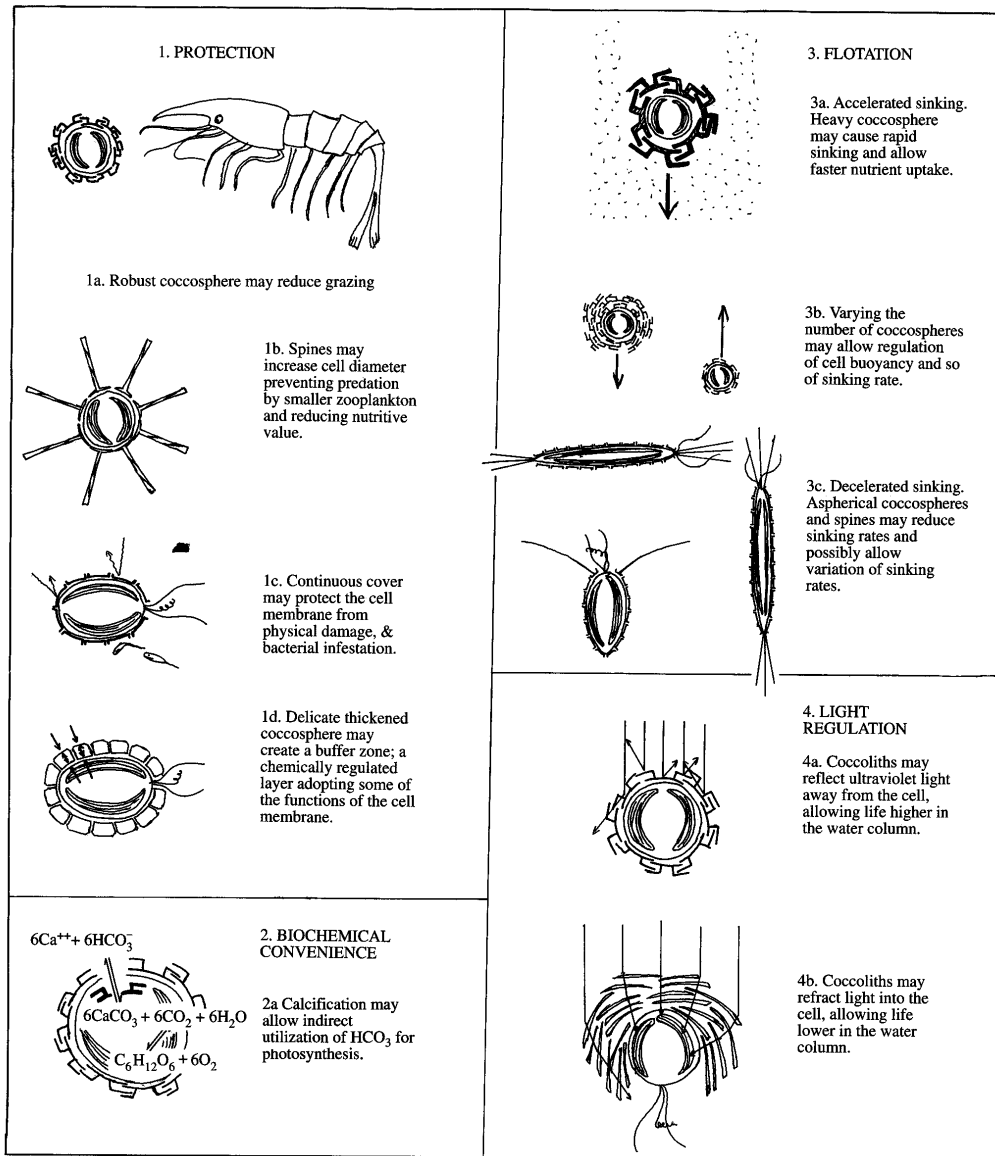


Figure 1.11 Possible functions of coccoliths (Figure 2 in Young 1994).

or in the shedding of coccoliths into the sea water medium.) From this it may be speculated that *E. huxleyi* is the only species that benefits significantly from function 2a (see Figure 2.4)(further reading: Winter & Siesser 1994).

Emiliania huxleyi

Emiliania huxleyi is a unicellular alga of about 5 μm . diameter (Figures 1.7, 1.8). It is a placolith producing coccolithophorid. *E. huxleyi* evolved only approximately 260,000 years ago (McIntyre 1970). Its phylogenetic position is indicated in Table 1.4. More detailed characterisations of several varieties of *E. huxleyi* have been performed by Bleijswijk et al. (1991) using immunofluorescent labelling of polysaccharides and morphometry, Young &

Table 1.4 Phylogenetic position of *Emiliana huxleyi* (from Jordan & Green 1994).

Phylum:	Haptophyta
Classis:	Prymnesiophyceae
Subclassis:	Prymnesiophycidae
Ordo:	Prymnesiales
Familia:	Noëlaerhabdaceae
Genus:	Emiliana
Species:	<i>Emiliana huxleyi</i>

Westbroek (1991) using morphometric analysis, and Medlin et al. (1996) using molecular biological techniques. Today, *E. huxleyi* has a cosmopolitan distribution, which excludes only the polar regions (McIntyre & Bé. 1967).

The ecological niche of *Emiliana huxleyi* is generally thought to include two main features: its competitive advantage under phosphate limitation, and its broad light optimum. The competitive advantage under phosphate limitation is due to both its high affinity for inorganic phosphate, and its ability to use organic phosphorus. The broad light optimum means that it has both a high affinity for light, and a high tolerance for high light intensities (Riegman et al. 1998). These two features make it understandable why blooms of *E. huxleyi* are generally found at times and places where there is a stable, relatively shallow upper mixed layer, because this tends to decrease the upward transport of nutrients, and thus gives rise to low nutrient concentrations, and it also increases the average amount of light that algae are exposed to. Such a stable shallow mixed layer is typically found in the summer months in the temperate regions, where blooms of coccolithophorids are most extensive, as can be seen in Figure 1.9 and in more detail in the seasonal subdivisions of this figure (Brown & Yoder 1994). A more detailed discussion of the (eco)physiology of *Emiliana huxleyi* can be found in the thesis of Bleijswijk (1996).

In the Global Emiliana Modelling initiative (GEM, Westbroek et al. 1993) the use of a

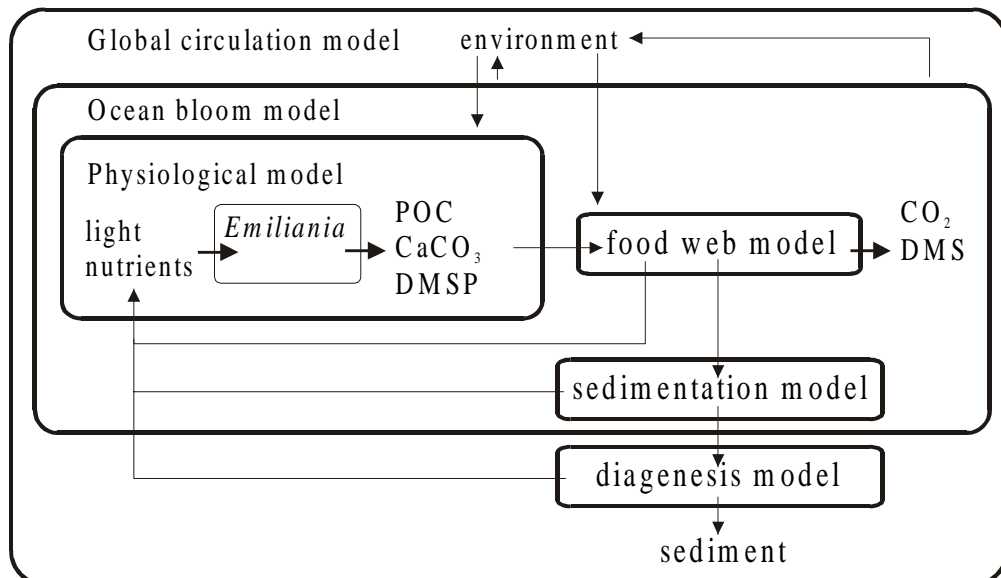


Figure 1.12 Simplified scheme of the Global *Emiliana* modelling initiative (GEM) approach with a hierarchical set of compatible models (adapted from Westbroek et al. 1993, 1994).

single organism, *Emiliana huxleyi*, is advocated as a model for the biological response to global change. The idea is to study one organism in detail and try to understand its workings at several levels of organisation (from the molecular through to the geological, Figure 1.12) and then test the general applicability of these workings on a wider range of organisms. The knowledge thus obtained should be easier to integrate than to study different levels with different subsets of organisms, and then to try to integrate that into knowledge. This thesis deals with the relationship between *E. huxleyi* and carbon on two of these levels of organisation: the physiological (chapters 1.3, 2 & 3) and the oceanic (chapters 1.4, 4 & 5)(further reading: <http://www.soc.soton.ac.uk/SOES/STAFF/tt/eh/>).

1.3 Intracellular processes

Enzyme kinetics

Enzymes act as catalysts in many reactions that take place inside the cell. This is done either by lowering the activation energy of exogenous (energy producing) reactions, or by coupling the reactions to an exogenous reaction (often the hydrolysis of ATP, which is the main energy carrier in the cell). In the simplest case, the rate of an enzyme-catalysed reaction is a function of the concentration of one rate-limiting substrate (= reactant), which is described by the Michaelis-Menten kinetics equation:

$$V = V_{\max} * [S] / ([S] + K_{1/2}) \quad (1.7),$$

in which V is the rate of the reaction, V_{\max} is the rate when the reaction is saturated with substrate, $[S]$ is the substrate concentration, and $K_{1/2}$ is the concentration at which the rate is half of V_{\max} (Michaelis & Menten 1913). Although strictly speaking Michaelis-Menten kinetics are only applicable for a single enzyme, it is often used to describe other cellular processes such as the growth rate (Figures 2.5b, 2.7c). Although it would be more correct to describe growth with a combined equation for diffusion of the substrate to the enzyme, and the enzyme reaction that limits the growth rate, the influence of the diffusion step is often smaller than the measurement error of the growth rate. In that case the description does not become more accurate with a more complicated equation (further reading: Morel 1987).

Carbonic anhydrase

Carbonic anhydrase is the enzyme that catalyzes the conversion between HCO_3^- and CO_2 . Since the conversion is not coupled to a free energy decreasing reaction, the enzyme catalyses the conversion towards chemical equilibrium. The function of carbonic anhydrase depends on its location: extracellular carbonic anhydrase tends to catalyse the conversion of HCO_3^- towards CO_2 in cells that take up CO_2 exclusively or in preference to HCO_3^- . Cytosolic carbonic anhydrase is sometimes thought to be associated with active uptake of CO_2 , and to catalyse the conversion of CO_2 towards HCO_3^- , to limit diffusive loss of CO_2 , which can pass through the cell membrane, while the charged HCO_3^- cannot. In the chloroplast the function of carbonic anhydrase is to catalyse the conversion towards CO_2 again, because the primary carbon fixing enzyme in C_3 plants is Rubisco (Ribulose-bis-phosphate carboxylase /oxygenase), which uses CO_2 as its substrate (Cooper et al. 1969). In *Emiliana huxleyi* carbonic anhydrase has been found in the chloroplast (Nimer et al. 1995) but no extracellular enzyme could be detected (Riebesell unpublished). Because of the presence of inhibitor(s) in the cytosol (Nimer et al. 1995) the presence of cytosolic carbonic anhydrase seems unlikely. The cofactor for carbonic anhydrase is Zn^{2+} , without which the enzyme is inactive. In chapter 3 this fact is used to determine the role of Zn^{2+} in HCO_3^- -use by *Emiliana huxleyi*, by growing the algae at varying Zn^{2+} concentrations (see 1.4 and chapter 3)(further reading: Graham et al. 1984).

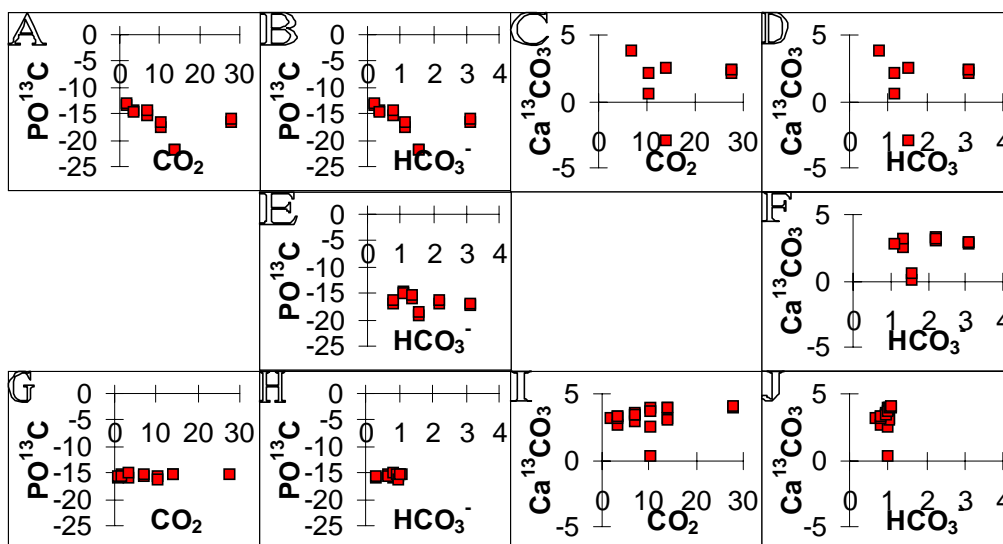


Figure 1.13 Data of $^{13}\text{C}/^{12}\text{C}$ ratios in POC and CaCO_3 , relative to medium DI^{13}C , in *Emiliana huxleyi* grown under inorganic carbon limitation (E. Buitenhuis, J. Engler, U. Riebesell, H. de Baar unpubl.). A-D) experiment at constant pH, E-F) experiment at constant CO_2 , G-J) experiment at constant alkalinity. See ‘Materials and methods’ in chapter 2 for details of the experimental setup.

^{13}C discrimination

Carbon is the 6th element in the periodic table because its nucleus contains 6 protons. Most carbon has 6 neutrons in the nucleus, bringing the atomic weight to 12: ^{12}C . A small fraction of the carbon atoms has more neutrons: 1.1% has 7 neutrons (^{13}C) and $10^{-10}\%$ (in atmospheric CO_2) has 8 neutrons (^{14}C). ^{13}C is a stable isotope, that is, it is not radioactive. ^{14}C is radioactive and emits an electron to become normal ^{14}N with 7 protons and 7 neutrons. ^{14}C is used in two types of studies in oceanography: for age determination using the very small amounts of natural ^{14}C (see ‘The dissolved inorganic carbon cycle’ and ‘Organic carbon in the biosphere’, chapter 1.1) and for the determination of carbon uptake rates using synthetic ^{14}C (rates of photosynthesis and calcification in chapter 2).

^{13}C is used for three types of studies in oceanography: for physiological studies of carbon uptake mechanisms (Spero et al. 1997), for measuring partitioning of carbon between reservoirs of the global carbon cycle (Ciais et al. 1995, Battle et al. 2000), and for paleoreconstruction of the global carbon cycle (Hayes et al. 1989). The basis for the use of ^{13}C in all of these approaches is the discrimination against ^{13}C in certain processes, such as photosynthetic carbon fixation. This discrimination is based on the preference of the carbon fixing enzyme Rubisco (Ribulose-bisphosphate carboxylase/oxygenase) for $^{12}\text{CO}_2$, that is, the reaction rate with ^{12}C is 1.029 times faster than with ^{13}C (Raven et al. 1993). Determination of the $^{13}\text{C}/^{12}\text{C}$ ratio is accurate enough to detect this small difference. This discrimination takes place under equilibrium conditions; it assumes that Rubisco always has an equilibrated pool of carbon to choose from. If Rubisco is inside a cell and CO_2 enters the cell by diffusion, then the diffusive exchange with the medium outside the cell must be faster than the rate at which Rubisco fixes CO_2 . If not, then Rubisco will use all CO_2 as fast as it enters the cell, because the rate limitation by diffusion will be bigger than the small rate limitation of ^{13}C fixation. From theoretical considerations it can be predicted that the ^{13}C discrimination will vary linearly with μ/CO_2^* (Laws et al. 1995, Rau et al. 1996), in which μ is the specific growth rate of the algae.

Because the difference in rates between the reaction that uses ^{12}C relative to the reaction that uses ^{13}C is so very small there are restrictions on the experimental design: If an experiment is conducted in a closed bottle then cells will first preferentially fix ^{12}C . If the amount of carbon that the cells use in the course of an experiment is a significant portion of the amount of dissolved carbon in the bottle (more than a few percent) then the $^{13}\text{C}/^{12}\text{C}$ ratio in the medium will increase because the cells are removing ^{12}C , and the fraction of ^{13}C that is incorporated into the biomass will increase with this ratio in the course of the experiment. This is called Rayleigh distillation. Disequilibrium conditions are not necessarily a disadvantage. If photosynthesis increases the ^{13}C pool of inorganic carbon inside the cell, then the $^{13}\text{C}/^{12}\text{C}$ ratio in calcite can be used to determine if calcification uses the same pool of inorganic carbon or fixes inorganic carbon that enters the cell through a separate route. Since the ^{13}C discrimination of enzymatic conversion of CO_2 to HCO_3^- by carbonic anhydrase is different from the uncatalysed discrimination, ^{13}C discrimination can provide information on the activity of carbonic anhydrase. As is mentioned in 'Materials and methods' of chapter 2 the ^{13}C discrimination was measured in samples of POC (particulate organic carbon) and CaCO_3 of *E. huxleyi* grown at different conditions of the dissolved inorganic carbon system (Figure 1.13). Since the experimental setup was designed for POC/PON analysis of these samples (chapter 2) rather than for ^{13}C discrimination, DIC-use was between 5 and 40%, and Rayleigh distillation will have influenced the results. This is probably the reason that the quality of the data is poor, and no conclusions could be drawn from them (further reading: Raven et al. 1993, McConnaughey 1989a, b).

1.4 The influence of the inorganic carbon system on *E. huxleyi* in the laboratory

The production of coccoliths is an energy requiring process (cf. Anning et al. 1996). Thus, although the function of these coccoliths is not known, the evolution theory predicts that they convey an advantage to the coccolithophorids, for otherwise they would either have lost this ability to produce coccoliths, or they would have been replaced by other algae. Young (1994) has compiled possible functions that have been suggested. One of the suggested functions is to enable coccolithophorids to use HCO_3^- for photosynthesis (Paasche 1962), the concentration of which is 100 times that of CO_2 . Raven & Lucas (1985) have outlined which data will be necessary to calculate the energy costs for algae to depend on diffusive entry of CO_2 , or of using a carbon concentrating mechanism (CCM). Anning et al. (1996) have determined some of the parameters that will be needed to calculate the cost for a coccolithophorid to use its particular method of DIC uptake. There is still some way to go, but when this line of investigation is completed it should be possible to define under which conditions coccolithophorids will do better or worse than algae that use a CCM. In chapter 2 no new suggestions are made as to the possible function of calcification or the mechanism of carbon-use, but the tight coupling that was found between the use of bicarbonate (HCO_3^-) in calcification and photosynthesis suggests that this coupling is functional. It is also shown that the $K_{1/2}$ of CO_2 -use in photosynthesis is lower than was previously found (Paasche 1964, Raven & Johnston 1991). This means that photosynthesis is saturated with CO_2 under normal oceanic conditions.

Tortell & Morel (1999) have observed a lower calcification rate of coccolithophorids at a higher CO_2 concentration of 800 μatm . However, at constant alkalinity *E. huxleyi* shows an increase in calcification rate with increasing CO_2 concentration. For fast increases in atmospheric CO_2 (30% during the last 150 years) relative to the exchange rate of alkalinity in the ocean (on the order of 100,000 years) the ocean has a constant alkalinity. At constant alkalinity, a doubling of $f\text{CO}_2$ from 360 to 720 μatm would increase the HCO_3^- concentration by 10%, the calcification rate by 8%, the photosynthesis rate by 7% and the C/P ratio by 0.9% (chapter 2). A 7% increase in growth rate and an 0.9% increase in the C/P ratio would lead to a

1% smaller atmospheric sink (potential flux in chapter 5) for a bloom of *E. huxleyi* (statement 4). At constant DIC, constant pH and constant CO_3^{2-} (experimental details are not given in the abstract of Tortell & Morel, 1999) the HCO_3^- concentration also increases with $f\text{CO}_2$. Although the coccolithophorids that Tortell & Morel (1999) studied may not have been *E. huxleyi* there is no reason to assume that other coccolithophorids would use CO_3^{2-} rather than HCO_3^- as a substrate for calcification.

Having quantified the use of CO_2 and HCO_3^- by *E. huxleyi* (chapter 2), we then investigated the coupling between calcification and photosynthesis (chapter 3). It can be calculated that the rate at which calcification generates protons (H^+) is higher than the spontaneous rate of hydration of bicarbonate (HCO_3^- , Table 3.1). Thus, given the observed tight coupling between calcification and photosynthesis (Figure 2.4) the enzyme carbonic anhydrase must be present to catalyse this hydration (Figure 2.1). Indeed, carbonic anhydrase has been detected in the chloroplasts of *E. huxleyi* (Nimer et al. 1994a). Since zinc (Zn) is a cofactor of carbonic anhydrase, the enzyme will not be active without zinc, and a reduced activity can be expected under zinc limitation. Our hypothesis, then, was that the coupling between calcification and photosynthesis would become less efficient under zinc limitation. It was found that the interactions between zinc and inorganic carbon use were more complicated than predicted. On the one hand it was found that zinc limitation reduces the efficiency with which bicarbonate is used (Figures 3.2 & 3.3). On the other hand it was also seen that under zinc limitation the use of CO_2 is compromised, as can be seen from the negative growth rates at low zinc, low bicarbonate and high CO_2 (Figures 3.2 & 3.3). This had not been expected since CO_2 can be used directly in the photosynthetic fixation of inorganic carbon into organic carbon (CO_2^{ex} in Figure 3.4). Since this CO_2 limitation at low zinc was alleviated by HCO_3^- this must be directly attributed to the function of carbonic anhydrase in the cell, and not to an effect of zinc limitation in any of the many other cellular functions of zinc. It is possible that this is connected with the intracellular pH regulation, since HCO_3^- is the main cellular pH buffer (Brownlee et al. 1995).

1.5 The influence of *E. huxleyi* on the inorganic carbon system in the sea

On geological time scales the amount of calcite that gets buried in the sediment is not a function of the amount that is produced. At steady state the amount of calcium that gets buried must equal the amount that enters the sea, mostly by rivers (see: the global carbonate cycle). Approximately 3 times as much CaCO_3 is produced as ends up in the sediment (Figure 1.2). The rest is dissolved, either below the lysocline where the water is undersaturated with respect to calcite, or above the lysocline coupled to the oxidation of organic matter (see chapter 4).

This argument applies on geological time scales where steady state can be assumed. However, our interest lies in global change on decadal time scales: the departure from steady state that is caused by human actions, as distinguished from, but also concurrent with, departures that are caused by other natural changes. The human impact on the global carbon cycle is caused for a large part by the burning of more fossil fuels than are being buried in the sediments. In Table 1.2 it is indicated that 30 % of the anthropogenic CO_2 ends up in the ocean. While it is clear that life in the ocean is transporting carbon from the surface ocean into the deep sea and onto the sea floor, it is not clear whether this transport has become faster through global change.

As to the coccolithophorids there is an active debate whether they are less or more efficient contributors to this biological carbon pump relative to other algal species. The reason for this uncertainty is that calcification by itself changes the equilibria of inorganic carbon in the seawater towards an increase in the concentration of CO_2 . However, calcification is performed by plants, and thus is coupled to photosynthesis, which reduces the concentration of CO_2 . The overall effect is of a reduction in the concentration of CO_2 , but it has been argued that

this reduction is smaller than would have been accomplished by other organisms (Robertson et al. 1994) and by inference that if global change shifted the species composition towards fewer coccolithophorids, or lower calcification rates (Tortell & Morel 1999, see section 1.4), the biological carbon pump might run more effectively. Wal et al. (1995) found evidence to the contrary: within a bloom of *E. huxleyi* fecal pellets contained coccoliths and sank more rapidly due to the high density of calcite, while outside the bloom the fecal pellets remained suspended in the upper ocean longer and were broken down to a greater extent. Indeed, within the bloom the concentration of CO₂ was lower than outside (chapter 4). By compiling a model based on the observed fluxes of carbon in a bloom (chapter 5) we are able to reconcile the observations of Robertson et al. (1994), Wal et al. (1995) and Buitenhuis et al. (1996, chapter 4). In the model the sedimentation rate was proportional to the sinking rate of fecal pellets. The sinking rate was calculated from Stokes' law, in which the density of the fecal pellets was calculated using the standing stocks of particulate organic carbon (POC) and CaCO₃ in the upper mixed layer. It was then possible to calculate the air-sea flux of CO₂ as a function of the C/P production ratio (Figure 5.5), and it was shown that blooms of *E. huxleyi* are more efficient carbon sinks than non-calcifying algae (statement 5).

This argument becomes even more important under steady state conditions, as is discussed above. The amount of calcite produced is not the controlling factor in the oceanic calcium budget, because the amount of calcite that is buried is matched to the amount of alkalinity entering the oceans, while any extra calcite that is produced is dissolved. A higher abundance of coccolithophorids would thus lead to a higher burial rate of organic carbon while leaving the burial rate of calcite unchanged. In other words, the alkalinity budget of the ocean would be unchanged while decreasing the DIC content, resulting in a lower atmospheric CO₂ concentration. In fact, if the alkalinity budget is governed by the atmospheric CO₂ concentration, as has been suggested by Broecker & Sanyal (1998), then a negative feedback may operate to keep the atmospheric CO₂ concentration within certain boundaries. If atmospheric CO₂ increases the weathering of calcareous rocks on land then this mechanism alone would tend to buffer the CO₂ concentration, because this weathering uses CO₂. Additionally, an increased input of alkalinity into the ocean by the rivers may decrease the dissolution of CaCO₃ in the surface ocean and thus increase the sedimentation of CaCO₃ and the POC associated with it from the organisms that precipitated the CaCO₃. This POC may then transport enough C downwards to bring the atmospheric CO₂ concentration to the original value, and thus also the original lower weathering rate. Thus, the coupling of the global carbonate and organic carbon cycles may function to maintain the CO₂ concentration in the air within a range that is optimal for life on earth.

Chapter 2: Photosynthesis and calcification by *Emiliana huxleyi* (Prymnesiophyceae) as a function of inorganic carbon species.

Erik T. Buitenhuis, Hein J. W. de Baar & Marcel J.W. Veldhuis

Journal of phycology (1999) **35** (5) 949-959*

Abstract

In order to test the possibility of inorganic carbon limitation of the marine unicellular alga *Emiliana huxleyi* (Lohmann) Hay and Mohler, its carbon acquisition was measured as a function of the different chemical species of inorganic carbon present in the medium. Since these different species are interdependent and covary in any experiment in which the speciation is changed, a set of experiments was performed to produce a multi-dimensional carbon uptake scheme for photosynthesis and calcification. This scheme shows that CO₂ that is used for photosynthesis comes from two sources. The CO₂ in seawater supports a modest rate of photosynthesis. HCO₃⁻ is the major substrate for photosynthesis by intracellular production of CO₂ (HCO₃⁻ + H⁺ → CO₂ + H₂O → CH₂O + O₂). This use of HCO₃⁻ is possible due to the simultaneous calcification using a second HCO₃⁻, which provides the required proton (HCO₃⁻ + Ca²⁺ → CaCO₃ + H⁺). HCO₃⁻ is the only substrate for calcification. By distinguishing the two sources of CO₂ used in photosynthesis it was shown that *E. huxleyi* has a K_{1/2} for external CO₂ of 'only' 1.9 ± 0.5 μM (and a V_{max} of 2.4 ± 0.1 pmol•cell⁻¹•d⁻¹). Thus, in seawater that is in equilibrium with the atmosphere ([CO₂] = 14 μM, [HCO₃⁻] = 1920 μM, at fCO₂ = 360 μatm, pH = 8, T = 15 °C), photosynthesis is 90 % saturated with external CO₂. Under the same conditions the rate of photosynthesis is doubled by the calcification route of CO₂ supply (from 2.1 to 4.5 pmol•cell⁻¹•d⁻¹). However, photosynthesis is not fully saturated since calcification has a K_{1/2} for HCO₃⁻ of 3256 ± 1402 μM, and a V_{max} of 6.4 ± 1.8 pmol•cell⁻¹•d⁻¹. The H⁺ that is produced during calcification is used with an efficiency of 0.97 ± 0.08, leading to the conclusion that it is used intracellularly. A maximum efficiency of 0.88 can be expected since NO₃⁻ uptake generates a H⁺ sink (OH⁻ source) for the cell. Because of the efficient coupling between H⁺ generation in calcification and CO₂ fixation in photosynthesis we conclude that this is the evolutionary reason for the success of *E. huxleyi* as a coccolithophorid.

Key index words: calcification rate; CO₂ (carbon dioxide); coccolithophorid; dissolved inorganic carbon system; *Emiliana huxleyi*; Haptophyta; HCO₃⁻ (bicarbonate); pH; photosynthetic carbon fixation.

Abbreviations: C/P calcification rate / photosynthetic rate, CCM carbon concentrating mechanism, DIC dissolved inorganic carbon, fCO₂ fugacity of CO₂, μ specific growth rate, POC/PON particulate organic carbon / particulate organic nitrogen

Introduction

Emiliana huxleyi is a coccolithophorid alga with a world-wide distribution. It usually forms blooms in the temperate regions after the spring diatom bloom. *E. huxleyi* produces coccoliths, platelets of distinctive shape that are made of CaCO₃ in the mineral form of calcite. These are produced intracellularly by an energy requiring process in specialised vesicles that are derived from the Golgi apparatus (Westbroek et al. 1989).

There are several theories that link the production of coccoliths to the success of *E.*

* This article received additional review for the Provasoli Award 1999.

huxleyi (Young 1994). As early as 1962 Paasche suggested that calcification and photosynthesis in *E. huxleyi* might be linked by a mechanism equivalent to the symbiosis of corals. By precipitating CaCO_3 it shifts the equilibrium of dissolved inorganic carbon (DIC) towards CO_2 , which can be used in photosynthesis. Thus, calcification may represent an alternative to a carbon concentrating mechanism (CCM) in decreasing photorespiration by the oxygenase activity of ribulose-bisphosphate-carboxylase-oxygenase (rubisco). In view of the widespread occurrence of blooms of *E. huxleyi* (e.g. Brown and Yoder 1994) this mechanism may be more efficient than a CCM in using resources such as energy, PO_4^{3-} and / or Zn^{2+} . Anning et al. (1996) have shown the potential merit of calcification as an energy efficient way of supplying Rubisco with CO_2 , but the actual balance of the comparison with a CCM depends on the -as yet unknown- transport route of the ions involved. While the competitive ability of *E. huxleyi* for PO_4^{3-} is well documented (Riegman et al. 1992, Egge & Heimdahl 1994) no mechanism to link this feature with calcification has been identified. Raven & Johnston (1991) have pointed out that an alga with a CCM would need more Zn^{2+} than an alga that depends on diffusive CO_2 entry. Calcification may represent an intermediate requirement of Zn^{2+} as a cofactor in the enzyme carbonic anhydrase (Morel et al. 1994).

The half-life time of the conversion of HCO_3^- into CO_2 is 38 seconds at 18 °C (Wolf-Gladrow & Riebesell 1997). The inorganic carbon species that are incorporated into calcite and photosynthetic organic carbon have been investigated using this relatively long equilibration time (Sikes et al. 1980). The ^{14}C was added at non-equilibrium concentrations (as $^{14}\text{CO}_2$ or $\text{H}^{14}\text{CO}_3^-$) and its incorporation was measured during the time-interval in which this ^{14}C equilibrated. It was found that ^{14}C added as HCO_3^- is preferentially incorporated into calcite while CO_2 is preferentially incorporated into organic carbon. From these results it was concluded that inside the cell two HCO_3^- are split into CO_3^{2-} and CO_2 . The CO_3^{2-} is precipitated as calcite (CaCO_3), and the CO_2 is fixed by the enzyme Rubisco to produce organic carbon (Equation 2.1-2.3):



The conversion of HCO_3^- into CO_3^{2-} was not discussed. The half-life time is 77 msec at 18 °C (Wolf-Gladrow & Riebesell 1997), and therefore these experiments did not distinguish between HCO_3^- and CO_3^{2-} . The disequilibrium experiments with ^{14}C were confirmed with equilibrium ^{13}C discriminations in calcite and photosynthetic carbon (Sikes and Wilbur 1982). However, while the equilibrium discrimination between HCO_3^- and CO_2 is -9.8 ‰ at 18 °C (Vogel et al. 1970, Mook et al. 1974), the equilibrium discrimination between HCO_3^- and CO_3^{2-} is only -0.5 ‰ at 18 °C (Thode et al. 1965). Therefore this method did not adequately distinguish between HCO_3^- and CO_3^{2-} either. By contrast, foraminifera were reported to use CO_3^{2-} in calcification (Spero et al. 1997). In view of these uncertainties we have looked in more detail at the finding of Paasche (1964) that *E. huxleyi* uses HCO_3^- rather than CO_3^{2-} for calcification.

Nimer et al. (1994) reported carbonic anhydrase in the chloroplasts of *E. huxleyi*. This suggests that carbonic anhydrase may convert HCO_3^- into CO_2 at the site of fixation by Rubisco and minimise diffusive loss of CO_2 . Nimer et al. (1995) formulated a model of inorganic carbon use in which photosynthesis and calcification are linked to maintain intracellular pH.

We have adapted this model, which is based on the reviewed data on inorganic carbon acquisition by *E. huxleyi*, as represented in Figure 2.1. We have tested this model by growing *E. huxleyi* at varying conditions in the DIC system. The four main species in the DIC system are HCO_3^- , CO_3^{2-} , CO_2 and H^+ (the concentration of H_2CO_3 is very low, and is included within CO_2 ,

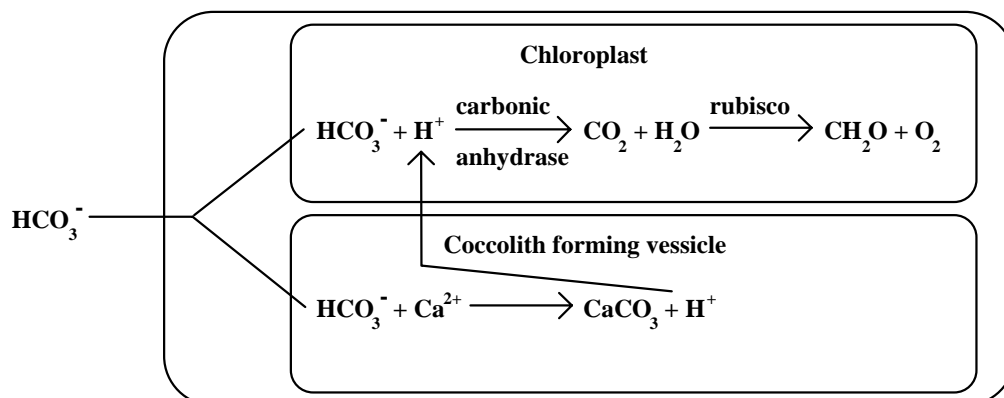


Figure 2.1 Uptake of inorganic carbon by *Emiliana huxleyi*, and mechanism of photosynthetic HCO_3^- use. CO_2^{ex} and CO_2^{in} represent the external and internal source of CO_2 respectively, that are used for photosynthesis. As explained in the results section these two sources were distinguished by performing several complementary experiments in the dissolved inorganic carbon system. Adapted after Nimer et al. 1995.

Weiss 1974). These are correlated by two dissociation constants. Thus, there are two degrees of freedom in the system, and it is not possible to vary one while keeping all the others constant. Therefore, we have performed a set of experiments in which, for each experiment, only one species of DIC was kept constant. The concentrations of the other species were calculated using the dissociation constants. The rates of photosynthesis and calcification were measured. The results are used to elucidate the modes of inorganic carbon acquisition by *E. huxleyi*.

While the geographic distribution of *E. huxleyi* has a wider temperature range, major blooms tend to occur in waters between about 10°C and 20°C (Brown and Yoder 1993). Therefore we have used a uniform 15 °C in our experiments as being representative of bloom conditions. This corresponds with $\text{CO}_2 = 14 \mu\text{M}$ and $\text{HCO}_3^- = 1920 \mu\text{M}$ for oceanic conditions when CO_2 is in equilibrium with the atmosphere ($f\text{CO}_2 = 360 \mu\text{atm}$ at $\text{pH} = 8$).

Materials & methods

Emiliana huxleyi strain Ch 24-90 (morphotype A, isolated from the North Sea, van Bleijswijk et al. 1991; characterised by van Bleijswijk et al. 1994) was adapted to the culture media in dilution cultures under nutrient replete and light saturated conditions. The media contained varying concentrations of HCO_3^- , CO_3^{2-} , CO_2 and H^+ .

In each of four experiments one species in the dissolved inorganic carbon (DIC) system was kept constant while the others varied. The four species are H^+ expressed as pH, CO_3^{2-} , alkalinity and CO_2 . Alkalinity is the titer of the weak bases:

$$\text{Alkalinity} = [\text{HCO}_3^-] + 2*[\text{CO}_3^{2-}] + \text{minor constituents} \quad (2.4),$$

(Dickson 1981). The experiment at constant CO_2 was performed twice, the results are presented as average values. Except in the experiment at constant CO_2 the CO_2 concentrations were $1/8$, $1/4$, $1/2$, $3/4$, 1 and 2 times ambient ($13.8 \mu\text{M}$ or $f\text{CO}_2 = 360 \mu\text{atm}$). In the experiment at constant CO_2 the CO_3^{2-} concentrations were $1/8$, $1/4$, $1/2$, 1, 2 and 4 times ambient ($123 \mu\text{M}$). Dissolved inorganic carbon is the main pH buffer in sea water. However, the conditions in the experiments were chosen in such a way that the pH varied only between 7.5 and 8.5. Over this range Paasche

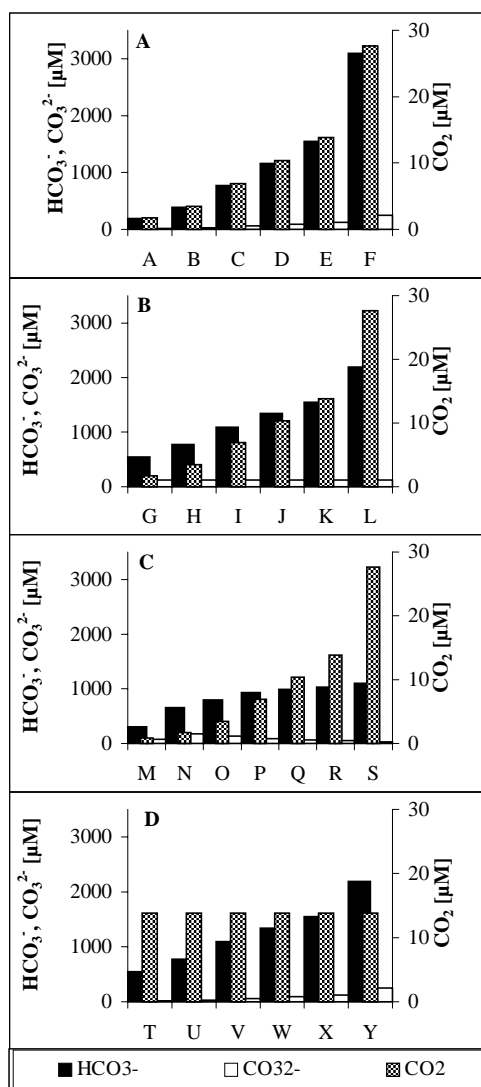


Figure 2.2 Concentrations of dissolved inorganic carbon species in the experiments. Black areas: HCO₃⁻; white areas: CO₃²⁻; grey bars: CO₂. a) At a constant pH of 8.0. b.) At a constant CO₃²⁻ concentration of 123 μM. c) At a constant alkalinity of 1214 μequivalents•L⁻¹ (condition M: 661 μequivalents•L⁻¹). d) At a constant CO₂ concentration of 13.8 μM.

(1964) found no indication of a direct pH effect on carbon uptake by *E. huxleyi*. Speciation of the DIC system was calculated with the dissociation constants of Roy et al. (1993). The calculated concentrations of CO₂, HCO₃⁻ and CO₃²⁻ in each medium are presented in Figure 2.2.

The DIC to be added was calculated as the final DIC concentration - 13.8 μM (the DIC concentration after removal of HCO₃⁻ and CO₃²⁻, see below). Speciation of the DIC system was calculated on the total pH scale (pH_T). The pH was adjusted on the NBS scale (pH_{NBS}). To correct for the residual liquid junction potential across the pH electrode in the dilute NBS buffers 0.05 pH unit was subtracted from the pH_T (Bates 1975).

The medium was based on natural low-nutrient sea water with additions of 250 μM NO₃⁻, 25 μM PO₄³⁻, vitamins according to Paasche (1964) and trace metals according to Guillard (1975). The HCO₃⁻ and CO₃²⁻ were removed by addition of HCl to a concentration of 2.4 mM, and bubbling with air overnight. After that the DIC was adjusted with 0.2 M

NaHCO₃. The pH was adjusted with 0.1 M NaOH. Thus there always was an adequate supply of nutrients except C.

Cells were grown at 15°C in a 16:8 hours light:dark cycle with 300 μmol photons•m⁻²•s⁻¹ of fluorescent light on a rotating shaker at 120 rpm in serum bottles with a small headspace. Cells were precultured in the medium for 3 to 5 days, and were then maintained at about 100,000 cells mL⁻¹, by diluting them 1.5 to 3-fold every day for 5 or 6 consecutive days. Dilutions of the cultures with a low fugacity of CO₂ (fCO₂, which is the partial pressure, corrected for the non-ideal behaviour of the gas mixture (Weiss 1974)) were performed in a glove-bag filled with synthetic air containing either 61 ppm or 162 ppm CO₂. Headspaces of the media and the cultures with an fCO₂ of 360 μatm or 720 μatm were replaced with pressurised air and synthetic air containing 706 ppm CO₂ respectively after each dilution. For the experiment at constant CO₂ the media were bubbled with pressurised air for 16 hours prior to the experiment and for a few minutes after each dilution.

The rates of photosynthetic carbon incorporation and calcification were determined in triplicate with the microdiffusion technique according to Paasche & Brubak (1994) with some adaptations. Briefly, the method entails incubation of the cells with DI^{14}C , then filtering and washing with unlabeled sea water, and then separating the calcite carbon from the organic carbon by dissolving the calcite in H_3PO_4 and trapping the liberated $^{14}\text{CO}_2$ into a filter wetted with NaOH in a closed scintillation vial, and then counting the two fractions separately. The adaptations were that 60 mL of cell suspension was incubated with 37 kBq of $\text{NaH}^{14}\text{CO}_3$ for 24 hours in order to measure over a full light-dark cycle. Incubations were started after the daily dilution at the end of the dark period. Subsamples of 1 mL were used without Carbo-sorb for determining the specific activity of the medium. Cultures were filtered onto 25 mm diameter Whatman GF/F filters. No carrier solution was used, since this was not needed to make the filters adhere to the wall of the scintillation vials. The concentration of the 30 μL of NaOH for trapping the calcite carbon was only 5 M, since 12.5 M NaOH resulted in an unclear solution with the scintillation fluid (Instagel plus). This also gave a full transfer ($96 \pm 1\%$, $n = 3$). After addition of scintillation fluid the samples were stored in the dark for at least 16 hours before counting. Counting efficiency (by channels ratio) was between 80 and 87 %. The average standard deviation for triplicate samples was 21 % for the organic and calcite fractions, and 10 % for the medium. All reported errors are standard deviations. Error bars in the figures are the standard deviations of the numerators.

Cells were counted in triplicate using flow-cytometry. Samples were taken at the end of the dark period, before the ^{14}C incubations, and after 24 hours from cultures run in parallel to the ^{14}C incubations. Samples were preserved by addition of 0.36 % formalin, buffered with 0.2 % hexamine and stored at -20°C . Samples were thawed in tepid water before analysis. The flow-rate was calibrated with 3 μm beads. The average standard deviation for triplicate cell counts was 3.5 %. Specific growth rates were calculated as $\ln(N_{t=24}) - \ln(N_{t=0})$. The ^{14}C incorporation rates were expressed on the basis of the cell numbers at the beginning of the incubations.

Duplicate samples of 45 mL were filtered onto precombusted 11 mm diameter GF/F glass filters at a vacuum of 0.2 bar. Samples were taken from unlabeled incubations run in parallel with the ^{14}C incubations. These were stored in the dark for 4-6 hours following the end of the dark period before sampling. In some experiments these samples were analysed for particulate organic carbon (POC) and particulate organic nitrogen (PON) with a Carlo Erba 1500NA series 2 NCS analyser according to Verardo et al. (1990). In the other experiments these samples were analysed for $\delta\text{PO}^{13}\text{C}$ and $\delta\text{Ca}^{13}\text{CO}_3$. The latter results will be presented in a separate paper.

Calculations of $K_{1/2}$ and V_{max} were performed using a Michaelis-Menten kinetics model:

$$\text{rate} = \frac{[\text{substrate}] * V_{\text{max}}}{[\text{substrate}] + K_{1/2}} \quad (2.5)$$

or Equation 2.7 (see results section). This was preferred over a linearization of the data (such as the one of Lineweaver-Burk), since a direct fit to the model equation gives equal weight to all data points, and allows the calculation of errors for the fitted parameters (J. van der Meer, NIOZ, The Netherlands, pers. comm.).

Results

Constant pH

At a constant pH of 8.0, the increasing concentrations of CO_2 , HCO_3^- and CO_3^{2-} are proportional to each other (Figure 2.2a). The results show that *Emiliania huxleyi* becomes carbon limited over the range of concentrations tested (Figure 2.3a - c). Because the species in

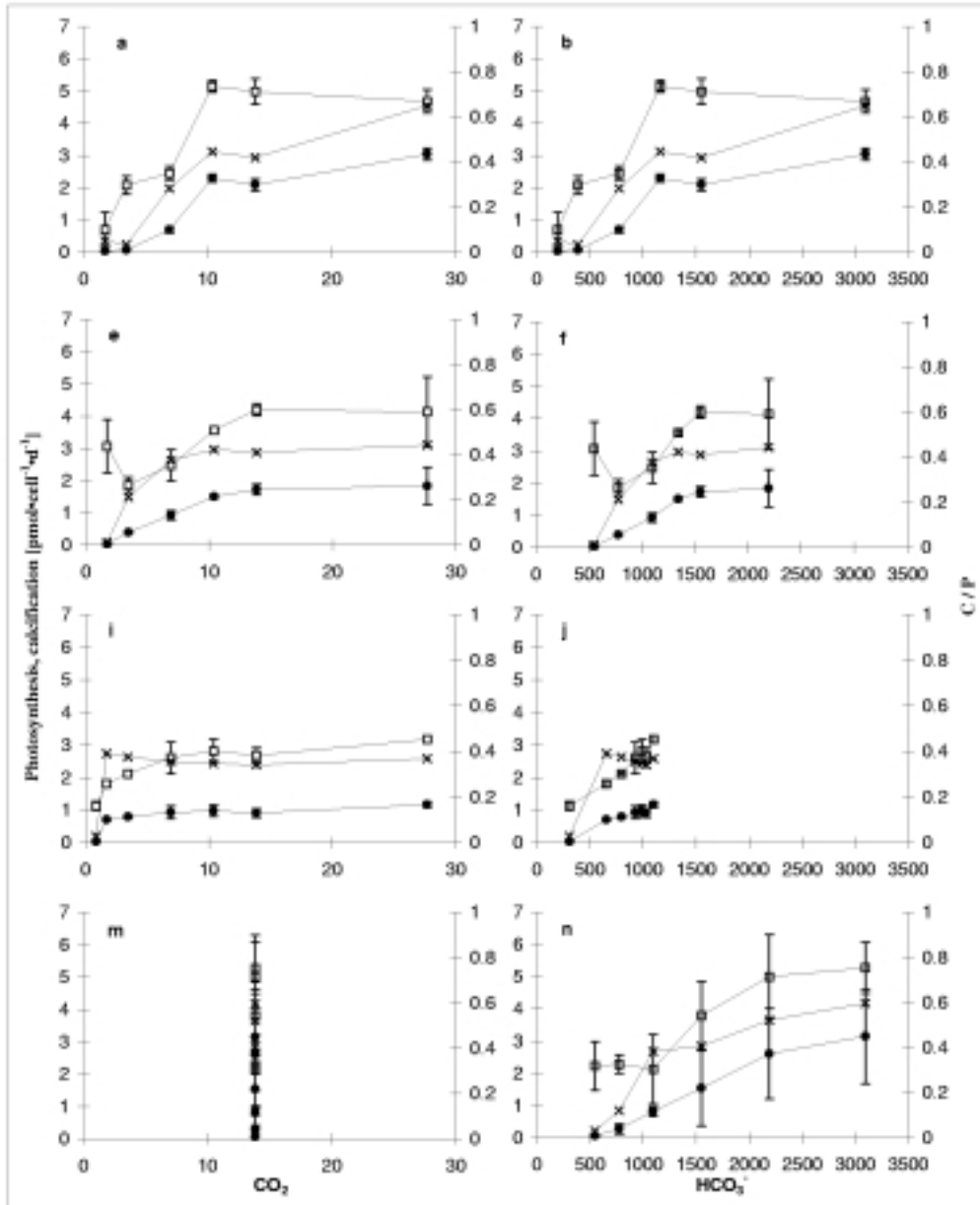


Figure 2.3 Rates of ^{14}C incorporation. Left y-axis: \square photosynthetic rates (P), \bullet calcification rates (C). Right y-axis: \times C/P ratios (calcification / photosynthesis). a - d) At constant pH. e - h) At constant CO_3^{2-} . i - l) At constant alkalinity. m - p) At constant CO_2 . Error bars indicate standard deviations (a - l: $n=3$; m-p: average of two experiments: $n=6$).

the dissolved inorganic carbon (DIC) system are interdependent, it cannot be proven that pH has no direct effect on carbon assimilation. However, the opposite trends with pH that are observed between Figures 2.3h, l and Figure 2.3p shows that at least any effect of pH on the

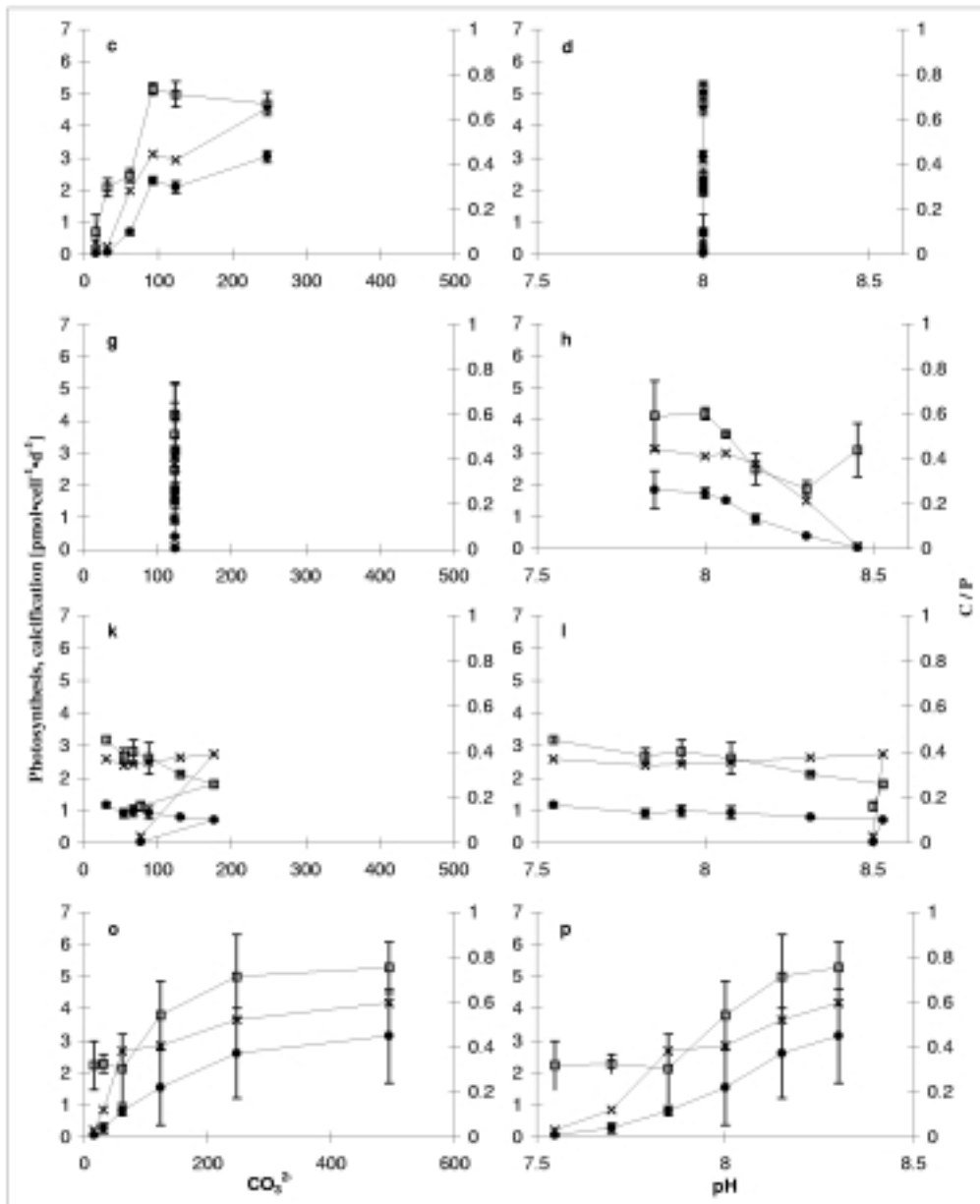


Figure 2.3 Continued.

rates of photosynthesis and calcification is smaller than the effect of the other species, and from here onwards we will assume that pH has no direct effects between 7.5 and 8.5.

Calcification stops at low DIC concentrations, while photosynthesis continues at a reduced rate (Figure 2.3a - c). In fact, calcification does not show the typical saturation curve, in which the initial rate of increase is highest, as is observed for the photosynthetic rates. This does not mean that calcification and photosynthesis compete for inorganic carbon, since it can be calculated from the chemical speciation of the DIC system that calcification increases the

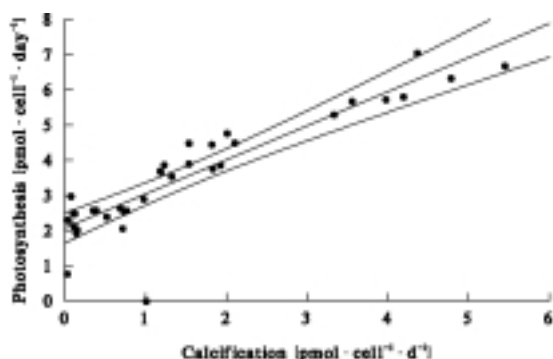


Figure 2.4 Rate of photosynthetic carbon incorporation as a function of calcification rate, fitted by linear regression with 95 % confidence levels shown. Results from the two experiments (12 cultures) at constant CO_2 . For parameter values see text.

availability of CO_2 for photosynthesis. When the rate of photosynthesis is fitted to a Michaelis-Menten kinetics equation the $K_{1/2}$ is $7.5 \pm 4.4 \mu\text{M CO}_2$. However, by fitting photosynthesis to CO_2 alone the increase of photosynthesis with HCO_3^- is ignored (see below).

Constant CO_3^{2-}

At a constant CO_3^{2-} concentration of $123 \mu\text{M}$ and with an increase in DIC, CO_2 increases faster than HCO_3^- (Figure 2.2b). Opposite trends in carbon assimilation rates as a function of CO_3^{2-} are observed between Figure 2.3k and Figures 2.3c, o for both photosynthesis and calcification. This shows that CO_3^{2-} is not the substrate for either photosynthesis or calcification.

Constant alkalinity

At a constant alkalinity of $1214 \mu\text{eq}\cdot\text{L}^{-1}$ and with increasing concentrations of CO_2 and HCO_3^- , the concentration of CO_3^{2-} decreases (conditions N - S in Figure 2.2c). An additional condition was set up in which the concentrations of CO_2 , HCO_3^- and CO_3^{2-} were all lower (condition M in Figure 2.2c, alkalinity = $661 \mu\text{eq}\cdot\text{L}^{-1}$). There is an increase in the calcification rate with HCO_3^- (Figure 2.3j), while there is no trend with CO_3^{2-} (Figure 2.3k). The same increase in the calcification rate with HCO_3^- is observed in the other experiments (Figure 2.3b, f, n, 2.5b). This clearly shows that for *E. huxleyi* HCO_3^- is the substrate for calcification.

Constant CO_2

At a constant CO_2 concentration of $13.8 \mu\text{M}$ and an increase in DIC, the concentration of CO_3^{2-} increases faster than the concentration of HCO_3^- (Figure 2.2d). Photosynthesis increases with HCO_3^- (Figure 2.3n). The increase is proportional to the increase in calcification rate (Figure 2.3n, 2.4). This is consistent with the model for DIC uptake by *E. huxleyi* (Figure 2.1), which would mean that it uses the protons that are generated by calcification to form CO_2 (Equations 2.1 and 2.2), and uses this extra CO_2 for photosynthesis (Equation 2.3). The tight coupling between the production of protons in calcification and the fixation of the generated CO_2 in photosynthesis can be seen from Figure 2.4. The equation for the line is:

$$\text{Photosynthesis} = \text{Calcification} * \text{efficiency} + \text{intercept} \quad (2.6).$$

The efficiency with which the protons are used is 0.97 ± 0.08 , and the extrapolated rate of photosynthesis at a calcification rate of $0 \text{ pmol}\cdot\text{cell}^{-1}\cdot\text{d}^{-1}$ (intercept) is $2.07 \pm 0.17 \text{ pmol}\cdot\text{cell}^{-1}\cdot\text{d}^{-1}$ ($n = 36$).

In this experiment again there was a minimum concentration of HCO_3^- required for calcification. This indicates that CO_2 is not a substrate for calcification, because CO_2 was constantly high at the air-saturated concentration of $13.8 \mu\text{M}$.

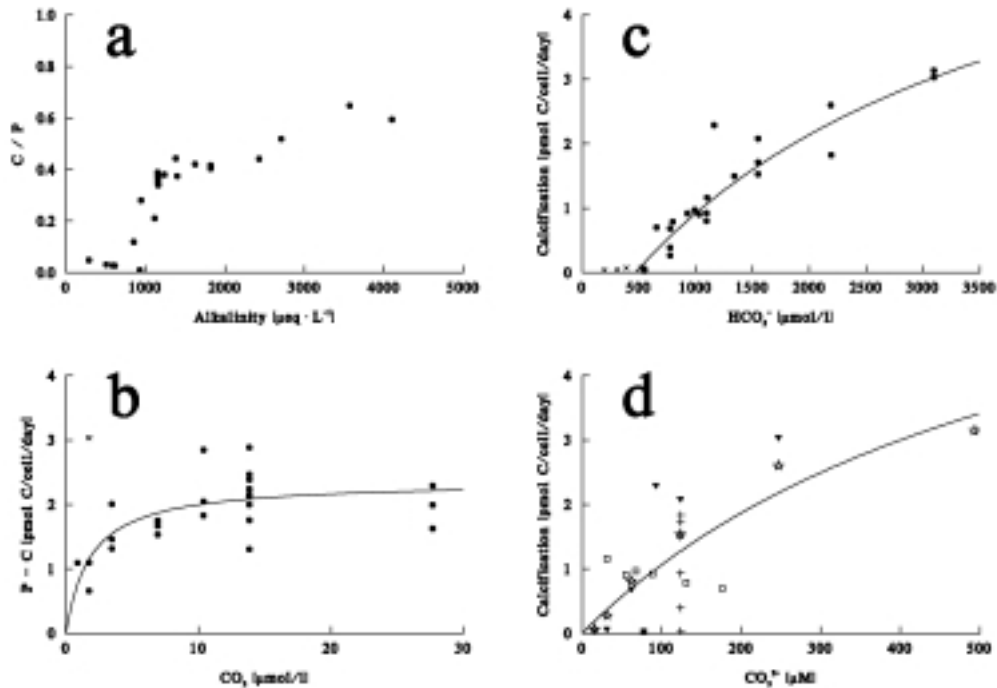


Figure 2.5 a) C/P ratio as a function of alkalinity. b) Part of the photosynthetic rate that is supported by CO_2 from the medium (photosynthesis - calcification) fitted to Michaelis-Menten kinetics Equation 2.5 (excluding condition G at constant carbonate, indicated by x). c) Calcification rate as a function of HCO_3^- fitted to Equation 2.7 (excluding the points below $\text{MIN}_{\text{HCO}_3^-}$, indicated by x). d) Calcification rate as a function of CO_3^{2-} . \blacktriangledown constant pH, \star constant CO_2 , + constant CO_3^{2-} , \square constant alkalinity conditions N-S, \blacksquare 'constant alkalinity' condition M. Curve fitted to Michaelis-Menten kinetics using all data points. For parameter values see text.

C/P and POC/PON ratios

The calcification/photosynthesis ratio (C/P, right-hand scales in Figure 2.3) shows the best correlation with alkalinity (Figure 2.5a). This reflects the fact that at constant CO_2 the C/P ratio increases with HCO_3^- , because the calcification rate increases faster than photosynthesis (Figure 2.3n), and at constant HCO_3^- the C/P ratio decreases with CO_2 (data not shown), because the photosynthetic rate increases with CO_2 while the calcification is not a function of CO_2 . Qualitatively, alkalinity reacts in the same way.

The particulate organic carbon/particulate organic nitrogen (POC/PON) ratios were independent of the concentrations of CO_2 , HCO_3^- and CO_3^{2-} and of pH (data not shown). The average POC/PON ratio was 7.4 ± 1.1 .

Michaelis-Menten kinetics

The CO_2 fixed during photosynthesis originates from two sources. One source is the external CO_2 in the sea water medium, and the other source is the internal CO_2 that is generated by calcification (CO_2^{ex} and CO_2^{in} in Figure 2.1). In the experiment at constant ambient CO_2 the external source was kept constant, and indeed the difference between photosynthesis and calcification was fairly constant as well ($2.0 \pm 0.4 \text{ pmol} \cdot \text{cell}^{-1} \cdot \text{d}^{-1}$). Using this finding we have calculated the rate of photosynthesis that is supported by the external CO_2 as the difference between total photosynthesis and calcification. We have

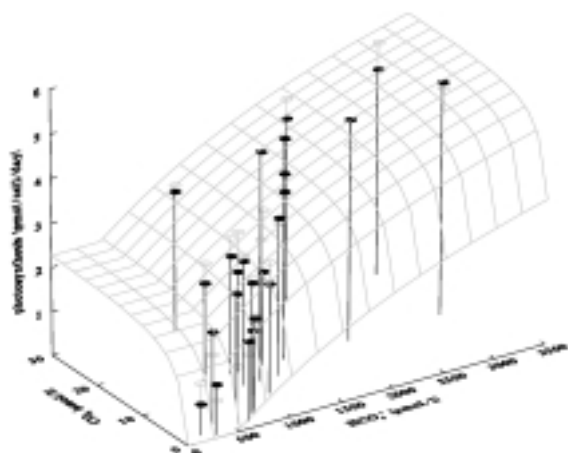


Figure 2.6 Photosynthetic rates as a function of CO_2 and HCO_3^- . The plotted 3-D function is the sum of the functions plotted in Figure 2.5a and b. Filled circles represent experimental data points, open circles represent the corresponding calculated photosynthetic rates, that lie on the surface of the function. Please note that below $[\text{HCO}_3^-] = 506 \mu\text{M}$ the calcification rate is zero, and photosynthesis depends solely on CO_2 .

plotted this part of the photosynthesis as a function of the external concentration of CO_2 . Fitting a Michaelis-Menten kinetics curve through these data gives a $K_{1/2}$ of $1.9 \pm 0.5 \mu\text{M CO}_2$, and a V_{max} of $2.4 \pm 0.1 \text{ pmol}\cdot\text{cell}^{-1}\cdot\text{d}^{-1}$ (Figure 2.5b). At low HCO_3^- concentrations the calcification stopped. This was seen both in the measurements of the calcification rates (Figure 2.5c) and in the side scatter characteristics of the cells in the flow-cytometer (data not shown). The calcification rate was independent of the carbonate concentration (Figure 2.3c, k, o), indicating that undersaturation of the sea water medium with respect to calcite was not the determining factor in preventing calcification. Therefore, the calcification rate was fitted to a modified Michaelis-Menten equation in which a minimum HCO_3^- concentration for calcification was included:

$$\text{calcification rate} = \frac{([\text{HCO}_3^-] - \text{MIN}_{\text{HCO}_3^-}) \cdot V_{\text{max}}}{([\text{HCO}_3^-] - \text{MIN}_{\text{HCO}_3^-}) + K_m} \quad (2.7)$$

The results of this fit are $\text{MIN}_{\text{HCO}_3^-} = 506 \pm 74 \mu\text{M}$, $K_m = 2750 \pm 1328 \mu\text{M}$ and $V_{\text{max}} = 6.4 \pm 1.8 \text{ pmol}\cdot\text{cell}^{-1}\cdot\text{d}^{-1}$. The HCO_3^- concentration at which half of V_{max} is reached $K_{1/2} = K_m + \text{MIN}_{\text{HCO}_3^-} = 3256 \mu\text{M}$.

Despite the fact that the calcification rate was not dependent on the carbonate concentration, it was possible to fit the results to a Michaelis-Menten kinetics curve with a V_{max} of $6.6 \pm 1.7 \text{ pmol}\cdot\text{cell}^{-1}\cdot\text{d}^{-1}$ and a $K_{1/2}$ of $488 \pm 179 \mu\text{M}$ (Figure 2.5d). This fortuitous result is caused by the partial correlation between HCO_3^- and CO_3^{2-} , as is explained in the discussion.

Combining the calculated rates of photosynthesis on both the external CO_2 in the sea water and the internal CO_2 generated from HCO_3^- by calcification gives the total rate of photosynthesis as a function of both CO_2 and HCO_3^- (Figure 2.6).

Specific growth rates

The specific growth rate (μ) was a function of both CO_2 and HCO_3^- (Figure 2.7a, b). Growth rate was approximately half maximal both at low CO_2 and at low HCO_3^- , indicating that both substrates contributed about equally to the growth rate. We were unable to get a meaningful fit for the separate contributions of the two substrates. This was caused in the first place by a lack of data on the separate contributions of photosynthesis and calcification to the growth rate. A fit with separate $K_{1/2}$'s and μ_{max} 's for CO_2 and HCO_3^- gave a negative

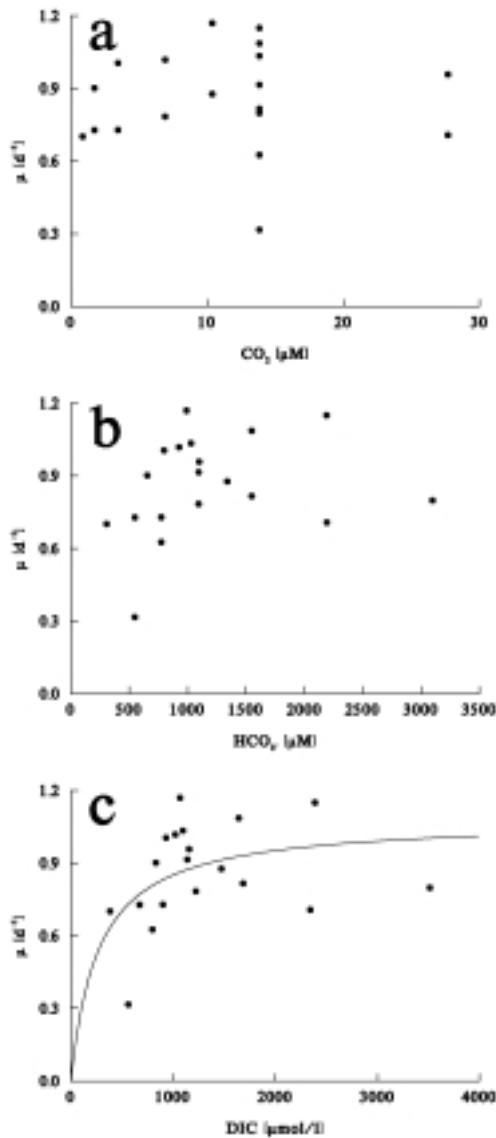


Figure 2.7 Specific growth rates (μ) as a function of a) CO_2 , b) HCO_3^- , c) dissolved inorganic carbon (DIC). Results of the experiments at constant CO_3^{2-} , constant alkalinity and constant CO_2 . The fitted curve is likely to be dependent on the experimental procedure, and does not reflect the physiology of this strain of *Emiliania huxleyi* (see text for details).

contribution of HCO_3^- . Fitting the data to the DIC concentration gave a $\mu_{max} = 1.1 \pm 0.1 d^{-1}$ and a $K_{1/2} = 270 \pm 169 \mu M$ (Figure 2.7c), however, as noted for the fit of the photosynthetic rate as a function of CO_2 (or DIC) at constant pH, this result is likely to be influenced by the average ratio of CO_2 to HCO_3^- in the experiments.

Discussion

The described experiments under saturation of light and all nutrients except C, confirm that calcification enhances photosynthetic carbon uptake, presumably through intracellular formation of CO_2 . The $K_{1/2}$ of photosynthesis that was reported by Raven & Johnston (1991) based on data of Paasche (1964) was $9 \mu M CO_2$. This was calculated from experiments conducted at constant pH, and therefore incorporates the increase in photosynthesis due to all inorganic carbon species and not just CO_2 . If we follow the same method of calculation we arrive at a similar $K_{1/2}$ of $7.5 \pm 4.4 \mu M CO_2$.

The present set of experiments in the dissolved inorganic carbon (DIC) system indicates that the $K_{1/2}$ for photosynthesis that is calculated in this way depends on both CO_2^{ex} and HCO_3^- . Thus, the calculated $K_{1/2}$ does not describe the dependence of photosynthetic carbon fixation on the CO_2 concentration, but also depends on the pH at which the experiment is performed. By separating the contributions of CO_2 and HCO_3^- we found a $K_{1/2}$ of $1.9 \mu M$ for CO_2 , and a $K_{1/2}$ of $3256 \mu M$ for HCO_3^- .

The published half-saturating CO_2 concentrations ($K_{1/2}$) for other algae (e.g. Table 1 in Raven & Johnston 1991) may also be subject to the reinterpretation that is presented here for *Emiliania huxleyi*. When the influence of CO_2 has not been separated from the influence of the other parameters of the DIC system, then the published $K_{1/2}$'s will incorporate these influences for those algae that do not solely use CO_2 . Thus these $K_{1/2}$'s will depend on the experimental setup that was used to determine them. The experiments described here can also be used as an alternate procedure for determining whether algae can use HCO_3^- (or CO_3^{2-}), which may be preferable to using extremely high pH or estimating diffusive fluxes of CO_2 towards the cell.

The fact that the $K_{1/2}$ for HCO_3^- is much higher than the $K_{1/2}$ for CO_2 can be partially explained by the lower pH inside the cell, which reduces the intracellular abundance of HCO_3^- relative to CO_2 . However, at a pH change across the cell membrane from 8 to 7 (Brownlee et al. 1995), the relative abundances change by a factor 10 only as opposed to the ratio in the $K_{1/2}$'s of 1687. Apparently there is a large difference in affinity between CO_2 and HCO_3^- . The difference in affinity by a factor of 169 is subject to some uncertainty since the $K_{1/2}$ for HCO_3^- is poorly constrained. The reason for this is that, because of the narrow pH range that was chosen (see materials and methods), the HCO_3^- concentrations did not become high enough to observe the level part of the Michaelis-Menten curve that defines V_{\max} . We can show the extent of this uncertainty by recalculating $K_{1/2}$ under the assumption that calcification is saturated at the highest HCO_3^- concentration of 3096 μM . Refitting the data with a V_{\max} of 3.1 $\text{pmol}\cdot\text{cell}^{-1}\cdot\text{d}^{-1}$ we calculated a $\text{MIN}_{\text{HCO}_3^-} = 576 \pm 35 \mu\text{M}$ and $K_m = 724 \pm 84 \mu\text{M}$. This gives a $K_{1/2}$ of 1300 μM , which is still a factor 674 higher than the $K_{1/2}$ for CO_2 . Thus, the affinity of the cell for CO_2 appears to be at least 67 times larger than the affinity for HCO_3^- .

Calcification stops below a certain HCO_3^- concentration (Figure 2.5b). Below this $\text{MIN}_{\text{HCO}_3^-}$ the cells are apparently unable to realise a concentration product of Ca^{2+} and CO_3^{2-} above the saturation point within the coccolith forming vesicle. Calcification did not depend on the CO_3^{2-} concentration in the medium, so we can tentatively conclude that the pH in the coccolith forming vesicle depends on the transport of HCO_3^- across the cell membrane. Brownlee et al. (1995) measured the cytosolic pH of *E. huxleyi*, and found an increase from 6.3 to 7.0 upon addition of DIC to DIC-starved cells. They suggested that HCO_3^- may act as an intra-cellular pH buffer. In the coccolith-forming vesicles the HCO_3^- may buffer the acidic polysaccharides that control the precipitation of calcite.

In the experiments at constant CO_3^{2-} and constant alkalinity it was shown that HCO_3^- and not CO_3^{2-} is the substrate for calcification (Figure 2.3f, g, j, k). This confirms the results of Paasche (1964), and shows that calcification in the plant *E. huxleyi* is different from that in the animal foraminifera (cf. Spero et al. 1997).

Despite the fact that HCO_3^- is the substrate for calcification, there still was a positive correlation between the calcification rate and CO_3^{2-} (Figure 2.5c) because there was a bias in the experiments towards a correlation of HCO_3^- and CO_3^{2-} . This bias is caused by the speciation of the DIC system. At constant pH the concentrations of HCO_3^- and CO_2 both increase 16-fold (Figure 2.2a). At constant CO_2 the concentration of CO_3^{2-} increases 16-fold as the HCO_3^- concentration increases 4-fold (Figure 2.2d). Accordingly the calcification rate increases with the CO_3^{2-} concentration (Figure 2.5c, \blacktriangledown constant pH, \star constant CO_2). At constant alkalinity the CO_3^{2-} concentration increases 6-fold as the HCO_3^- concentration decreases 1.6-fold (Figure 2.2c). The concomitant decrease in calcification rate can be traced in Figure 2.5c (\square constant alkalinity), but due to the small change in calcification rate this has little influence on the fit to Michaelis-Menten kinetics. This is an example of the complex equilibria within the DIC system, and it shows that conclusions about the influence of either the DIC system on C use or of C use on the DIC system need to be addressed with due caution.

As mentioned in the results section, photosynthesis in *E. huxleyi* is proposed to depend on two sources of CO_2 : an external CO_2 source in the sea water medium, and an internal CO_2 source that is generated by calcification. In the experiment at constant CO_2 the external source was constant, and indeed the difference between photosynthesis and calcification was fairly constant. By plotting the remainder (the photosynthesis that is fixed from the internal source) against the calcification rate, it can be calculated that the CO_2 that is generated by calcification is used with an efficiency of 0.97 ± 0.08 (Figure 2.4). Since *E. huxleyi* was grown on NO_3^- , and NO_3^- constitutes a H^+ sink for the cell (or OH^- source, Brewer and Goldman 1976), the maximum expected efficiency is only 0.88 (at an average POC/PON ratio of 7.4). The latter

consideration also indicates that the V_{\max} , but not $K_{1/2}$, of photosynthesis on external CO_2 (Figure 2.5a) may be dependent on the nitrogen source.

The ratio of calcification versus photosynthesis (C/P in Figure 2.3) was between 0 and 1 under all conditions tested for this strain. This means that at nutrient saturated growth there is no increase in CO_2 concentration associated with the decrease in alkalinity due to calcification, and no liberation of gaseous CO_2 from the sea water. Thus, in contrast with recent suggestions (Crawford and Purdie 1997, and references therein), during the nutrient-saturated productive phase of blooms of *E. huxleyi* no increase in $f\text{CO}_2$ is to be expected. Only during the transient nutrient limited phase a C/P ratio of greater than 1 is likely to occur (Paasche 1998), with a short-lived increase in $f\text{CO}_2$, as was observed during a mesocosm study (Purdie & Finch 1994). In fact, from our results the expected decrease in $f\text{CO}_2$ is stronger than that which is expected from a C/P ratio of 1, which is often used as the standard ratio. This extra decrease in $f\text{CO}_2$ is due to the photosynthetic use of CO_2 from the sea water medium, next to the use of HCO_3^- in both photosynthesis and calcification.

It might be expected that the calcification rate would have increased at low CO_2 concentrations to generate more CO_2 for photosynthesis, but this was not found. The energy requirement of calcification should not be a factor in our experiments, since *E. huxleyi* was grown at nutrient and light saturation. Apparently, the calcification rate is only dependent on the HCO_3^- concentration and is not regulated by the CO_2 concentration. Regulation does not seem to be required, because *E. huxleyi* was able to use all the extra CO_2 that was generated under all conditions that were tested. The apparently optimal efficiency with which the protons, that are generated by calcification, are used in photosynthesis gives some indication that this is the major physiological reason, in the evolutionary sense, for *E. huxleyi* to calcify. More specifically, we suggest that the unique feature of *E. huxleyi* among coccolithophorids to continue calcification after a complete coccosphere is formed makes it possible to optimise the use of dissolved inorganic carbon. This may be the reason that it is the most successful coccolithophorid species. Whether the highly organised form in which CaCO_3 is precipitated and the incorporation of the coccoliths into a coccosphere constitute additional advantages for *E. huxleyi* (Young 1994), falls outside the scope of this study.

In this study it was shown that calcification allows *E. huxleyi* to efficiently use both HCO_3^- and CO_2 in photosynthesis (Figure 2.6). This is also reflected in the dependence of the specific growth rate (μ) on both HCO_3^- and CO_2 (Figure 2.7a, b). However, unlike μ , the rate of photosynthesis is not saturated with HCO_3^- up to a concentration of 3500 μM . This is a rather puzzling result since the cells were adapted to the media for at least five divisions, and unbalanced growth seems rather unlikely after that time. Cells do produce DOC at high light conditions (W. Stolte, NIOZ, pers. comm.), but this cannot be the explanation because the rate of photosynthesis was based on ^{14}C incorporation into the particulate fraction. Moreover, the photosynthetic rate per cell was based on the same cell counts that were used to calculate the growth rates.

The conspicuous presence of *E. huxleyi* as blooms in the upper mixed layer of the temperate zones of the oceans, and as coccoliths in sediments throughout the greater part of the oceans is rather surprising in view of its relatively low μ_{\max} of 1.1 d^{-1} . We have already mentioned the inconsistency between an increase in photosynthetic rates while μ is saturated with inorganic carbon. This may be a pointer towards a surplus of cell resources which may stimulate the efficient use of other resources such as PO_4^{3-} and Zn^{2+} .

Acknowledgements

We would like to thank Santiago Gonzalez for performing the POC/PON analyses. We would like to thank E. Paasche, J. Raven, V. Schoemann, K. Timmermans and an anonymous reviewer for their helpful criticism of the manuscript. This is NIOZ publication nr. 3320.

Chapter 3: Zn^{2+} - HCO_3^- colimitation of *Emiliana huxleyi* (Prymnesiophyceae).

Erik T. Buitenhuis, Klaas R. Timmermans, Hein J. W. de Baar.

Abstract

In analogy to the iron-hypothesis, the Zn-hypothesis has been put forward, which states that Zn may limit primary production and therefore influence the global carbon cycle. The proposed mechanism is that photosynthesis would be carbon limited due to a lack of the cofactor Zn in carbonic anhydrase. We have determined the $K_{1/2}$ for growth of *Emiliana huxleyi* at 19 ± 8 pM Zn^{2+} and a minimum requirement of 9 ± 3 pM. The lowest Zn^{2+} concentration in the North Pacific is about 2 pM, showing that Zn-limitation may indeed occur. From our results with additions of both EDTA and ZnCl_2 we conclude that EDTA is not detrimental for *E. huxleyi* up to a concentration of 200 μM .

In the current model for inorganic carbon use by *E. huxleyi* carbonic anhydrase is present in the chloroplast to generate CO_2 from HCO_3^- at the site where it is fixed by Rubisco (Ribulose biphosphate carboxylase oxygenase). The H^+ that is required in this reaction is produced in calcification. From this it can be expected that carbonic anhydrase affects the use of HCO_3^- in photosynthesis. We have tested this by growing *E. huxleyi* under Zn^{2+} - HCO_3^- colimitation. The results are partly inconsistent with the model. The experiment was conducted at a constant high concentration of CO_2 , but at low Zn^{2+} the efficiency with which CO_2 was used also decreases. This shows that Zn^{2+} and possibly carbonic anhydrase activity are needed for CO_2 fixation also. In accordance with the model, it was found that Zn^{2+} affects the efficiency of HCO_3^- -use by *E. huxleyi*.

Key words: calcification to photosynthesis coupling; coccolithophorid; EDTA; *Emiliana huxleyi*; Haptophyta, HCO_3^- (bicarbonate); Zinc limitation.

Abbreviations: CA, carbonic anhydrase; EDTA, ethylene-diamine-tetra-acetic-acid; μ , specific growth rate; POC, particulate organic carbon.

Introduction

Emiliana huxleyi is an interesting alga for studying use of inorganic carbon, since it produces both particulate organic carbon (POC) in photosynthesis and particulate inorganic carbon as CaCO_3 in calcification. Moreover, it is a cosmopolitan algae, that has been suggested to be the most productive coccolithophorid (Westbroek et al. 1985). Paasche (1962) suggested that calcification and photosynthesis are coupled in a manner equivalent to the symbiosis of corals and their associated algae. Later, it was confirmed that there is a direct link between calcification and photosynthesis. Due to this link HCO_3^- , which is about 100-fold more abundant than CO_2 , can be used as a substrate for photosynthesis (Nimer et al. 1995, Buitenhuis et al. 1999).

It was found that the efficiency with which calcification stimulates the part of photosynthesis that is supported by HCO_3^- is 0.97 ± 0.08 (Buitenhuis et al. 1999). In the results section we calculate that the uncatalyzed conversion rate of HCO_3^- to CO_2 is not fast enough to support this coupling between calcification and photosynthesis. Indeed, it has previously been shown that during logarithmic growth *E. huxleyi* synthesizes carbonic anhydrase in the chloroplast only (Nimer 1994a).

Since Zn^{2+} is the cofactor of carbonic anhydrase it can be expected that under Zn^{2+} limitation the coupling between calcification and photosynthesis, which permits the direct use

of HCO₃⁻ in photosynthesis, becomes less efficient. Zn²⁺ plays a role in a great number of cellular processes (Faústro da Silva & Williams 1991), thus there is potential for ascribing effects of Zn²⁺ limitation to the lack of carbonic anhydrase while in fact another cellular process is responsible for this effect. We consider that the risk of such a misinterpretation is limited, firstly because it was found that in a diatom most of the cellular Zn²⁺ was contained in carbonic anhydrase (Morel et al. 1994), and secondly, and more importantly, we have attempted to specifically address the role of carbonic anhydrase by growing *E. huxleyi* under Zn²⁺-HCO₃⁻ colimitation, in order to distinguish between general effects of Zn²⁺-limitation and those effects that are linked to inorganic carbon use.

When carbonic anhydrase is present in the chloroplast, where it can facilitate the use of HCO₃⁻ in photosynthesis (Nimer et al. 1995), but not as a cell membrane associated enzyme, where it has been reported to facilitate the uptake of CO₂ in other microalgae (Price & Badger 1989), then the effect of Zn²⁺ on the use of dissolved inorganic carbon (DIC) could be limited to the efficiency with which HCO₃⁻ is used in photosynthesis. Therefore we varied the concentration of HCO₃⁻ at a constant CO₂ concentration in the Zn-C colimitation experiments. Given the speciation of DIC in sea water this choice resulted in the increase of pH and CO₃²⁻ in the medium concomitant with the increase of HCO₃⁻. It was previously shown that over the range we have used there was no measurable effect of these two parameters on carbon fixation in *E. huxleyi* (Buitenhuis et al. 1999).

Zn²⁺ concentrations can get as low as 2 pM in the North Pacific Ocean (Bruland 1989). Since optimum Zn²⁺ concentrations for oceanic microalgae are often higher than that, Morel et al. (1994) have proposed that Zn²⁺ may limit carbon fixation in the open ocean, and thus affect the efficiency of the biological carbon pump.

In this study we have only measured the effect of Zn²⁺ and Zn²⁺-HCO₃⁻ colimitation on the specific growth rate. Thus we were not able to reach detailed conclusions about the function of carbonic anhydrase, but have reviewed to what extent our results are consistent with the current model of inorganic carbon use by *E. huxleyi*.

Materials & methods

Medium was prepared from low nutrient seawater. The concentration of trace metals was further reduced by addition of 50 µM MnO₂. After 24 h. with stirring the water was filtered over two connected filters of 0.2 µm and 0.07 µm pore size. To this we added 250 µM NO₃⁻, 25 µM PO₄³⁻, vitamins according to Paasche (1964) and 50 nM FeCl₂. The concentration of Zn²⁺ at which *E. huxleyi* becomes Zn-limited was found to lie in the low pM range (Figure 3.1). Since it was impossible to directly produce medium with such low concentrations, the availability of Zn was reduced by the addition of the metal ion chelator EDTA. Since the Zn-EDTA complex is not available to the algae, the available concentration of Zn²⁺ can be reduced to concentrations in the low pM range with the total Zn concentration (Zn_T) in the low nM range by addition of up to 200 µM EDTA. All handling was done in a laminar flow hood.

In order to test for the possible detrimental effect of EDTA on growth, the concentration of Zn²⁺ was controlled by addition of EDTA and in some cases also ZnCl₂. The concentration of EDTA was between 6 and 300 µM. The total concentration of Zn (Zn_T) was between 4 and 200 nM. No Co was added to the cultures. Co was not measured, but in medium that was prepared in the same way Co_T was 4 to 7 nM (A. Daniel, U. of Liverpool, pers. comm.). Since Co is complexed by EDTA 40 times more efficiently than Zn, there was little Co²⁺ available relative to Zn²⁺. Cells were grown in 30 to 1000 ml acid cleaned (1 M HCl) polycarbonate square bottles. The final dilution of the inoculum was at least 10,000 fold from a culture with high trace metal concentrations (~600 nM Zn_T). The C speciation was not controlled in the

Table 3.1 HCO_3^- to CO_2 conversion in the chloroplast. Rate of uncatalyzed conversion from HCO_3^- to CO_2 , and minimum Zn^{2+} concentration as cofactor in carbonic anhydrase (CA) required for catalyzed conversion.

		Uncatalyzed			CA catalyzed
H^+_i [M]	α	$1.3\text{E}-8^{\text{A}}$	pH _i		7.9^{A}
HCO_3^- [M]	β	$5.0\text{E}-4^{\text{B}}$	k_{cat} (pH) [s^{-1}]	η	$3.6\text{E}+4^{\text{E}}$
k_{-1} [s^{-1}]	γ	$1.2\text{E}+4^{\text{C}}$	K_m [M]	θ	$3.0\text{E}-2^{\text{F}}$
$V_{\text{chloroplast}}$ [$\text{l}\cdot\text{cell}^{-1}$]	δ	$1.4\text{E}-14^{\text{D}}$	calcification rate [$\text{mol}\cdot\text{cell}^{-1}\cdot\text{day}^{-1}$]	ι	$1.8\text{E}-12^{\text{G}}$
Light period [$\text{s}\cdot(16\text{h.})^{-1}$]	ϵ	$5.8\text{E}4$	cells [l^{-1}]	κ	$1.0\text{E}+8^{\text{H}}$
$\text{HCO}_3^- \rightarrow \text{CO}_2$ $\alpha*\beta*\gamma$ [M s^{-1}]	ζ	$7.4\text{E}-8$	CA required $\iota*(\beta+\theta)(\theta*\beta)^{-1}* \epsilon^{-1}$ [$\text{mol}\cdot\text{cell}^{-1}$]	λ	$5.3\text{E}-20$
CO_2 generation $\delta*\epsilon*\zeta$ [$\text{mol}\cdot\text{cell}^{-1}\cdot\text{day}^{-1}$]		$6.0\text{E}-17$	Zn^{2+} in CA $\kappa*\lambda$ [M]		$5.3\text{E}-12$

^A Anning et al. 1996, ^B Brownlee et al. 1995, determined in whole cells, ^C Wolf-Gladrow & Riebesell 1997, ^D estimated from van der Wal et al. 1985, ^E Graham et al. 1984, ^F Pocker & Bjorkquist 1977, ^G Buitenhuis et al. 1999, ^H this study.

Zn^{2+} limitation experiment, but at an alkalinity of about 2540 $\mu\text{eq/kg}$ and a typical $f\text{CO}_2$ in the laboratory of around 500 μatm , concentrations of 2161 μM HCO_3^- and 19 μM CO_2 can be calculated.

In the experiment with varying HCO_3^- concentrations at constant CO_2 the alkalinity was lowered by addition of 10 M HCl (quartz distilled, Zn_T undetectable) or increased by addition of 1 M NaHCO_3 (129 nM Zn_T , no significant change in Zn_T). The CO_2 concentration was manipulated by bubbling overnight at 15 °C with air from a gas cylinder with a slightly elevated CO_2 content corresponding to an $f\text{CO}_2$ of 444.6 μatm before the start of the experiment. The alkalinity of the medium was calculated from DIC and $f\text{CO}_2$ with the dissociation constants of Roy et al. (1993), using a program by Lewis & Wallace (<http://cdiac.esd.ornl.gov/oceans/co2rprt.html>). DIC was determined according to DOE (1994), $f\text{CO}_2$ in the gas cylinder was calculated from the gas mixing ratio $x\text{CO}_2$ according to Weiss (1974). $x\text{CO}_2$ was determined as described in Buitenhuis et al. (1996).

Cells were counted as described in Buitenhuis et al. (1999) starting after 3 days of adaptation to the medium over a 4 to 12 day period.

Specific growth rates (μ) were calculated as the slope of $\ln(\text{cell counts})$ against time (in days).

Curve fitting of the growth rates to Eqs. 3.1 and 3.2 was done as described in Buitenhuis et al. (1999).

Results

Conversion of $\text{HCO}_3^- \rightarrow \text{CO}_2$

In the second column of Table 3.1 we have calculated the rate of uncatalyzed conversion of HCO_3^- into CO_2 in the chloroplast. This is small relative to the calcification rate (Table 3.1). As calcification was found to be tightly coupled to photosynthetic use of HCO_3^- (Buitenhuis et al. 1999), this must mean that the conversion is catalyzed by carbonic anhydrase (CA). In the fourth column of Table 3.1 we have calculated the amount of CA that is needed for enzyme catalyzed conversion. Since CA contains one atom of Zn^{2+} as a cofactor this directly gives the minimum cellular Zn^{2+} requirement in carbonic anhydrase, which at a maximum cell density in our experiments of $\sim 10^8$ cells ml^{-1} gives a minimum concentration in the medium of 5 pM, disregarding other cellular requirements for Zn^{2+} .

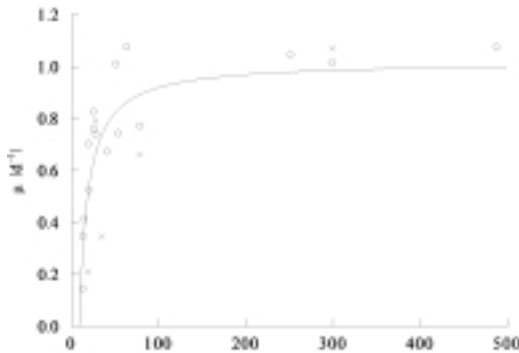


Figure 3.1 Growth rate as a function of Zn²⁺. Circles represent measurements made at a constant Zn_T concentration (either 3.7 or 10.0 nM), crosses represent measurements at a constant EDTA concentration (200 μM). See text for fitted equation (Equation 3.1) and parameter values.

Zn²⁺ limitation

The Zn²⁺ requirement of *Emiliania huxleyi* was determined. At the highest EDTA concentration (300 μM) growth rates increased after addition of either ZnCl₂ or CoCl₂ (data not shown). This confirmed that the cells were limited by Zn²⁺, and that Zn²⁺ can be replaced by Co²⁺ (cf. Sunda & Huntsman 1995). In Figure 3.1 it can be seen that the growth rate as a function of Zn²⁺ can be described by the modified Michaelis-Menten equation:

$$\mu = \frac{([Zn^{2+}] - [Zn^{2+}_{min}]) * \mu_{max}}{[Zn^{2+}] - [Zn^{2+}_{min}] + K_m} \quad (3.1)$$

Fitting the data to this function gives $[Zn^{2+}_{min}] = 9 \pm 3$ pM, $\mu_{max} = 1.03 \pm 0.07$ d⁻¹ and $K_{1/2} = K_m + [Zn^{2+}_{min}] = 19 \pm 8$ pM. There is no systematic difference between growth rates obtained at low Zn_T and low EDTA concentrations and the same Zn²⁺ concentrations at high Zn_T and high EDTA. This showed that EDTA was not poisonous to the cells up to a concentration of 200 μM. 6 pM Co²⁺ gave a half-maximum growth rate (0.51 d⁻¹) when Zn²⁺ was below the minimum required by *E. huxleyi*.

Zn²⁺-HCO₃⁻ colimitation

We first tested whether Zn²⁺ and HCO₃⁻ were dependent nutrients, for which colimitation occurs, or whether they are independent, in which case the law of the minimum would apply. At two Zn²⁺ concentrations the growth rate was determined as a function of the HCO₃⁻ concentration. Figure 3.2 clearly shows that the Zn²⁺ concentration affects the ability of the cells to use HCO₃⁻, and thus that these are dependent nutrients.

To quantify this colimitation we have determined the growth rate as a function of both Zn²⁺ and HCO₃⁻ (Figure 3.3). The positive growth rates were fitted to the function:

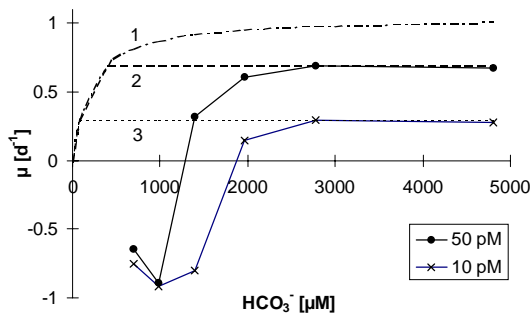


Figure 3.2 Growth rate as a function of HCO₃⁻ at 10 (×) and 50 (●) pM Zn²⁺. Zn²⁺ decreases 5% with the increasing HCO₃⁻, due to a change in Zn speciation with pH. Curve 1 from Buitenhuis et al. (1999) at saturated Zn²⁺. Curves 2 & 3 predicted by the law of the minimum, adjusted to the maximum growth rates measured at the two Zn²⁺ concentrations.

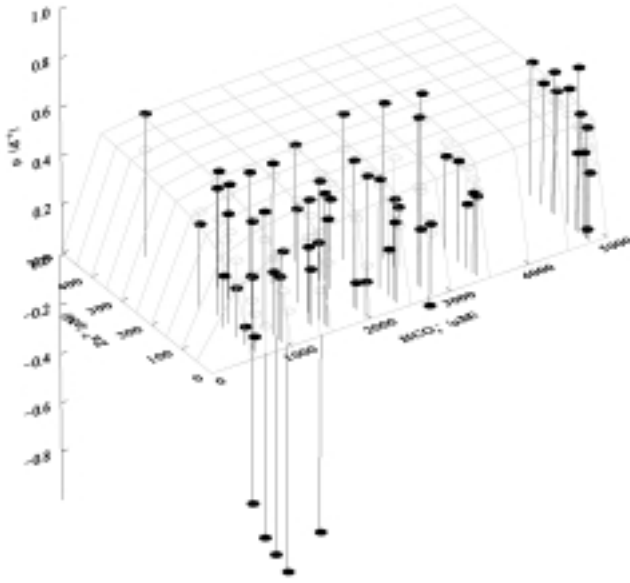


Figure 3.3 Growth rate as a function of HCO_3^- and Zn^{2+} . Filled circles represent experimental data points. Open circles represent the corresponding calculated photosynthetic rates, calculated from Eq. 3.2. See text for equation and parameter values.

$$\mu = \frac{[\text{HCO}_3^-] * \mu_{\max}}{[\text{HCO}_3^-] + ([\text{Zn}^{2+}] + K_m) / [\text{Zn}^{2+}]} \quad (3.2).$$

Our choice of this equation to fit the results is presented in the discussion. The parameter values for Equation 3.2 are: $\mu_{\max} = 0.46 \pm 0.03 \text{ d}^{-1}$ and $K_m = 27761 \pm 12940$.

Discussion

In order to test for the possible detrimental effect of EDTA (Muggli & Harrison, 1996), the Zn^{2+} concentration was manipulated either by addition of EDTA or by addition of ZnCl_2 at a high EDTA concentration (200 μM). In Figure 3.1 it can be seen that there is no significant difference between growth rates measured at high EDTA concentrations and high Zn_T concentrations and at low EDTA concentrations and low Zn_T concentrations, corresponding to the same Zn^{2+} . We therefore conclude that the reduced growth rates measured by Muggli & Harrison (1996) was caused by limitation of growth by the availability of Zn^{2+} , which varied in their experiments. In fact, they measured a growth rate at 16 pM Zn^{2+} which was 47% of that at 251 pM Zn^{2+} , which is almost in perfect agreement with our $K_{1/2}$ of 19 pM Zn^{2+} . Their interpretation of the detrimental effect of EDTA was possibly suggested by the results of Sunda & Huntsman (1992) that the Zn^{2+} requirement of *Emiliania huxleyi* is extremely low. This was subsequently shown to be due to the presence of Co^{2+} in the medium, which can replace Zn^{2+} (Sunda & Huntsman 1995). Both Muggli & Harrison (1996) and we used low Co^{2+} concentrations (see Materials & Methods). Given our finding that EDTA has no direct poisonous effect on *E. huxleyi* the advantage of using EDTA is that it buffers the Zn^{2+} concentration, so that it remains constant in solution as the algae grow and use Zn^{2+} . This made it possible to simplify the experimental approach to a batch culture and still get cells that were adapted to a specific Zn^{2+} concentration (see Materials & Methods).

We discuss our results in relation to Zn^{2+} , although it is possible that the cells react to Zn' (inorganically complexed Zn). However, we find good agreement between the experimentally determined minimum requirement of 9 pM dissolved Zn^{2+} in the modified Michaelis-Menten kinetics (Equation 3.1) and the calculated 5 pM particulate Zn^{2+} required in carbonic anhydrase

(Table 3.1). This is in agreement with the finding of Morel et al. (1994) that most of the cellular Zn is present in carbonic anhydrase.

According to the model of C use by *E. huxleyi* Zn²⁺ is directly involved in the C metabolism, that is, in its ability to use HCO₃⁻ in photosynthesis. This led us to suspect that, unlike all other tested combinations of nutrient limitations (Droop 1983, Zonneveld 1996), Zn and C might be dependent nutrients where the law of the minimum would not apply, but rather some form of synergy would occur. In Figure 3.2 it is shown that this is indeed the case. Curves 1-3 in Figure 3.2 show the theoretical growth curves that are predicted by the law of the minimum. Curve 1 represents Zn-saturated growth. At low Zn²⁺ concentrations the law of the minimum predicts that the growth rate would be C limited at the low HCO₃⁻ concentrations, which would give the same results for the two Zn²⁺ concentrations. Then at higher HCO₃⁻ concentrations the cells would become Zn limited. At 10 pM Zn²⁺ the changeover from C to Zn limitation should have occurred at a lower HCO₃⁻ concentration than at 50 pM Zn²⁺. After that the growth rate would remain constant at the Zn limited rate. This theoretical case is illustrated by curves 2 and 3 in Figure 3.2. The data in Figure 3.2 show no such abrupt change. Instead the affinity for HCO₃⁻ is affected by Zn²⁺ with a Michaelis-Menten type saturation curve for both Zn²⁺ concentrations. Moreover, the growth rates become negative at low HCO₃⁻ concentrations in both cases, which was not observed for C limitation at Zn saturated conditions (Buitenhuis et al. 1999).

Colimitation of two nutrients may be expressed in several ways. We have compared four possibilities:

a) multiplication of two Michaelis-Menten type saturation curves:

$$\mu = \frac{[\text{HCO}_3^-]}{[\text{HCO}_3^-] + K_{m,\text{HCO}_3^-}} * \frac{[\text{Zn}^{2+}]}{[\text{Zn}^{2+}] + K_{m,\text{Zn}^{2+}}} * \mu_{\max} \quad (3.3),$$

b) the minimum of two Michaelis-Menten type saturation curves:

$$\mu = \text{MIN} \left(\frac{[\text{HCO}_3^-] * \mu_{\max}}{[\text{HCO}_3^-] + K_{m,\text{HCO}_3^-}}, \frac{[\text{Zn}^{2+}] * \mu_{\max}}{[\text{Zn}^{2+}] + K_{m,\text{Zn}^{2+}}} \right) \quad (3.4),$$

c) μ_{\max} depends on Zn²⁺ at a constant affinity (α) for HCO₃⁻ ($\alpha = \mu_{\max}/K_m$):

$$\mu = \frac{[\text{HCO}_3^-] * [\text{Zn}^{2+}] * \mu_{\max} / ([\text{Zn}^{2+}] + K_{m,\text{Zn}^{2+}})}{[\text{HCO}_3^-] + [\text{Zn}^{2+}] * \mu_{\max} / ([\text{Zn}^{2+}] + K_{m,\text{Zn}^{2+}}) / \alpha_{\text{HCO}_3^-}} \quad (3.5),$$

d) affinity for HCO₃⁻ depends on Zn²⁺:

$$\mu = \frac{[\text{HCO}_3^-] * \mu_{\max}}{[\text{HCO}_3^-] + ([\text{Zn}^{2+}] + K_m) / [\text{Zn}^{2+}]} \quad (3.2).$$

From Figure 3.4 it can be seen that a μ -S₁-S₂ curve is not a good way to decide between these options, especially between a) to c). With a modelling approach, using measured cell quota for nutrients, it has been shown that for those cases where data are available option b) describes the data better than option a) (Zonneveld 1996). We expect the situation to be different from these reviewed cases for Zn²⁺-HCO₃⁻ colimitation. This is because in the current hypothesis on the carbon use of *E. huxleyi*, Zn²⁺ is directly involved in carbon acquisition as a cofactor of

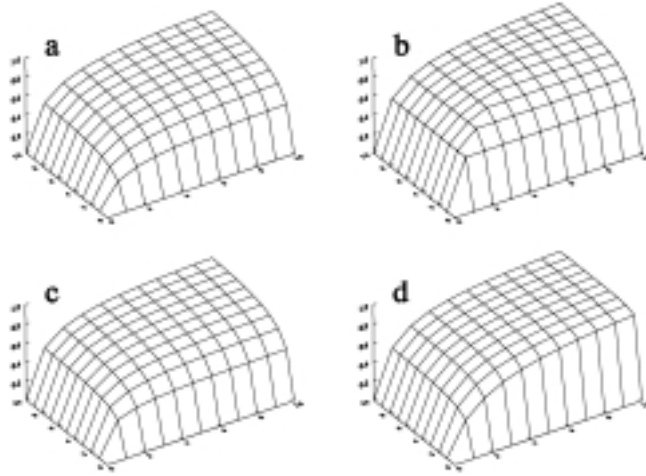


Figure 3.4 Four possible ways to express the dependence of growth rate on two nutrients.

a) Multiplication of limitations. b) Law of the minimum. c) Variable μ_{\max} , constant affinity. d) Variable affinity, constant μ_{\max} . See text for a description of these cases.

carbonic anhydrase (Figure 3.5). Therefore, we expect Zn^{2+} to affect the affinity for HCO_3^- , and we have chosen to fit our data to Equation 3.2 (option d). More data are needed to decide whether this provisional conclusion is correct.

From the hypothesis of carbon use by *E. huxleyi* shown in Figure 3.5 it is expected that:

- 1) the efficiency of HCO_3^- use in photosynthesis declines with Zn^{2+} , whereas
- 2) the use of CO_2 in photosynthesis should be unaffected.

To 1) Figure 3.3 shows that at a high Zn^{2+} concentration the specific growth rate decreases with HCO_3^- , and this decrease is more pronounced at a low Zn^{2+} concentration. We suggest three possible explanations for this effect of Zn^{2+} :

- a) The simplest explanation is that Zn^{2+} is involved in the use of HCO_3^- . This is consistent with the hypothesis presented in Figure 3.5, in which Zn^{2+} acts as the cofactor of carbonic anhydrase. In this case Zn^{2+} increases the efficiency with which HCO_3^- is converted to CO_2 , which is the substrate for Rubisco.
- b) Zn^{2+} and HCO_3^- can partly replace each other in maintaining intracellular pH within the range needed for cell survival. It has been shown that HCO_3^- affects the cytoplasmic pH, from which it was concluded that the intracellular speciation of DIC acts as a pH buffer (Nimer et al. 1994b). Carbonic anhydrase would be needed to keep this pH buffer functioning at low HCO_3^- concentrations if the flux of HCO_3^- into the cell is much higher than the uncatalysed equilibration of intracellular DIC. The rate of uncatalysed equilibration would be 10 times faster in the more acidic cytosol (pH 6.9, Anning et al. 1996) This would still mean that this rate is slow compared to the rate of HCO_3^- use. However, since no carbonic anhydrase was found in the cytosol (Nimer et al. 1994a) this doesn't appear to be a good explanation.
- c) The cells produce more carbonic anhydrase at low concentrations of HCO_3^- , and the Zn^{2+} in this enzyme competes with the other sites where Zn^{2+} is used in the cell, and thus leads to an indirect Zn^{2+} limitation at low HCO_3^- . This explanation seems to be directed against survival of the cell when they could grow on CO_2 only, but since HCO_3^- never becomes low enough in the sea for this problem to occur it might still be functional.

To 2) In Figure 3.3 it can be seen that at low Zn^{2+} and low HCO_3^- the cells die (negative μ), even though the CO_2 concentration is constantly high at 17 μM . This shows that Zn^{2+} is needed for use of CO_2 . This seems surprising since CO_2 is the direct substrate for Rubisco. This lends some credibility to explanations b) and c) above, in which there are other effects of Zn^{2+} limitation in addition to the reduced efficiency of HCO_3^- use. It is important to note that the negative growth rates cannot be explained by just Zn^{2+} limitation, since they only become

apparent at low HCO₃⁻ concentrations. Neither is it just a lack of HCO₃⁻, since cells can perform photosynthesis using CO₂ at HCO₃⁻ concentrations where calcification stops (Buitenhuis et al. 1999). An alternative explanation from b) and c) that accounts for this colimitation, and inability to use CO₂, would be conversion of CO₂ into HCO₃⁻ at the cell membrane, transportation of HCO₃⁻ to the chloroplast, and conversion of HCO₃⁻ into CO₂ at the site of fixation by Rubisco. This relatively convoluted mechanism could possibly function to prevent diffusive loss of inorganic carbon, since the charged HCO₃⁻ ion can be retained in the cell, while CO₂ diffuses through the cell membrane. Again, with carbonic anhydrase measured only in the chloroplast under normal conditions (Nimer et al. 1994a) the experimental evidence for this mechanism is lacking.

In summary, we have shown that there is a variable cellular requirement for Zn²⁺ that is a function of the HCO₃⁻ concentration, and thus any explanation that is forwarded concerning the Zn requirement must focus on the C physiology, including pH regulation. We conclude that while the presented results are in large part in agreement with the current model for C use by *E. huxleyi* (Figure 3.5), the picture is not complete, and more experimental evidence (such as rates of photosynthesis and calcification and discrimination against ¹³C in the organic and inorganic fractions both at constant CO₂ and at constant HCO₃⁻) will be needed to resolve the problem we have outlined here.

Acknowledgements

We would like to thank Patrick Laan for technical assistance, Loes Gerringa for help with MINEQL, Ulf Riebesell for help with the reaction kinetics, and Patrick Laan and Loes Gerringa for helpful comments on the manuscript. KRT and HJWdB acknowledge the support from the European Commission's Marine Science and Technology Program (MAST III) under contract MAS3-CT95-0005 (MERLIM). This is NIOZ publication nr. 3407.

Chapter 4: Trends in inorganic and organic carbon in a bloom of *Emiliana huxleyi* in the North Sea.

Erik Buitenhuis, Judith van Bleijswijk, Dorothee Bakker, Marcel Veldhuis.

Marine Ecology Progress Series (1996) **143** (1-3) 271-282

Abstract

During a survey of the end phase of an *Emiliana huxleyi* bloom in the northern part of the North Sea we measured total inorganic carbon (TIC) and the fugacity of CO₂ (fCO₂), as well as standing stocks of CaCO₃ and particulate organic carbon (POC). Production of CaCO₃ by *E. huxleyi* resulted in an immediate increase of fCO₂, but led to a long-term decrease in fCO₂. Observations during a surface survey and at 24-hours stations showed a large increase of fCO₂ with the standing stock of CaCO₃. The immediate increase of fCO₂ is caused by a shift in the chemical equilibria in the inorganic carbon system when alkalinity decreases relative to dissolved inorganic carbon (DIC). Average fCO₂ in the high reflectance area (with high numbers of detached coccoliths) was lower than average fCO₂ in the reference areas, located outside the *E. huxleyi* bloom. The long-term decrease in fCO₂ is due to an enhanced sedimentation of both organic and inorganic carbon in faecal pellets containing heavy calcite. This enhanced sedimentation is reflected in the vertical gradient of TIC between the surface mixed layer and the aphotic zone, which increased from the POC-rich zone to the CaCO₃ maximum. The overall effect of production, air-sea exchange, mineralisation and sedimentation was a decrease of fCO₂ due to a net transport of carbon to below the pycnocline. We tentatively calculate an atmospheric carbon sink of 1.3 mol•m⁻² for this bloom of *E. huxleyi*.

Key words: TIC, fCO₂, CaCO₃, POC, algal bloom, coccolithophorid.

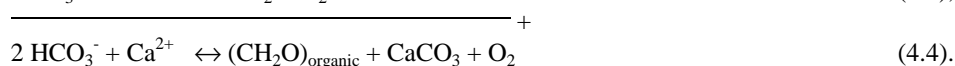
Introduction

Emiliana huxleyi (Lohmann) Hay and Mohler is a coccolithophorid of the class of Prymnesiophyta. It is a unicellular alga that produces organic carbon through photosynthesis and inorganic carbon through coccolithogenesis. The coccoliths of *E. huxleyi* are oval platelets which are formed intracellularly by precipitation of CaCO₃ in a coccolith vesicle (Westbroek et al. 1989). After completion they are transported out of the cell and retained on the cell surface.

Massive blooms of this species are a regular (yearly) phenomenon, especially in the temperate regions. Surface waters with spectral signatures similar to that of *E. huxleyi* blooms annually covered an average of 1.4 *10⁶ km² (Brown and Yoder, 1994). *E. huxleyi* may influence global climate by three mechanisms. i) By affecting the inorganic carbon system of the sea water. ii) By altering the heat exchange between the sea water and the atmosphere, due to increased light scattering by detached coccoliths. iii) By contributing to emissions of dimethylsulphide (DMS), which increases cloud albedo. In this paper we focus mainly on the first mechanism and to some extent on the second.

All algae contain the enzyme ribulose biphosphate carboxylase oxygenase (Rubisco). Rubisco fixes CO₂ into organic carbon (Equation 4.1), which decreases the CO₂ concentration in the sea water. Besides organic carbon, *E. huxleyi* also produces CaCO₃ (Equation 4.2). Production of CaCO₃ generates CO₂ intracellularly (Equation 4.3). The ratio between the production of organic carbon and CaCO₃ determines the net effect on the CO₂ concentration in the sea water. Production of organic carbon and CaCO₃ in a ratio of 1:1 (Equation 4.4) results in a small decrease of the CO₂ concentration. This decrease is caused by the buffering effect of sea water: removal of bicarbonate is partially compensated for by hydration of CO₂. The concentration of CO₂ remains constant if the ratio is 1:1.2. Higher ratios result in elevated CO₂

concentrations.



Laboratory experiments have shown that the ratio between organic carbon and CaCO_3 production is affected by the growth conditions of *E. huxleyi*. CaCO_3 production has been observed to exceed photosynthesis when cells are limited by phosphate (van Bleijswijk et al. 1994a, Paasche & Brubak 1994). Such a situation may occur at the end of a bloom.

In the field the situation is complicated by the variability of environmental factors. Furthermore sedimentation may play an important role in the field, whereas it cannot be measured in the laboratory. Therefore no a priori conclusions can be drawn with respect to the effect of *E. huxleyi* blooms on the CO_2 concentration of surface waters. In order to resolve this question we have measured the concentrations and standing stocks of carbon (fCO_2 , TIC, CaCO_3 , POC) in various stages of a bloom of *E. huxleyi* in the summer of 1993 in the North Sea. We derive a carbon budget for the development of the bloom (in time) based on the various stages of the bloom encountered on a transect from the edge to the centre of the bloom (in space).

The fugacity of CO_2 (fCO_2) is proportional to the chemical activity (μ) of CO_2 in air (equivalent to the activity of a dissolved ion). fCO_2 is about 0.5% lower than the partial pressure of CO_2 (pCO_2 , equivalent to the concentration of a dissolved ion). Total inorganic carbon (TIC) is the sum of dissolved inorganic carbon (DIC) and CaCO_3 . Calcium carbonate (CaCO_3) is precipitated by *E. huxleyi* into coccoliths in the mineral form calcite (Young et al. 1991). Particulate organic carbon (POC) here designates the organic carbon in algae, calculated from flow cytometer data. Alkalinity is the excess of strong cations over strong anions or the amount of acid needed to titrate the weak bases to their protonated forms. Alkalinity was calculated from DIC and fCO_2 .

Materials & methods

During a cruise in the northern part of the North Sea (Figure 4.1a) from 28 June until 12 July 1993 total inorganic carbon (TIC), the fugacity of CO_2 (fCO_2), standing stocks of CaCO_3 and particulate organic carbon (POC) (see Table 4.1) were measured on board the research vessel Pelagia. For TIC, fCO_2 , and CaCO_3 both discrete samples at CTD stations and on-line measurements, when the ship was sailing, were taken. For POC only discrete samples were taken.

Sampling

Discrete samples were taken from a CTD rosette sampler (Neil Brown) equipped with 10.5 l NOEX bottles. Samples were not poisoned; they were stored in the dark and analysed shortly after sampling. Discrete samples for TIC were taken in gas tight bags made of Mailar (aluminium foil coated with plastic) fitted with gastight tubing (Masterflex 6542-24). TIC was measured within 2 hours after sampling. Discrete samples for fCO_2 were taken in 1100 ml bottles of dark glass, which were flushed with 3 volumes of sea water. The fCO_2 was measured within an hour after sampling.

On-line samples for TIC were taken at approximately 10 minute intervals from a 10 l debubbling tank. This tank was flushed with water from the aqua flow system (flow approximately $8 \text{ l} \cdot \text{min}^{-1}$) which took in water at a depth of approximately 3 m at the bow of the

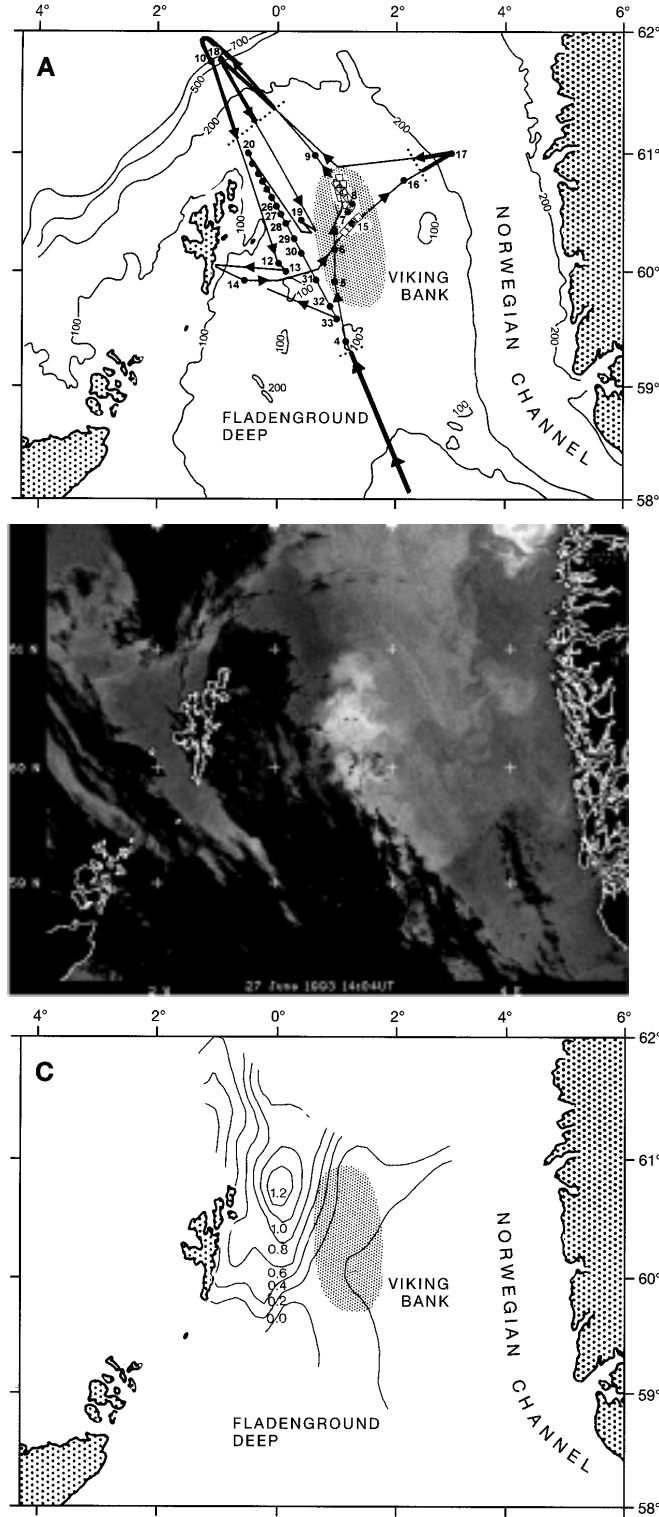


Figure 4.1 The research area. a) cruise track (from 28 June until 12 July) with the station numbers. Station 19N and 19S are represented by a single dot. Station numbers 20 to 33 are referred to as the transect. Shaded area indicates the average position of the high reflectance area between 27 June and 13 July. Open squares: on-line data in the high reflectance area. Bold lines: on-line data in the reference areas. b) AVHRR photograph of the investigated area on 27 June 1993. The high reflectance area can be recognised as a light spot between The Shetlands and Norway. Dark spots are cloud cover. c) Contour plot of the fluorescence (arbitrary units) at 3 m depth in the investigated area.

Table 4.1 Parameters that are mentioned in this paper.

Parameter	Abbreviation	Unit	Description
Alkalinity		$\mu\text{equivalents}\cdot\text{kg}^{-1}$	$2 * [\text{CO}_3^{2-}] + [\text{HCO}_3^-] + [\text{B}(\text{OH})_4^-] + [\text{OH}^-] - [\text{H}^+]$ etc.
Calcite	CaCO_3	$\mu\text{mol}\cdot\text{l}^{-1}$	Particulate Ca ($> 0.8 \mu\text{m}$)
Chlorophyll <i>a</i>		$\mu\text{g}\cdot\text{l}^{-1}$	Measured fluometrically or with the HPLC
Dissolved inorganic carbon	DIC	$\mu\text{mol}\cdot\text{kg}^{-1}$	$[\text{HCO}_3^-] + [\text{CO}_3^{2-}] + [\text{CO}_2]$
Fugacity of CO_2	$f\text{CO}_2$	μatm	Activity of CO_2 gas in water
Mole fraction of CO_2	$x\text{CO}_2$	ppm	Gas mixing ratio [$\mu\text{mol}\cdot\text{mol}^{-1}$]
Particulate organic carbon	POC	$\mu\text{mol}\cdot\text{l}^{-1}$	Phytoplankton carbon (flowcytometer)
Total inorganic carbon	TIC	$\mu\text{mol}\cdot\text{kg}^{-1}$	$[\text{HCO}_3^-] + [\text{CO}_3^{2-}] + [\text{CO}_2] + \text{CaCO}_3$

ship. On-line samples for $f\text{CO}_2$ were taken directly from the aqua flow system. Water temperature, salinity, fluorescence and atmospheric pressure were logged automatically at one minute intervals.

Total inorganic carbon

Total inorganic carbon (TIC) was measured with an automated coulometer (DOE 1991). Measurements were calibrated with standard water obtained from A. G. Dickson (Scripps institution of oceanography, USA). The extraction efficiency as determined with this standard water was 99.3%. The standard deviation was $8 \mu\text{mol}\cdot\text{kg}^{-1}$ ($n=19$). This relatively large standard deviation was probably caused by variation between titration cells (A. A. J. Majoor, pers. comm., NIOZ, The Netherlands), which were not calibrated separately. All measurements at a station were performed with the same cell, probably leading to less variation.

Fugacity of CO_2

The mole fraction of CO_2 ($x\text{CO}_2$) in air equilibrated with sea water was measured with an IRGA (infra-red gas analyser, Licor 6252). The instrument resembles the underway system described by Wanninkhof & Thoning (1993), with three improvements (design by M. H. C. Stoll and J. M. J. Hoppema, NIOZ, The Netherlands): (i) The $x\text{CO}_2$ is measured in non-flowing gas to guarantee that measurements are taken at atmospheric pressure and to obtain a stable signal. Typical standard deviation of ten measurements was 0.05 ppm. (ii) During equilibration the gas is circulated through both the sample cell and the equilibrator. This prevents the flow of unequilibrated air into the system which Wanninkhof & Thoning (1993) mention as a possible source of error. (iii) Measurements were performed in dry gas to circumvent the need for water vapour correction, and to facilitate comparison between samples and calibration gases.

The IRGA was calibrated every hour with three mixtures of CO_2 in synthetic air. The raw data were fitted by a second order function. The polynomial function supplied by the manufacturer gives less reproducible results for $x\text{CO}_2$, because the zero and span settings vary with changes in pressure and temperature (F. A. Koning, pers. comm., NIOZ, The Netherlands).

The three calibration gases were calibrated on a gas chromatograph (GC) against three standards of the NMI (Dutch bureau of standards). Similarly, a calibration gas of NOAA (national oceanographic and atmospheric administration, USA) was measured on the GC. The difference between the measured value based on the NMI calibration and the value given by NOAA was + 1.3 ppm. The reproducibility of the IRGA, calculated as the standard deviation of air samples ($n = 133$), was 1.2 ppm.

Discrete samples for $x\text{CO}_2$ were measured in bottles of dark glass after equilibration of 1 l sea water with 100 ml laboratory air plus the volume of air in the instrument. On-line samples were taken by equilibrating a circulated flow of air with a continuous flow of sea water from the aqua flow system (approximately $2 \text{ l} \cdot \text{min}^{-1}$) in an equilibrator equipped with a calibrated temperature sensor. The design of the equilibrator was adopted from A. Watson (Robertson et al. 1993). Every hour we measured 10 samples from the sea water equilibrator and one sample of air, taken at about 15 m above the sea surface.

For the discrete samples, fugacity of CO_2 ($f\text{CO}_2$) was calculated using $x\text{CO}_2$, the temperature measured by the CTD and the ambient pressure (Weiss 1974). This calculated $f\text{CO}_2$ was higher than the *in situ* $f\text{CO}_2$ due to warming of the samples. We estimate an increase of less than $10 \mu\text{atm}$. for surface samples and less than $60 \mu\text{atm}$. for samples taken at 125 m.

For the on-line samples, $f\text{CO}_2$ in the equilibrator was calculated using the temperature in the equilibrator and the ambient pressure. $f\text{CO}_2$ at the *in situ* temperature was calculated from TIC and alkalinity according to Goyet et al. (1993). The use of TIC instead of DIC introduced an error smaller than $0.1 \mu\text{atm}$. TIC at the time of measurement of $f\text{CO}_2$ was obtained by linear interpolation. Alkalinity was calculated using TIC and $f\text{CO}_2$ in the equilibrator.

Dissolved inorganic carbon and alkalinity

Dissolved inorganic carbon (DIC) was calculated by subtracting CaCO_3 from TIC. Alkalinity was calculated from DIC and $f\text{CO}_2$, using the dissociation constants of Goyet and Poisson (1989). The uncertainty in alkalinity due to the standard deviation of $8 \mu\text{mol} \cdot \text{kg}^{-1}$ in TIC is about $10 \mu\text{eq} \cdot \text{kg}^{-1}$. The uncertainty due to the standard deviation of 1.2 ppm in $f\text{CO}_2$ is about $1 \mu\text{eq} \cdot \text{kg}^{-1}$.

Standing stock of CaCO_3

Particulate calcium ($>0.8 \mu\text{m}$) standing stock was determined according to van Bleijswijk et al. (1994b) using atomic absorption spectroscopy. The reproducibility of the measurements (average standard deviation of duplicates) was 6 %. The CaCO_3 standing stock was calculated from particulate calcium by assuming a 1:1 Ca:C molar ratio in coccoliths (K. M. Fagerbakke, pers. comm., University of Bergen, Norway).

Dissolution of CaCO_3

The dissolution rate of CaCO_3 was determined by incubating 5 l of sea water in the dark. Duplicate samples were taken in the dark from single 10.5 l NOEX bottles. Samples were incubated unfiltered or after filtration over $10 \mu\text{m}$ and $200 \mu\text{m}$ filters to remove micro and mesozooplankton respectively. Samples were incubated in a sea water tank on deck of the ship. Subsamples were taken after 0, 24 and 48 or 72 hours, until the bottles were empty. Three series of subsamples in which a decrease in CaCO_3 alternated with an increase were discarded. Apparently the bottles had not been shaken sufficiently to resuspend the coccoliths and algae before taking one of the subsamples.

Saturation of sea water with CaCO_3

The concentration of calcium ($[\text{Ca}^{2+}]$) was measured by atomic absorption spectroscopy. The concentration of carbonate ($[\text{CO}_3^{2-}]$) was calculated from DIC and $f\text{CO}_2$, using the dissociation constants of Goyet and Poisson (1989). The extent of oversaturation of CaCO_3 in sea water was calculated according to Mucci (1983).

Particulate organic carbon

Particulate organic carbon (POC) standing stock of the phytoplankton was calculated from cell numbers and estimated spherical diameters (ESDs), as determined by flow cytometry (Veldhuis 1995). ESD was calibrated with standard beads (high density $2.0 \mu\text{m}$ and $10.0 \mu\text{m}$,

Coulter Counter), and checked by fractionated filtration and microscopical observations. ESDs were used to estimate cell volumes (assuming spherical cells), that were converted to carbon. For cyanobacteria a constant factor of $400 \text{ fg C} \cdot \mu\text{m}^{-3}$ was used (Takahashi et al. 1985). For pico-eukaryotes a factor of 1800 to $3000 \text{ fg} \cdot \text{cell}^{-1}$ was used, depending on size (Campbell & Vaultot 1993). For larger cells the formula $\log C = -0.422 + 0.758 * \log V$ was used (Strathmann 1967). Detritus was not included.

Results

Research area

Before the start of the cruise the research area was located by AVHRR (advanced very high resolution radiometry). An area with high reflectance was observed in the North Sea. During the cruise it was located east of the Shetland Islands (Figure 4.1b). The high reflectance area could be recognised from the ship as a milky white colouring of the sea. It was characterised by low nutrient concentrations (NO_3^- and $\text{PO}_4^{3-} < 0.1 \mu\text{M}$), low particulate organic carbon ($\approx 4 \mu\text{M POC}$), low numbers of living *Emiliania huxleyi* ($\approx 2000 \text{ ml}^{-1}$) and high numbers of detached coccoliths ($\approx 100,000 \text{ ml}^{-1}$). These conditions are typical for the end phase of a bloom of *E. huxleyi*. Small cyanobacteria ($\approx 100,000 \text{ ml}^{-1}$) contributed about 50 % to POC.

To the northwest of the high reflectance area we observed a POC-rich zone (cf. Figure 4.1c). This zone was characterised by high nutrient concentrations ($4 \mu\text{M NO}_3^-$, $0.3 \mu\text{M PO}_4^{3-}$) and a high standing stock of POC ($\approx 30 \mu\text{M}$). A mixed phytoplankton community was present, with *E. huxleyi* ($\approx 3500 \text{ ml}^{-1}$) constituting about 40 % of POC.

In the Atlantic Ocean and to the east and south of the high reflectance area nutrient concentrations ($0.1 - 6 \mu\text{M NO}_3^-$ and $0.1 - 0.4 \mu\text{M PO}_4^{3-}$) and POC ($2 - 15 \mu\text{M}$) were variable. In these areas, which we will call the reference areas (Figure 4.1a), the numbers of *E. huxleyi* cells ($\approx 2000 \text{ ml}^{-1}$) and detached coccoliths ($\approx 16,000 \text{ ml}^{-1}$) were low.

On-line measurements

Total inorganic carbon (TIC; Table 4.1) averaged at $2048 \pm 31 \mu\text{mol} \cdot \text{kg}^{-1}$ ($n = 172$) in the high reflectance area, and at $2058 \pm 31 \mu\text{mol} \cdot \text{kg}^{-1}$ ($n = 182$) in the reference areas. TIC varied between 1970 and $2110 \mu\text{mol} \cdot \text{kg}^{-1}$ in both areas. The fugacity of carbon dioxide ($f\text{CO}_2$) in the high reflectance area was $303 \pm 24 \mu\text{atm}$ on average ($n = 464$, ranging from 257 to $440 \mu\text{atm}$). In the reference areas $f\text{CO}_2$ was $324 \pm 29 \mu\text{atm}$ on average ($n = 416$, ranging from 227 to $421 \mu\text{atm}$).

Apparently the two regions, that show large differences in detached coccoliths, do not show significant differences in average TIC and $f\text{CO}_2$. However, we found a positive correlation between $f\text{CO}_2$ and on-line CaCO_3 standing stock measured at the same time (Figure 4.2; $f\text{CO}_2 [\mu\text{atm}] = 259.7 + 3.5 * \text{CaCO}_3 [\mu\text{M}]$, $n = 94$, $p < 0.05$). When $f\text{CO}_2$ was corrected to a constant temperature of $10.6 \text{ }^\circ\text{C}$ it increased slightly less with CaCO_3 ($f\text{CO}_2\text{-corr.} [\mu\text{atm}] = 260.0 + 3.0 * \text{CaCO}_3 [\mu\text{M}]$, $n = 94$, $p < 0.05$). We also observed a positive correlation between temperature and CaCO_3 standing stock ($T [^\circ\text{C}] = 10.6 + 0.03 * \text{CaCO}_3 [\mu\text{M}]$, $n = 94$, $p < 0.02$). Ackleson et al. (1988) and Holligan et al. (1993) found a much larger temperature difference between CaCO_3 rich and CaCO_3 poor waters.

The mole fraction of CO_2 ($x\text{CO}_2$) in dry air was $358.8 \pm 1.2 \text{ ppm}$. ($n = 133$) during the first week of the cruise. The same average $x\text{CO}_2$ was presented in Boden (1994) for June 1993 north of 35° N (357.6 ± 3.7 , $n=8$, excluding the data of the industry-influenced Waldhof station). $f\text{CO}_2$ in the air, at a pressure of $1.013 * 10^5 \text{ Pa}$ and an average water temperature of $11.6 \text{ }^\circ\text{C}$, was $357.5 \mu\text{atm}$.

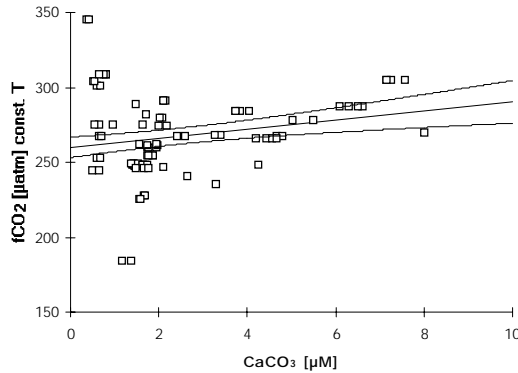


Figure 4.2 Plot of $f\text{CO}_2$, corrected to a constant temperature of $10.6\text{ }^\circ\text{C}$, versus CaCO_3 . Linear regression with 95 % confidence levels, $f\text{CO}_2 = 260.0 + 3.0 * \text{CaCO}_3$, $n = 94$, $p < 0.05$.

24-hours stations

At four 24-hours stations (stations 12, 19N, 19S and 15; Figure 4.1a) we measured several vertical profiles of TIC, $f\text{CO}_2$, CaCO_3 and POC over a 24 hours period. The position of the ship was maintained in relation to the sampled water mass by using a drifting buoy with sediment traps at 10 m and 50 m depth. Station 12 was located just outside the high reflectance area. To the west of the high-reflectance area there were two 24-hours stations on the same day (sampled alternatingly). One (station 19N) was located in the POC-rich zone, and the other (station 19S) was located 9 nautical miles to the south, towards the high reflectance area. The fourth 24-hours station (station 15) was in the high reflectance area.

At none of the stations $f\text{CO}_2$ or TIC showed a distinct diel rhythm. In order to better distinguish the differences between stations data of all CTD casts were averaged to produce a single profile per station. We order these stations as progressive stages of the bloom: first the reference areas, then the POC-rich zone and then the high reflectance area (successively stations 12, 19N, 19S and 15). During these stages concentrations of TIC decreased in the upper mixed layer (from 2070 to 2060 $\mu\text{mol}\cdot\text{kg}^{-1}$). In contrast, below the pycnocline TIC increased (from 2120 to 2150 $\mu\text{mol}\cdot\text{kg}^{-1}$) (Figure 4.3a). These observations indicate that sedimentation was higher in the high reflectance area than in the reference areas. Sedimentation decreases TIC in the upper mixed layer, and subsequent mineralisation below the pycnocline increases TIC. The $f\text{CO}_2$ increased from station 12 to station 15 over the entire water column (from 286 to 354 μatm at the surface, Figure 4.3b). Stations 19S and 19N showed intermediate values.

The standing stock of CaCO_3 increased from station 19N via 19S to station 15, whereas the standing stock of POC decreased (Figure 4.3c, d). At station 12 the standing stocks of CaCO_3 and POC were intermediate between those at stations 19N and 19S.

At station 15 a high standing stock of CaCO_3 (8 μM) and a low standing stock of POC (11 μM) coincided with a high $f\text{CO}_2$ (354 μatm at the surface). Most likely, this high $f\text{CO}_2$ is the result of the acidification of the sea water due to CaCO_3 production (Equations 4.2 & 4.3). At another station in the high reflectance area (station 7, Figure 4.1a) a high CaCO_3 standing stock (15 μM) and low POC (4 μM at the surface) coincided with a low $f\text{CO}_2$ (330 μatm at the surface, data not shown). The vertical gradient in TIC (2040 at the surface; 2150 at 125 m depth) was even sharper here than at station 15. We conclude that so much carbon was removed from the upper mixed layer through sedimentation that this had a greater effect on $f\text{CO}_2$ than the production of coccoliths did.

Dissolution experiments

At stations 7, 12 and 15 (Figure 4.1a) samples were incubated in the dark for determination of the dissolution rate of CaCO_3 . In order to determine the effect of grazing on the dissolution rate we compared samples that had been filtered before incubation (either 10 μm or 200 μm)

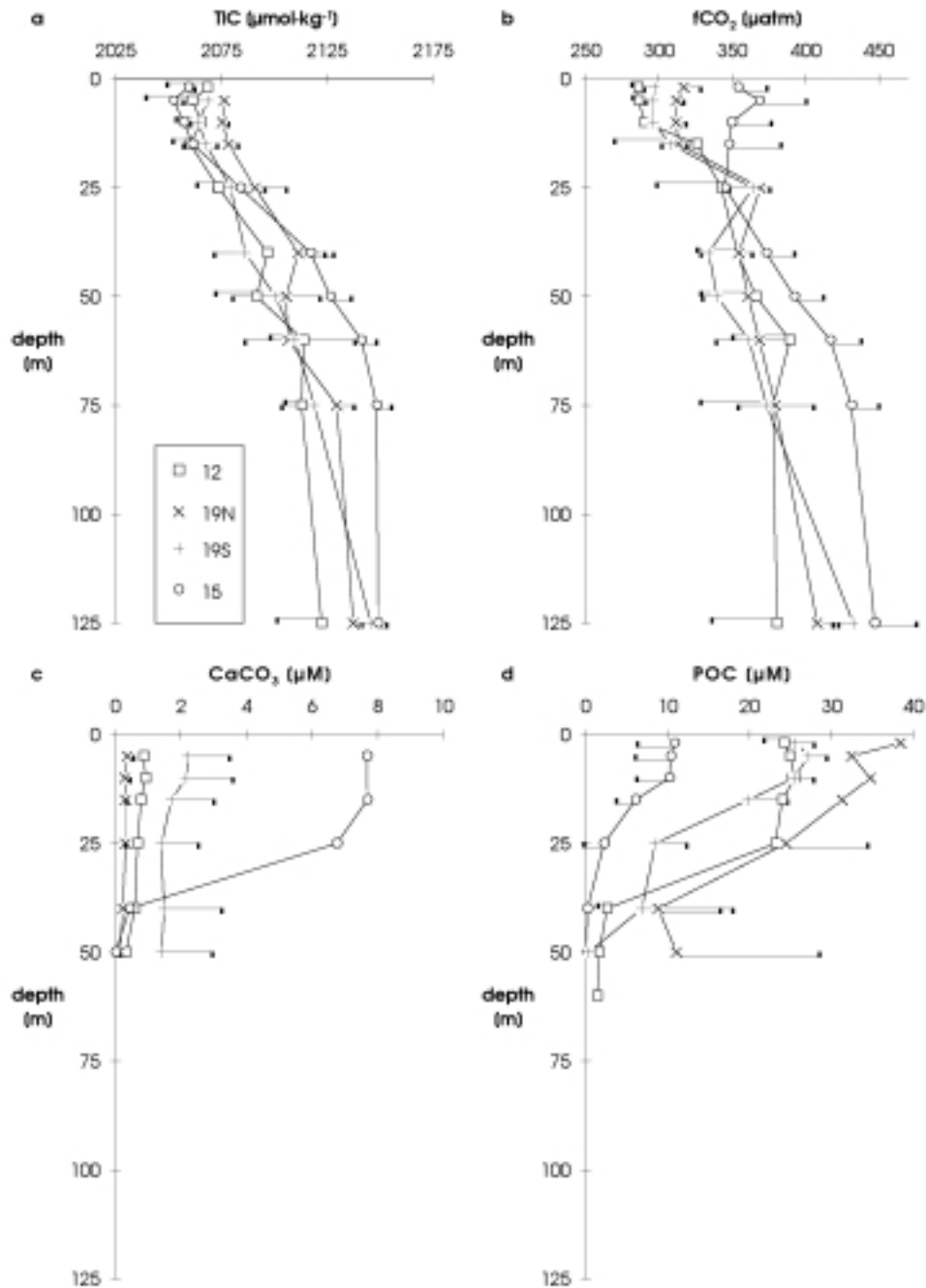


Figure 4.3 Depth profiles of 24-hour stations, averaged values over all CTD casts at a single station, with standard deviations. □ Station 12, outside the bloom ($n = 3$, except CaCO_3), × Station 19 N, at the fluorescence maximum ($n = 3$, except CaCO_3), + Station 19 S, at the lower fluorescence ($n = 4$, except CaCO_3), ○ Station 15, at the high reflectance area ($n = 5$, except CaCO_3). a) TIC, b) $f\text{CO}_2$, c) CaCO_3 , (n = 1 or 2 for (19N, S)) d) POC.

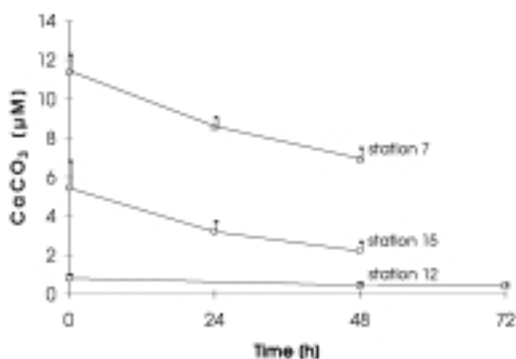


Figure 4.4 Changes in standing stocks of CaCO_3 [μM] of samples stored in the dark, with standard deviations. \square Station 12, \circ Station 15, Δ Station 7.

with unfiltered samples. Removal of grazers had no significant effect on the dissolution rate of CaCO_3 (data not shown). Therefore the results were averaged per station (Figure 4.4). At all stations 25 % (± 11 %, $n=27$) of the CaCO_3 standing stock dissolved per 24 hours.

The sea water at stations 7, 12 and 15 was 3.8 to 4.5 times oversaturated with respect to CaCO_3 . Even if all the POC in the samples had been mineralised to CO_2 during the incubations the sea water would still be oversaturated 3.6 to 4.1 times with respect to CaCO_3 .

Transect

Within a period of 24 hours vertical profiles were taken along a transect (stations 20-33, Figure 4.1a). This transect ran from the edge of the Atlantic Ocean, through the POC-rich zone, along the edge of the high reflectance area where coccoliths were abundant.

TIC and the density of the water (SigmaT) showed comparable patterns (Figure 4.5a, b). Towards the high reflectance area the gradients of TIC and SigmaT with depth became more pronounced. An increased gradient of TIC with depth was already noted before (section 24-hours stations), and indicates increased sedimentation. The $f\text{CO}_2$ was clearly influenced by uptake of CO_2 by algae, expressed as POC (Figure 4.5c, d). A minimum of $f\text{CO}_2$ was located in the POC-rich zone. Low values of $f\text{CO}_2$ persisted in the high reflectance area. There was no apparent relationship between CaCO_3 and $f\text{CO}_2$ (Figure 4.5d, e). Calculated alkalinity in the upper mixed layer decreased from the POC-rich zone to the high reflectance area. This agrees with the observed increase of the standing stock of CaCO_3 (Figure 4.5e, f).

The CaCO_3 standing stock, as measured by atomic absorption, showed a close correlation with the CaCO_3 standing stock calculated from flow cytometer data ($\text{CaCO}_3^{\text{AAS}} = 0.99 * \text{CaCO}_3^{\text{flow cytometer}} - 0.052$, $p < 0.001$, $n=39$). For the stations 20, 22, 30 and 32 we assumed that each *E. huxleyi* cell was covered with 20 coccoliths. The total number of coccoliths (attached and detached) was multiplied by 0.26 pg carbon per coccolith (Balch et al. 1992). At stations 24, 26 and 28 (the POC-rich zone) CaCO_3 was calculated from detached coccoliths only, because the numbers of *E. huxleyi* cells were probably overestimated due to the presence of small diatoms (P. van der Wal, pers. comm., NIOZ, The Netherlands). At station 33 (95 nautical miles after the start of the transect) CaCO_3 was not measured by atomic absorption spectrophotometry (AAS), but estimated using this equation.

The organic carbon to chlorophyll ratio ($\text{POC} [\mu\text{M}] / \text{chlorophyll } a [\mu\text{g}\cdot\text{L}^{-1}]$) was 6.7 ± 3.8 ($n = 43$) on average. In the POC-rich zone the ratio was 9 ± 5 ($n = 17$). In the high reflectance area it was 4 ± 2 ($n = 15$). Because organic carbon was calculated from flow cytometer data for living algae, the ratio is a direct measure of the average algal composition.

Total carbon content (TIC + POC, Figure 4.6) was calculated over the photic zone (0-40 m, penetration depth of 0.5% of surface irradiance) and the aphotic zone (40-80 m), and over the entire sampled depth (0-80 m). Proceeding from the POC-rich zone towards the high reflectance area the total carbon content decreased in the photic zone, whereas it increased in

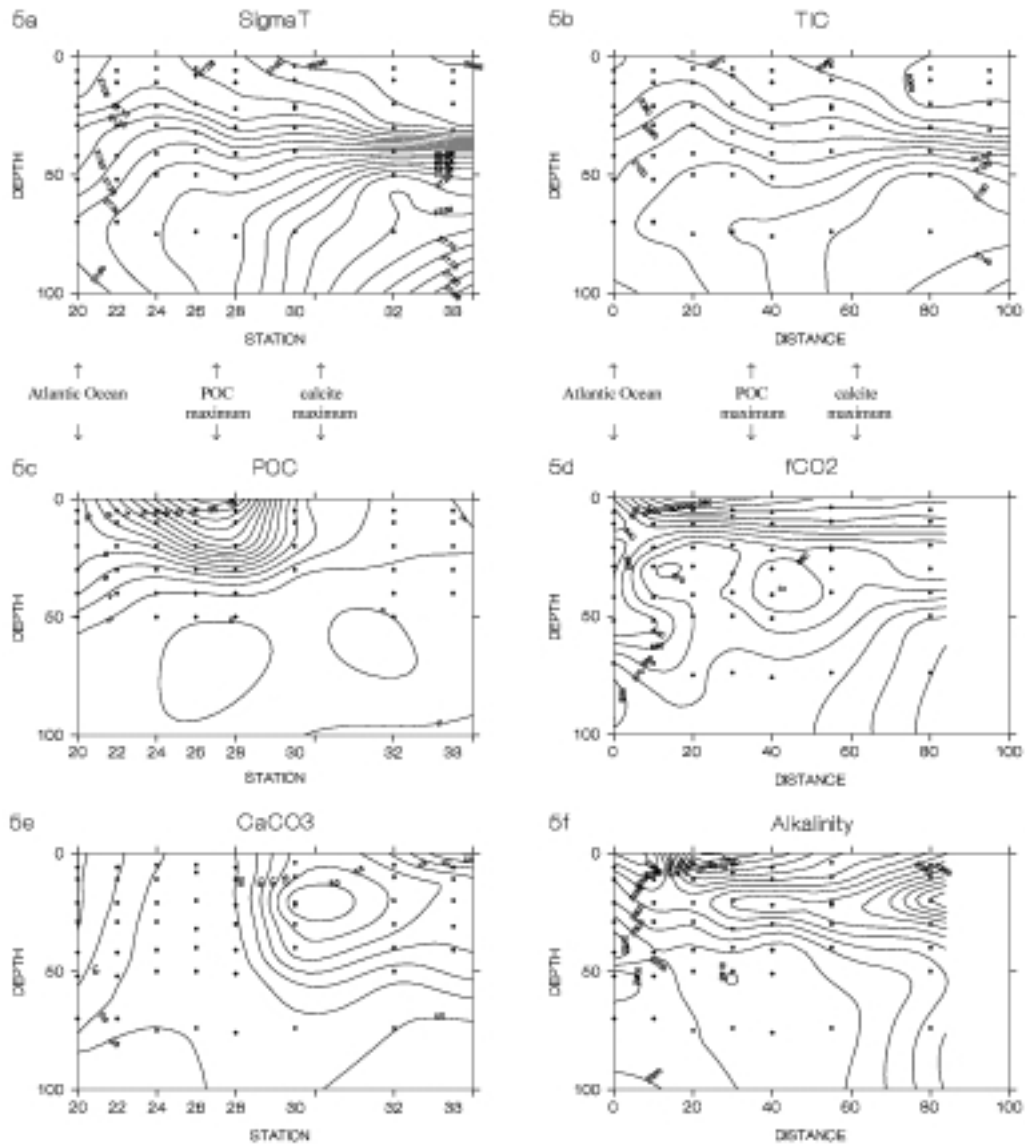


Figure 4.5 Contour plots (using least squares method) of the transect, distance from the first station in nautical miles, depth in meters. Diamonds represent sampling depths. fCO₂ and CaCO₃ were not measured at the last station. a) SigmaT (density [kg l^{-1}] - 1) \times 1000. b) TIC [$\mu\text{mol}\cdot\text{kg}^{-1}$]. c) POC [μM]. d) fCO₂ [μatm]. e) CaCO₃ [μM] at 95 nautical miles was calculated from flow cytometer data using the correlation of flow cytometer data with atom adsorption measurements at the other stations (see text). f) Calculated alkalinity [$\mu\text{equivalents}\cdot\text{kg}^{-1}$].

the aphotic zone (Figure 4.6a). We ascribe these trends to the sinking of CaCO₃ and POC through the stratified layer, and the subsequent dissolution of CaCO₃ and degradation of POC below 40 m. Van der Wal et al. (1995) found enhanced sedimentation of both CaCO₃ and POC in the high reflectance area due to the increased density of faecal pellets that contained coccoliths.

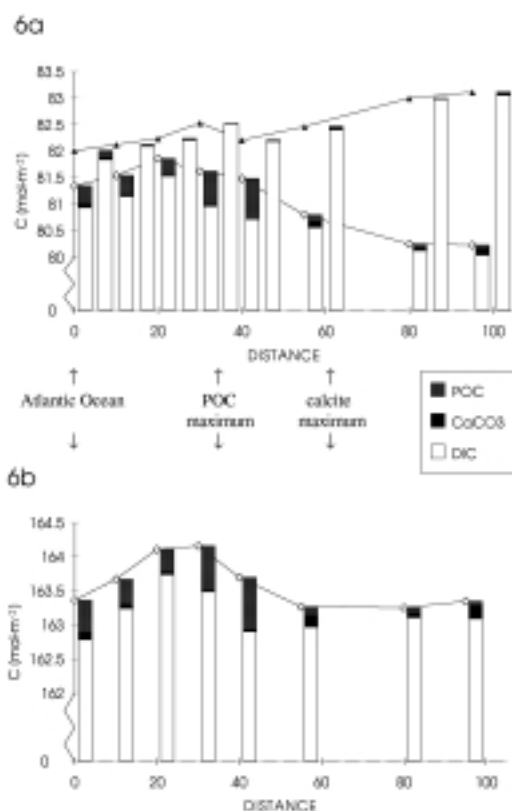


Figure 4.6 Total carbon content (ΣC : the sum of TIC and POC) of the water column along the transect, distance from the first station in nautical miles. Open bars: DIC. Filled bars: CaCO_3 . Dotted bars: POC. a) \diamond (odd bars) ΣC in the photic zone: 0-40 m depth, \blacktriangle (even bars) ΣC in the aphotic zone: 40-80 m depth. b) ΣC in the sampled water layer: 0-80 m depth.

Total carbon content measured over the entire sampled depth was highest in the POC-rich zone (Figure 4.6b). Algal growth and the resultant minimum in $f\text{CO}_2$ has probably led to a high atmosphere-ocean flux of carbon dioxide into this area. In the high reflectance area the total amount of CaCO_3 exceeded the total amount of POC (Figure 4.6b).

Dissolved organic carbon (DOC) was only measured in the photic zone. DOC was constant at $3.0 \pm 0.2 \text{ mol}\cdot\text{m}^{-2}$ (C. P. D. Brussaard pers. comm., NIOZ, The Netherlands, data not shown).

Discussion

In a bloom of *Emiliania huxleyi* in the North Atlantic in 1991 Robertson et al. (1994) have found that the fugacity of CO_2 ($f\text{CO}_2$) was $15 \mu\text{atm}$. higher in waters with high CaCO_3 standing stocks ($>18 \mu\text{M}$) than in waters with low CaCO_3 standing stocks ($<5.5 \mu\text{M}$). We will argue here that while the short-term effect of CaCO_3 precipitation was a rise in $f\text{CO}_2$ due to a decrease in alkalinity, the long-term effect of this bloom of *E. huxleyi* was a decrease in $f\text{CO}_2$ by enhanced sedimentation. First we discuss the influences that the physical properties of the water column and biological activities have on the concentrations of inorganic and particulate organic carbon and the speciation of the dissolved inorganic carbon system. Then we derive a carbon budget that shows that this bloom acted as a carbon sink for the atmosphere.

The influence of the physical structure was apparent from the similarity between the contour plots for total inorganic carbon (TIC) and the density of the water column (Figure 4.6a, b). In the high reflectance area the stratification was more pronounced than in the northern part of the research area (Atlantic Ocean side). As a result the phytoplankton was mixed over shallower depths, and the concentration gradient of inorganic carbon was steeper (Figure 4.5b,

see also Figure 4.6a). The enhancement of stratification is not necessarily the result of physical processes only. *E. huxleyi* may generate a positive feedback for an increase of the temperature in the upper mixed layer: the reflectance of coccoliths may increase the temperature by light scattering (Holligan & Balch 1991, Westbroek et al. 1993), this will make the upper mixed layer shallower which will increase the average light intensity, and this will stimulate growth. The observed positive correlation between temperature and the CaCO_3 standing stock illustrates these processes of calcification, stratification and positive feedback.

The influence of biological activities on the carbon speciation was manifested by the occurrence of the $f\text{CO}_2$ minimum in the POC-rich zone, and by the increase of $f\text{CO}_2$ with biologically produced CaCO_3 . Furthermore TIC was strongly depleted in the upper mixed layer of the high reflectance area, because in this area sedimentation was high due to the elevated sinking speed of faecal pellets containing CaCO_3 (van der Wal et al. 1995).

In a plot based on a surface survey over the entire cruise track, $f\text{CO}_2$ (corrected to a constant temperature) increased with an increase of the standing stock of CaCO_3 (Figure 4.2). This demonstrates that precipitation of CaCO_3 shifts the carbon equilibria in favour of CO_2 according to Equations 4.2 and 4.3. The $f\text{CO}_2$ increased $3.0 \mu\text{atm. per } \mu\text{M CaCO}_3$. This is much higher than the increase of $f\text{CO}_2$ that is predicted from CaCO_3 precipitation ($1 \mu\text{atm. per } \mu\text{M CaCO}_3$ at typical concentrations of alkalinity and DIC). The enhanced increase results from the apparent inverse correlation between the standing stocks of POC and CaCO_3 (Figure 4.3c, d, Figure 4.5c, e). There are three compatible explanations for this inverse correlation. Firstly, the production of CaCO_3 continues after the culmination of the bloom, so that the peak in CaCO_3 standing stock occurs after the peak in POC standing stock (P. van der Wal, pers. comm.). Secondly, other phytoplankton species may contribute relatively less to POC at the end of the bloom, when nutrient concentrations are low. At low nutrient concentrations *E. huxleyi* will outcompete other phytoplankton species as it has a high affinity for nutrients, especially phosphate (Egge, 1993). Thirdly, POC is degraded faster than CaCO_3 , so the relative contribution of CaCO_3 increases.

The relatively high $f\text{CO}_2$ in the surface water at station 15 (which has a high standing stock of CaCO_3) is in accordance with the trend shown in Figure 4.2. The profiles of the other 24-hours stations do not show a clear increase of $f\text{CO}_2$ with CaCO_3 . Also other data seem to contradict a positive correlation between CaCO_3 and $f\text{CO}_2$. At station 7, where the highest standing stock of CaCO_3 was found, $f\text{CO}_2$ was relatively low. Along the transect $f\text{CO}_2$ at the surface was fairly constant between stations 24 and 33. On-line surface measurements of $f\text{CO}_2$ integrated over wider areas were lower inside the high reflectance area than in the reference areas. The explanation is found in the trend in TIC along the transect towards lower concentrations in the upper mixed layer and higher concentrations below the pycnocline. This is consistent with sedimentation, which results in a decrease of $f\text{CO}_2$ at timescales that are slower than the increase of $f\text{CO}_2$ caused by production of CaCO_3 . We conclude that whether calcification is seen as a sink or source of CO_2 depends on the time scale on which these processes are observed: while on the basis of chemical equilibria production of CaCO_3 will lead to an instantaneous increase of $f\text{CO}_2$, the overall processes of production, remineralisation, dissolution, air-sea gas exchange and sedimentation lead to a net export of carbon from the upper mixed layer, hence a decrease of $f\text{CO}_2$.

About 25 percent of the standing stock of CaCO_3 was found to dissolve per 24 hours in the dark, despite the fact that the sea water at stations 7, 12 and 15 was about 4 times oversaturated with respect to CaCO_3 . Degradation of the standing stock of POC would not change this. Since there was no significant difference between filtered (either $10 \mu\text{m}$ or $200 \mu\text{m}$) and unfiltered samples, we conclude that dissolution was not caused by micro- or mesozooplankton. Therefore dissolution was probably caused by respiration of bacteria and algae, and by lysis of cells, which creates an acidified micro environment around the coccoliths.

Photosynthesis accompanied by production of CaCO_3 in a molar ratio of 1:1 amounts to bicarbonate utilisation, and leads to a smaller decrease in $f\text{CO}_2$ than in the case of CO_2 utilisation by photosynthesis alone. In either case there is an additional decrease in $f\text{CO}_2$ due to an increase in pH since uptake of NO_3^- by the cell is coupled to OH^- excretion (Brewer and Goldman 1976). This increase of pH is equivalent to an increase of alkalinity (Table 4.1). The ratio between calcification and photosynthesis (C/P-ratio) indicates how uptake of dissolved inorganic carbon will affect $f\text{CO}_2$. When the effect of simultaneous production of CaCO_3 and POC is calculated, $f\text{CO}_2$ remains constant at a C/P-ratio of 1.2:1. When the effect of PON production is also taken into account the C/P-ratio required for maintaining a constant $f\text{CO}_2$ increases to 1.3:1. The highest C/P production ratio that was observed in this bloom was 0.18 (station 7, van der Wal et al. 1995). The highest C/P sedimentation ratio was 1.3 (station 15, the unpoisoned trap at 50 m depth, van der Wal et al. 1995). Thus no indication for an increase of $f\text{CO}_2$ was observed at any stage of this bloom.

The particulate organic carbon to chlorophyll *a* ratio in the POC-rich zone was about twice the ratio in the high reflectance area. Although the difference is not significant, there is an explanation for this difference. The beam attenuation coefficient c_{530} was twice as large in the high reflectance area as in the POC-rich zone. This would lead to a higher chlorophyll content per cell as an adaptation to low light conditions.

Consecutive stages of the bloom development were encountered travelling southwards along the transect. Therefore we tentatively interpret Figure 4.6 as the development of the bloom in time. This interpretation is suggested by the seasonal northwesterly migration of the high reflectance area on satellite images taken before the cruise. This is corroborated by the observed decrease of nutrient concentrations from north to south. We have calculated the transport of carbon during the bloom from changes in the total carbon content (TIC + POC) of the sampled water column along the transect. For this purpose the water column was divided into an upper (0-40 m), an intermediate (40-80 m) and a deep (80-130m) box (Figure 4.7). The thermocline resides at approximately 40 metres depth (Figure 4.5a), whereas no samples were taken below 80 metres depth. The mass balance for the upper box involves an influx of CO_2 from the atmosphere, changes in carbon pools and downflux of biogenic particles:

$$\text{Influx} = \Delta\text{DIC} + \Delta\text{POC} + \Delta\text{CaCO}_3 + \text{Downflux} \quad (4.5).$$

Latter downflux is the source term for a similar balance for the intermediate box, where any residual carbon is assumed to represent an excess sedimentation term into the deep box :

$$\text{Downflux} = \Delta\text{DIC} + \Delta\text{POC} + \Delta\text{CaCO}_3 + \text{Excess sedimentation} \quad (4.6).$$

In the first 20 nautical miles of the transect from the Atlantic Ocean to the POC-rich zone the $f\text{CO}_2$ decreased to 286 μatm . at the surface, while the total carbon content from 0 - 80 m increased by 0.7 $\text{mol}\cdot\text{m}^{-2}$ (Figure 4.5d, 4.6b). This indicates uptake of CO_2 from the atmosphere. The air to sea flux (influx, Figure 4.7) was calculated with the exchange coefficient for average wind speeds given by Wanninkhof (1992) using the average wind speed during the cruise and the $f\text{CO}_2$ gradient at the chlorophyll maximum (20 nautical miles from the beginning of the transect). At a fugacity gradient of 72 μatm and an average wind speed during the cruise of 7.7 $\text{m}\cdot\text{s}^{-1}$ it would have taken 64 days for an amount of 0.7 $\text{mol}\cdot\text{m}^{-2}$ to be taken up from the atmosphere. This 64 day period is only an approximation since $f\text{CO}_2$ was only measured once at station 24 and the wind speed represents an average in time (13 days) and space. Blooms tend to be visible by AVHRR for shorter periods of typically 15 - 30 days (Westbroek et al. 1993). This

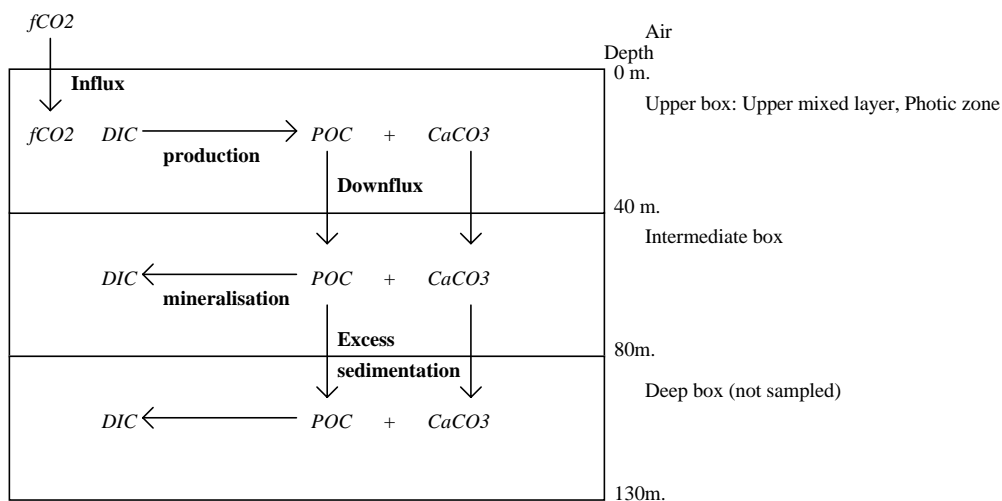


Figure 4.7 Box model for a carbon budget. See text for details.

would mean that either the air to sea flux has been underestimated or diffusion from below the thermocline plays an important role. We have not included latter diffusion in our calculations.

In the subsequent stretch (20 - 100 nautical miles) from the POC-rich zone (station 24) to the high reflectance area (station 33) the stratification increased (Figure 4.5a). As discussed above, this led to a decrease of DIC in the photic zone (0-40 m, Figure 4.6a). This decrease cannot be ascribed to increased photosynthesis since neither POC (Figure 4.5c, 4.6a), nor chlorophyll *a* (data not shown) increased, due to nitrogen limitation. Since the total carbon content in the aphotic zone increased while the total carbon content in the photic zone decreased (Figure 4.6a) we assume that these changes are caused by sedimentation.

From the POC-rich zone to the high reflectance area the decrease in total carbon content of $1.6 \text{ mol}\cdot\text{m}^{-2}$ in the upper mixed layer was larger than the increase of $0.9 \text{ mol}\cdot\text{m}^{-2}$ in the intermediate layer (Figure 4.6b). Since the upper mixed layer remained undersaturated (Figure 4.5d), the difference of $0.7 \text{ mol}\cdot\text{m}^{-2}$ cannot have escaped by sea to air outflux. The most straightforward explanation is that from 80 m to the bottom the total carbon content increased as well, as was found elsewhere at the 24-hours stations at 125 m depth (Figure 4.3). When the measured total carbon content at 80 m depth was extrapolated to the 80 - 130 metres interval an increase of $2.4 \text{ mol}\cdot\text{m}^{-2}$ for the aphotic zone (40-130 m.) was calculated over the whole transect (downflux + excess sedimentation in Figure 4.7). In the photic zone the total carbon content decreased $1.1 \text{ mol}\cdot\text{m}^{-2}$. This would yield an overall atmospheric carbon sink of $1.3 \text{ mol}\cdot\text{m}^{-2}$ for this bloom of *E. huxleyi*. This is consistent with the relatively high sedimentation rate of $45 \text{ mmol}\cdot\text{m}^{-2}\cdot\text{day}^{-1}$ that was measured at station 7 (Wal et al. 1995), if it is multiplied by 30 days.

If we calculate the global significance of this carbon sink of $1.3 \text{ mol}\cdot\text{m}^{-2}$ by multiplying it by the average area of *E. huxleyi* blooms of $1.4 \cdot 10^6 \text{ km}^2$ (Brown and Yoder, 1994) we arrive at 2.2 Mton C per year or 0.4 ‰ of the export production at 100 metres depth (Berger, 1989).

Acknowledgements

We thank Rob Kempers, Erica Koning and the captain and the crew of the RV Pelagia for technical assistance. We thank the blood bank in Alkmaar for providing the Mailar. We thank Steve Groom for processing the AVHRR data. Helpful discussions with Erica Koning, Paul van der Wal, Hein de Baar, Dieter Wolff-Gladrow, Ray Weiss, Hein de Wilde and Bram Majoor were appreciated. We thank the reviewers for comments that led to improvement of the manuscript.

Chapter 5: Blooms of *Emiliana huxleyi* are sinks of atmospheric carbon dioxide; a field and mesocosm study derived simulation.

Erik T. Buitenhuis, Paul van der Wal, Hein J. W. de Baar.

Submitted to *Global Biogeochemical Cycles*

Abstract

During field measurements in a bloom of *Emiliana huxleyi* in the North Sea in 1993, an apparently inconsistent combination of observations was measured:

- a) $f\text{CO}_2$ was lower in the centre of the bloom than in the surrounding non-bloom areas, and undersaturated with respect to the atmosphere in both cases,
- b) within the bloom enhanced sedimentation of coccoliths-containing fecal pellets was observed,
- c) a large atmospheric sink of $1.3 \text{ mol C}\cdot\text{m}^{-2}$ was derived,
- d) in the same bloom a positive correlation between CaCO_3 and $f\text{CO}_2$ was observed, which was interpreted as an increase of $f\text{CO}_2$ during production of CaCO_3 .

In order to resolve the inconsistency between observations (a, b, c) and d a one-dimensional three-layer model was constructed. A positive correlation between CaCO_3 and $f\text{CO}_2$ was obtained when the model was parameterised with data obtained from field and mesocosm studies. The correlation is a feature of the decay-phase of a bloom, and represents a decrease of $f\text{CO}_2$ with a decrease of CaCO_3 . Thus it represents the dissolution and sedimentation of CaCO_3 rather than its production. Having resolved the ambiguity within the field data by adding the dimension of time in the model, blooms of *E. huxleyi* can be identified as sinks for atmospheric carbon dioxide. This sink is a function of the calcification to photosynthesis (C:P) ratio of the nitrate-using phytoplankton, and is maximal when the C:P ratio is 0.42 (that is, *E. huxleyi* constitutes 97% of the nitrate-using phytoplankton). Rather than using the model for making accurate predictions about the magnitude of this sink a sensitivity analysis was performed to give a range of magnitudes for the range of parameter values that were obtained during previous studies. Furthermore gaps were identified in the current knowledge of carbon fluxes within blooms of *E. huxleyi*.

Key words: air-sea gas exchange, calcification, calcite (CaCO_3), carbon dioxide (CO_2), carbon flux, coccolithophorid, Prymnesiophyceae, sedimentation.

Introduction

Calcification (precipitation of CaCO_3) decreases alkalinity twice as much as dissolved inorganic carbon (DIC). As the chemical speciation of DIC in seawater has been accurately determined (Millero 1995), it follows that the fugacity of CO_2 ($f\text{CO}_2$) increases. However, calcification by *Emiliana huxleyi* is at least loosely coupled to photosynthesis, which decreases DIC and has a smaller effect on alkalinity. Alkalinity increases during uptake of nitrate (NO_3^-) and phosphate (HPO_4^{2-}), and decreases during uptake of ammonia (NH_4^+). The combined effect of calcification (C) and photosynthesis (P), then, results in a decrease of $f\text{CO}_2$ at C:P production ratios lower than 1.7 during use of nitrate (C:P < 1.2 during use of ammonia), and an increase of $f\text{CO}_2$ at higher C:P production ratios. Blooms of *Emiliana huxleyi* have therefore been suggested as potential sources of CO_2 for the atmosphere. Robertson et al. (1994) concluded that blooms of *E. huxleyi* may constitute smaller sinks than blooms of non-calcifying algae. This conclusion was based on observations in the North Atlantic Ocean, where $f\text{CO}_2$ was 15 μatm . higher in samples with $\text{CaCO}_3 > 18 \mu\text{M}$ than in samples with $\text{CaCO}_3 < 5.5 \mu\text{M}$. Crawford & Purdie (1997) calculated an actual increase of $f\text{CO}_2$ in blooms of *E. huxleyi*, but this was

found under the extreme conditions of 100% mineralisation of POC and 0% dissolution of CaCO_3 .

Wal et al. (1995) found that sedimentation of carbon is enhanced in a bloom of *E. huxleyi* due to the increased weight of fecal pellets that contain coccoliths. This physical effect of enhanced sedimentation complicates the above mentioned chemical effect of calcification on alkalinity, and thereby on fCO_2 . Sedimentation of particulate carbon itself will not change the air-sea gradient of CO_2 . However, if the carbon remains suspended in the surface waters, then it will eventually be mineralized again and the end result will be no different from the situation before the start of the bloom, while any material that is sedimented below the thermocline will leave the surface waters undersaturated for carbon dioxide.

To illustrate this point first a model is considered with two boxes: atmosphere and surface water. This model simulates a bloom with first production and then degradation of both particulate organic carbon (POC) and calcite (CaCO_3). If the C:P production ratio in the model is lower than 1.7 then during the productive stage CO_2 will decrease and gas exchange will transport CO_2 from the atmosphere to the sea. During the degradation stage CO_2 will increase and CO_2 will outgas from the sea to the atmosphere. At the end of the bloom the situation will be the same as at the start, so that the net exchange with the atmosphere will be zero.

This two box model can be used to illustrate the chemical effect of calcite production. To include the physical effect of calcite in sinking particles a third box is introduced: the deep sea. The same hypothetical model simulation can now be performed with a bloom in the upper ocean, which is later degraded, and some material being transported to the deep layer. Since exchange of dissolved constituents (DIC, alkalinity etc.) between the upper and the deep layer is slow relative to the production and degradation of the bloom, by the end of the bloom the effect of gas exchange with the atmosphere will be a function of the amount of POC and CaCO_3 that is sedimented to the deep layer. The more POC and the less CaCO_3 is sedimented the more CO_2 will be drawn down from the atmosphere. But if the amount of sedimented POC is stimulated by the amount of heavy CaCO_3 in the sedimenting particles then CaCO_3 both reduces and increases CO_2 drawdown from the atmosphere. Thus, it has to be determined whether the chemical effect of CaCO_3 precipitation is more or less important than the physical effect of CaCO_3 enhancing sedimentation. This was done by constructing a three box model using data from several studies of blooms of *E. huxleyi*.

The model that is presented here includes those processes that were found to occur during both a natural bloom of *E. huxleyi* in the North Sea in 1993 (Wal et al. 1995, Buitenhuis et al. 1996, Wiebinga et al. 2000) and a mesocosm study at the field station of the University of Bergen in Raunefjord in 1992 (Bleijswijk et al. 1994a, Wal et al. 1994, Bleijswijk & Veldhuis 1995). Parameter values were also taken from these studies.

Model description

The model simulates an algal bloom within a 1-D sea with three boxes: an atmosphere with constant fCO_2 , a mixed layer with a constant depth of 40 m and a deep layer of 80 m depth. The model contains 7 carbon pools, three nitrogen pools, two pools of alkalinity, and a fixed atmospheric fCO_2 (Figure 5.1). All simulations were run for 60 days with a variable time step to minimize integration errors. Cumulative integration errors were always less than 10^{-12} of the total pools. Most of the parameter values, and some of their ranges for the sensitivity analysis were taken from a field study in the North Sea in 1993 (Wal et al. 1995, Buitenhuis et al. 1996, Wiebinga et al. 2000) and a mesocosm study in Raunefjorden, Norway in 1992 (Bleijswijk et al. 1994a, Wal et al. 1994, Bleijswijk & Veldhuis 1995). Additional parameter values were taken or derived from Redfield et al. (1963), Alldredge & Gotschalk (1988), Bleijswijk et al. (1991, 1994b), Wanninkhof (1992), Chipman et al. (1993), Roy et al. (1993) and Buitenhuis et al. (1999).

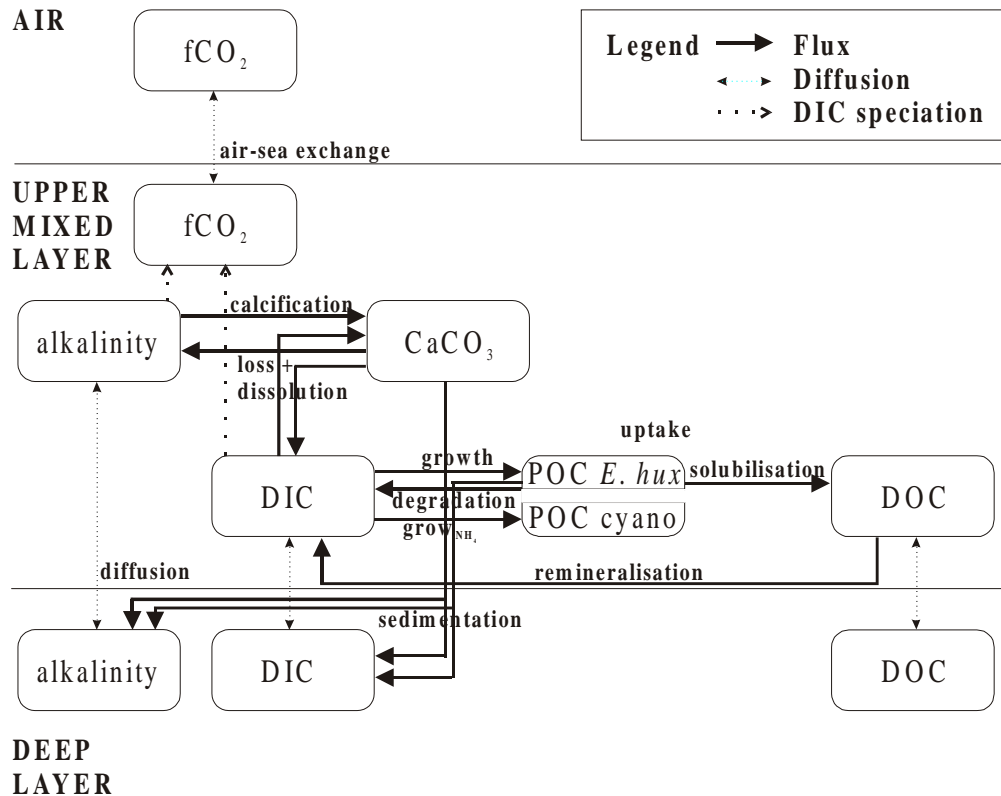


Figure 5.1 Simplified scheme of the model structure. Pools and fluxes of nitrogen and feedback controls have been omitted. Dotted arrows of DIC speciation indicate that $f\text{CO}_2$ was calculated from DIC and alkalinity (see the 'CO₂fromDIC,alkalinity' function in section 2.8 for details). Air-sea gas exchange was added to DIC.

Model structure

The model structure is shown in Figure 5.1, and is described from top to bottom and from left to right.

The air has a constant $f\text{CO}_2$ of 360 μatm . In the upper mixed layer $f\text{CO}_2$ is calculated from alkalinity and DIC with the dissociation constants of Roy et al. (1993). The starting values of alkalinity and DIC were chosen in such a way that the $f\text{CO}_2$ at the start of the model run was 360 μatm . at a temperature of 11.6 °C and a salinity of 35.2.

The calcification rate (C) is proportional (C:P parameter) to the growth rate (or photosynthesis P), but with a delay. At the start of the model runs, for the length of the delay period, the C:P production ratio is equal to the C:P parameter. After that the C:P production ratio becomes slightly higher than the C:P parameter, until it becomes close to infinite as the NO_3^- concentration approaches 0. The C:P production ratio stays very high for the length of the delay period, after which both calcification and photosynthesis are very small for the remainder of the model run. The delay is introduced because calcification continues after photosynthesis becomes nutrient-limited. In cultures, this delay was 2 to 3 days (Dong et al. 1993, Paasche 1998). In the mesocosm study calcification rates were still 41 % of the average rates four days after the peaks of *E. huxleyi* (Wal et al. 1994), possibly because nutrients were added daily

during this study. Even so, the standing stock of CaCO_3 also went through a distinct maximum two days after the peak in POC was reached (Bleijswijk et al. 1994a).

The sedimentation rate is proportional to the sinking rate, calculated with Stokes' law (see the SEDIMENTATION function in the Materials & Methods section). This is consistent with the observation that fecal pellets that contain CaCO_3 sink rapidly out of the upper mixed layer, whereas fecal pellets without CaCO_3 stay suspended in the upper mixed layer for longer periods, and are more prone to be degraded there (Wal et al. 1995).

The net growth rate is composed of a gross growth rate and loss factors (Bleijswijk et al. 1995). The gross growth rate is a function of nitrate (NO_3^-) according to Michaelis-Menten kinetics (Michaelis & Menten 1913). The loss rate is composed of sedimentation, solubilisation (to DOC) and degradation (to DIC). The declining phase of the bloom is then brought about by nutrient limitation of the gross growth rate, and a loss rate that continues unabated.

The standard model calculates only the C-fluxes due to *E. huxleyi*. In reality, the new production of *E. huxleyi* is followed by a secondary growth of cyanobacteria (Buitenhuis et al. 1996). In one of the runs of the sensitivity analysis an additional component ($\text{POC}_{\text{cyano}}$) was introduced to represent the C-flux associated with this secondary growth. In the model *E. huxleyi* uses only nitrate, while the cyanobacteria use only ammonia. This is a simplification of the observation that new production tends to depend mostly on nitrate, while recycled production uses mostly ammonia. It was chosen as a simple means of representing the complex factors that lead to bloom formation, rather than as a representation of the real situation (which is presented in Stolte 1996). The total primary production was found to be fairly constant throughout the bloom (Wal et al. 1995). Thus, the secondary growth appears to be a recycling pool of carbon, and therefore mineralisation and sedimentation of this pool are not included.

Diffusive exchange of dissolved constituents between the upper mixed layer and the deep layer is calculated as due to turbulent mixing. Water exchange by variations in the mixed layer depth were not included. For our objective of unraveling general trends an average wind speed was most suitable. When attempting to simulate a specific bloom, variations in the wind speed can have a large influence (see also 4.1 in the discussion and Bakker et al. [1997]).

Parameter values

The processes are described from top to bottom and from left to right as well (Figure 5.1).

The exchange rate between fCO_2 in the air and the upper mixed layer was calculated on the basis of the equation for average wind speeds given by Wanninkhof (1992) using the observed average wind speed of $7.2 \text{ m}\cdot\text{s}^{-1}$ (Buitenhuis et al. 1996). The sum of this exchange is presented as the air-sea flux. At the end of each model run all particulate and organic carbon in the upper mixed layer is mineralised and the flux of CO_2 is calculated to bring the upper mixed layer in equilibrium with the atmosphere. This is added to the air-sea flux during the model run. The results of this flux are presented as the potential flux. Thus, the potential flux is the effect of sedimentation and diffusive exchange between the upper mixed layer and the deep layer, expressed in units of $\text{mol CO}_2\cdot\text{m}^{-2}$.

The C:P parameter was calculated as 0.433, based on 20 coccoliths $\cdot\text{cell}^{-1}$ of 21.7 $\text{fmol CaCO}_3\cdot\text{coccoliths}^{-1}$ per 1 $\text{pmol POC}\cdot\text{cell}^{-1}$ (Wal et al. 1994, Buitenhuis et al. 1999).

Dissolution of newly produced coccoliths was undetectable for the first 2 days (Wal et al. 1995), but on the other hand the dissolution rate during the end phase of a bloom was 25 % per day (Buitenhuis et al. 1996). About 75 % of the coccoliths of a cell were dissolved during loss of a cell (Bleijswijk et al. 1994a). In an attempt to combine these observations, dissolution of CaCO_3 was composed of two components. During the growth phase of the bloom dissolution is associated by a 75% loss parameter with the three loss factors (sedimentation, solubilisation and degradation). Additionally, during the declining phase of the bloom 17 % of the standing stock of CaCO_3 dissolves per day, to bring the total dissolution rate to 25% per day.

Nitrate was set at 6 μM at the start of the model run, which was the concentration to the north of the North Sea bloom (Veldhuis 1993). Nitrate is taken up by $\text{POC}_{E.hux}$ with a C:N ratio of 7.4 (Buitenhuis et al. 1999) Ammonia is taken up by $\text{POC}_{\text{cyano}}$ with a C:N ratio of 6.625 (Redfield et al. 1963). For both nutrients the $K_{1/2}$ was 0.1 μM . The effect of uptake and excretion of nitrate, ammonia and phosphate (N:P = 16) on alkalinity was included in the model.

The sedimentation function was based on Stokes' law. In the sensitivity analysis the value of power was -1.32 and -1.08 to give the same total sedimented fluxes as calculated with fixed sedimentation rates of 0.02 and 0.12 d^{-1} (Wal et al. 1995). In the standard run power was set at -1.2. For details, see the description of the SEDIMENTATION function in the Materials & Methods section.

A gross growth rate of 0.69 d^{-1} is based on measurements during the growing phase in a mesocosm study (Bleijswijk & Veldhuis 1995). A solubilisation rate of 0.06 d^{-1} was chosen to give rise to a production of DOC of 0.6 $\text{mol}\cdot\text{m}^{-2}$ (Wiebinga et al. 2000). A degradation rate of 0.07 d^{-1} was used to give a total loss rate of 0.2 d^{-1} (Bleijswijk & Veldhuis 1995).

DOC is a composite of different molecules with differing biodegradabilities. For practical purposes DOC can be subdivided into three pools. The most labile fraction is degraded almost as fast as it is produced (viewed on a daily basis). The second fraction can accumulate during algal blooms, but is located in the upper mixed layer of these high productivity areas, and is thus degraded over timescales at which water transport takes place. The most refractory fraction is degraded only very slowly, and can be found as a constant concentration in the deep ocean, and as the background to the more labile pools in the upper ocean (cf. Wiebinga 1999) The first and last pools have turnover times that fall outside of the scope of this model, and the DOC pool in the model represents only the intermediately refractory fraction. A comparison of DOC profiles taken during different stages of the North Sea bloom of *Emiliania huxleyi* has shown that DOC increases up to the peak of the bloom to a concentration of 0.6 $\text{mol}\cdot\text{m}^{-2}$. The degradation rate was not fast enough to be detectable (Wiebinga et al. 2000). A low remineralisation rate of 0.003 d^{-1} (which gives a half life of 230 days) was used in the standard model, and a rate of 0.03 d^{-1} (which gives a half life of 23 days) in the sensitivity analysis.

Vertical diffusivities in stratified water vary between approximately 10^{-5} and 10^{-4} $\text{m}^2\cdot\text{s}^{-1}$ (Chipman et al. 1993). Since blooms of *E. huxleyi* are normally observed in stable water columns the lower diffusivity was used in the standard model run, and the higher of the two was used in the sensitivity analysis. Using the equation of Broecker (1981): $K_v = 3.7\cdot 10^{-8}\cdot\delta\rho^{-1}\cdot\delta z$ (with $\delta\rho\cdot\delta z^{-1}$ in $\text{kg}\cdot\text{m}^{-4}$), the diffusivities in the bloom in the North Sea varied between $1\cdot 10^{-6}$ and $6\cdot 10^{-6}$ $\text{m}^2\cdot\text{s}^{-1}$. Because the higher diffusivity mentioned above gave virtually the same model output as a diffusivity of 0 these lower values were not used.

In the model all sedimented material is remineralised instantaneously. Since the model results were not very sensitive to diffusion from the deep layer this assumption was not explored any further.

Differential equations

$$\begin{aligned} \mu_{E.hux} &= \mu_{\text{max}, E.hux} * [\text{NO}_3] / ([\text{NO}_3] + K_{1/2, E.hux}) \\ \mu_{\text{cyano}} &= \mu_{\text{max}, \text{cyano}} * [\text{NH}_4] / ([\text{NH}_4] + K_{1/2, \text{NH}_4}) \\ \text{sedim} &= \text{SEDIMENTATION} \\ \text{calcif} &= \text{CALCIFICATION} \\ \text{dissolution} &= \text{conditional (calcif} > \mu_{\text{max}, E.hux} / 2, \text{diss}_{\text{before}}, \text{diss}_{\text{after}}) \\ \delta[\text{NO}_3] \cdot \delta t^{-1} &= -\mu_{E.hux} * \text{POC}_{E.hux} / \text{cn} + \text{DIFN} / \text{mld} \\ \delta\text{POC}_{E.hux} \cdot \delta t^{-1} &= \mu_{E.hux} * \text{POC}_{E.hux} + (-\text{solubilisation} - \text{degradation} + \text{sedim}) * \text{POC}_{E.hux} \\ \delta[\text{POC}_{\text{cyano}}] \cdot \delta t^{-1} &= \mu_{\text{cyano}} * [\text{POC}_{\text{cyano}}] \\ \delta[\text{NH}_4] \cdot \delta t^{-1} &= \text{degradation} * \text{POC}_{E.hux} / \text{cn} - \text{remineralisation} * [\text{DOC}] / \text{cn} - [\text{POC}_{\text{cyano}}] * \\ &\quad \mu_{\text{cyano}} / \text{cn}_{\text{h}_4} \end{aligned}$$

$\delta[\text{DOC}] \cdot \delta t^{-1}$	= solubilisation* $\text{POC}_{E.hux}$ + remineralisation* $[\text{DOC}] + \text{DIFDOC} / \text{mld}$
$\delta[\text{DOC}_{\text{deep}}] \cdot \delta t^{-1}$	= $-\text{DIFDOC} / \text{dld}$
$\delta[\text{CaCO}_3] \cdot \delta t^{-1}$	= $\text{POC}_{E.hux} * (\text{calcif- loss} * (\text{degradation} + \text{solubilisation-sedim})) * \text{cp} + \text{dissolution} * [\text{CaCO}_3] + \text{sedim} * [\text{CaCO}_3]$
$\delta[\text{DIC}] \cdot \delta t^{-1}$	= $-(\mu_{E.hux} - \text{degradation}) * \text{POC}_{E.hux} - (\text{POC}_{E.hux} * (\text{calcif- loss} * (\text{degradation} + \text{solubilisation-sedim})) * \text{cp} + \text{dissolution} * [\text{CaCO}_3]) - \text{remineralisation} * [\text{DOC}] + \text{DIFDIC} / \text{mld} + \text{AIRSEA} - [\text{POC}_{\text{cyano}}] * \mu_{\text{cyano}}$
$\delta[\text{alkalinity}] \cdot \delta t^{-1}$	= $-2 * (\text{POC}_{E.hux} * (\text{calcif- loss} * (\text{degradation} + \text{solubilisation-sedim})) * \text{cp} + \text{dissolution} * [\text{CaCO}_3]) + \text{DIFalk} / \text{mld} - \delta[\text{NO}_3] \cdot \delta t^{-1} * \text{potAlk}_{\text{NO}_3} + \delta[\text{NH}_4] \cdot \delta t^{-1} * \text{potAlk}_{\text{NH}_4}$
$\delta[\text{NO}_{3\text{deep}}] \cdot \delta t^{-1}$	= $-\text{sedim} * \text{POC}_{E.hux} / \text{cn} * \text{mld} / \text{dld} - \text{DIFN} / \text{dld}$
$\delta[\text{DIC}_{\text{deep}}] \cdot \delta t^{-1}$	= $-\text{sedim} * (\text{POC}_{E.hux} + [\text{CaCO}_3]) * \text{mld} / \text{dld} - \text{DIFDIC} / \text{dld}$
$\delta[\text{alkalinity}_{\text{deep}}] \cdot \delta t^{-1}$	= $-2 * \text{sedim} * [\text{CaCO}_3] * \text{mld} / \text{dld} - \text{DIFalk} / \text{dld} - \Delta[\text{N}_{\text{deep}}] \cdot \delta t^{-1} * \text{potAlk}_{\text{NO}_3}$
$[\text{CO}_2]$	= $\text{CO}_2 \text{ from DIC, alkalinity}$
$f\text{CO}_2$	= $[\text{CO}_2] / K_0 \cdot 10^6$

Output [mol·m⁻²]

air sea flux	= $\Sigma \text{AIRSEA} * \text{mld} * 1000$
potential flux	= $(\Sigma \text{AIRSEA} + \text{POTFLUX}) * \text{mld} * 1000$
sedimented CaCO_3	= $\Sigma (\text{sedim} * [\text{CaCO}_3]) * \text{mld} * 1000$
sedimented $\text{POC}_{E.hux}$	= $\Sigma (\text{sedim} * \text{POC}_{E.hux}) * \text{mld} * 1000$
DOC	= $[\text{DOC}] * \text{mld} * 1000$

Rate constants

$\mu_{\text{max}, E.hux}$	maximum growth rate <i>E. huxleyi</i>	0.69 d ⁻¹
$\mu_{\text{max}, \text{cyano}}$	maximum growth rate cyanobacteria	0.69 d ⁻¹
degradation	$\text{POC}_{E.hux} \rightarrow \text{DIC} \ \& \ \text{alkalinity}$	0.07 d ⁻¹
solubilisation	$\text{POC}_{E.hux} \rightarrow \text{DOC}$	0.06 d ⁻¹
remineralisation	$\text{DOC} \rightarrow \text{DIC} \ \& \ \text{alkalinity}$	0.003 d ⁻¹
diss _{before}	$\text{CaCO}_3 \rightarrow \text{DIC} \ \& \ \text{alkalinity}$	0 d ⁻¹
diss _{after}		0.17 d ⁻¹

Constants

$K_{1/2, E.hux}$	half-saturation constant <i>E. huxleyi</i>	0.1 μM
$K_{1/2, \text{cyano}}$	half-saturation constant cyanobacteria	0.1 μM
cn	C:N ratio $\text{POC}_{E.hux}$ and DOC	7.4
cnh ₄	C:N ratio cyanobacteria	6.625
cp	calcification:photosynthesis ratio	0.433
loss	CaCO_3 loss associated with $\text{POC}_{E.hux}$ loss	0.75
potAlk _{NO₃}	effect of NO_3 and HPO_4^{2-} on alkalinity	1.1396 $\mu\text{eq} \cdot \mu\text{M}^{-1}$
potAlk _{NH₄}	effect of NH_4^+ and HPO_4^{2-} on alkalinity	0.875 $\mu\text{eq} \cdot \mu\text{M}^{-1}$
mld	mixed layer depth	40 m
dld	deep layer depth	80 m
k _{dif}	turbulent diffusion between ml & dl	0.0216 m·d ⁻¹
k _{av}	CO_2 gas transfer rate	4.229 m·d ⁻¹
delay	delay between calcification and photosynthesis	2 d

Initial concentrations

$\text{POC}_{E.hux}$	0.1 μM
$[\text{NO}_3, \text{deep}]$	6 μM

[DOC] = [POC _{cyano}] = [NH ₄]	0 μM
[DIC _{deep}]	2157 μM
[alkalinity _{deep}]	2372 μeq·L ⁻¹

Functions

$$\text{DIFx} = k_{\text{dif}} * (x_{\text{dld}} - x_{\text{mld}})$$

$$\text{AIRSEA} = k_{\text{av}} * (\text{CO}_{2,\text{air}} - [\text{CO}_2])$$

$$\text{CALCIFICATION} = \mu_{E,\text{hux}}(\text{time} - \text{delay}).$$

IF time < delay THEN CALCIFICATION = $\mu_{\text{max}, E,\text{hux}}$

CO₂fromDIC,alkalinity = CO₂ calculated from DIC and alkalinity based on the CO2SYSTEM program by Lewis & Wallace (<http://cdiac.esd.ornl.gov/oceans/co2rprt.html>), using K₁ and K₂ according to Roy et al. (1993) and other dissociation constants as compiled by Millero (1995).

POTFLUX = DICfromAlkalinity_{potflux}CO_{2,air} - DIC_{potflux}. Alkalinity_{potflux} and DIC_{potflux} are calculated after mineralisation of all particulate and organic carbon in the mixed layer. DICfromAlkalinity_{potflux}CO_{2,air} works like CO₂fromDICalkalinity.

SEDIMENTATION = -V_{sink}* 3600* 24/ mld. The sinking speed (V_{sink}) is calculated from Stokes' law by interpolation of the following equations:

$$V_{\text{sink}} = (2 * V * g * \Delta\rho / (A * \rho * C_d))^{0.5}$$

$$\text{Re} = V_{\text{sink}} * \rho * r / \eta$$

$$C_d = \text{intercept} * \text{Re}^{\text{power}}$$

The relationship between the drag coefficient (C_d) and the Reynolds number (Re) was of the form derived by Aldredge & Gotschalk (1988), and the parameter values are between those for diatom-dominated marine snow (C_d = 105*Re^{-0.97}) and other marine snow (C_d = 95*Re^{-1.87}, Aldredge & Gotschalk 1988). In the model intercept = 100. In the sensitivity analysis the value of power is varied to obtain sedimentation rates that were comparable to those obtained by using fixed rates of sedimentation between 0.02 and 0.12 d⁻¹ (Wal et al. 1995). V, A and r are the volume, area, and radius of the fecal pellets that constituted the main part of the sedimented material during the North Sea bloom (see Wal et al 1995 for details on the collection of samples). V = 3·10⁻¹³ m³, A = 2.14·10⁻⁹ m² and r = 4.153·10⁻⁵ m. ρ is the density of seawater = 1.0267 kg·L⁻¹. g is the gravitational constant = 9.8 m·s⁻². η is the kinematic viscosity = 1 g·m⁻¹·s⁻¹. The excess density of the sedimented material (Δρ = (M_{E,hux}* POC_{E,hux}+ 100*[CaCO₃])/ (M_{E,hux}*POC_{E,hux}/ ρ_{org}+ 100* [CaCO₃]/ ρ_{CaCO3}) - ρ) was calculated from the effective densities of CaCO₃ and POC_{E,hux} in the ratio of their standing stocks. M_{E,hux} was estimated as 240 g·mol⁻¹, since carbon is about 5% of wet biomass. ρ_{org} was estimated as 1.027 kg·L⁻¹. ρ_{CaCO3} = 1.66 kg·L⁻¹ was estimated from the density of calcite (2.8 kg·L⁻¹) and the amount of water included in the coccosphere, which was estimated from the cell radius with and without coccosphere (Bleijswijk et al. 1994b) and the amount of CaCO₃ per coccosphere (Bleijswijk et al. 1991). There was no sedimentation of CaCO₃ when POC_{E,hux} became 0 μM.

BOFS North Atlantic pCO₂ data

Data of the two cruises with the RRS Charles Darwin (CD60 and CD61) were retrieved from the CD-ROM (Lowry et al. 1994) of the biogeochemical ocean flux study (BOFS). The reported pCO₂ was converted to fCO₂ (Weiss 1974).

Results

Model output

The development of the bloom is characterised by four successive stages:

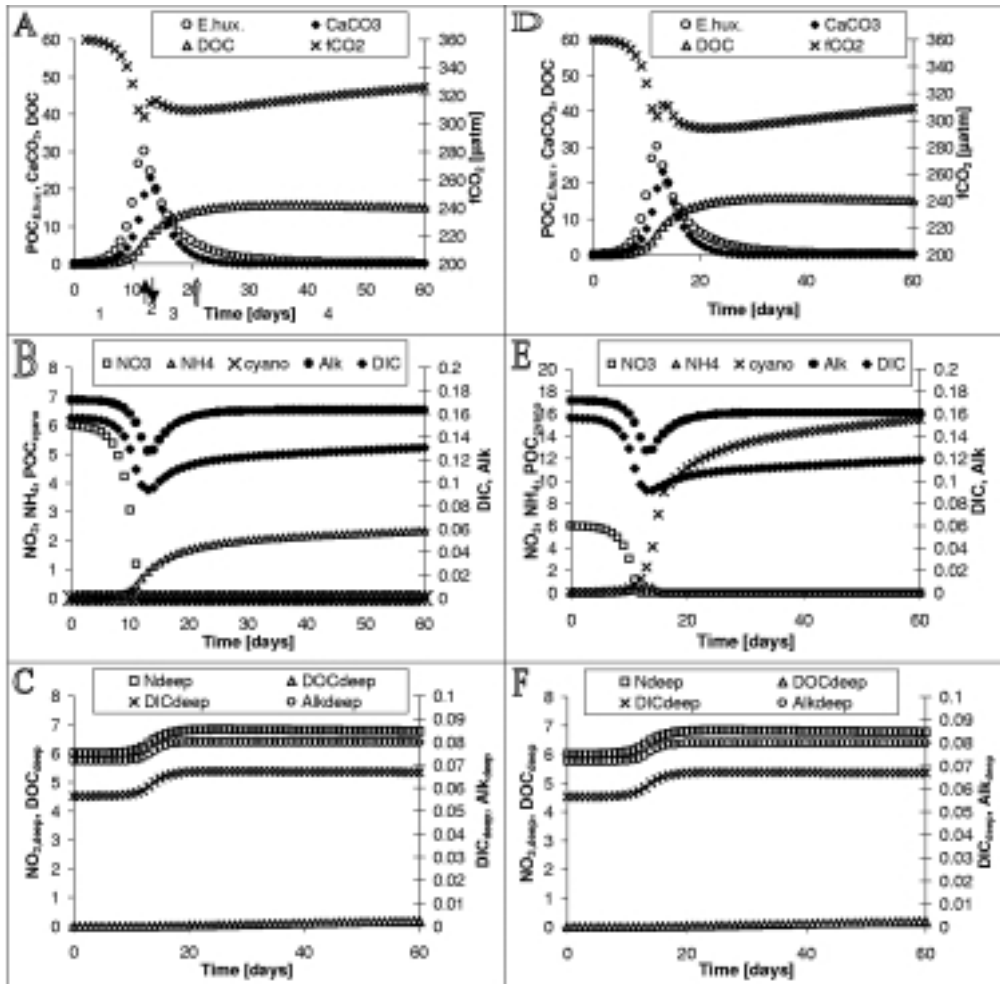


Figure 5.2 a-c) Results of the standard run. d-f) Results including POC_{cyano} using ammonia (NH_4). The successive stages of the bloom marked 1 to 4 are explained in the text. $\uparrow POC_{E.hux}$ maximum, $\downarrow CaCO_3$ maximum, $\uparrow\uparrow$ second fCO_2 minimum. $POC_{E.hux}$, $CaCO_3$, DOC , NO_3 , NH_4 , POC_{cyano} , $NO_{3,deep}$, DOC_{deep} in μM , DIC [mM -2], Alk [meq/L -2.2], DIC_{deep} [mM -2.1] and Alk_{deep} [meq/L -2.3].

Stage 1) The growth stage lasts as long as the gross growth rate is higher than the loss rate. At this point $POC_{E.hux}$ goes through a maximum, fCO_2 goes through a (local) minimum (Figure 5.2a, d) and nitrate (NO_3) is nearly depleted (Figure 5.2b, e). The loss rate is the sum of sedimentation, solubilisation ($POC_{E.hux}$ to DOC) and degradation ($POC_{E.hux}$ to DIC). Degradation and remineralisation (DOC to DIC) release ammonia (Figure 5.2b, e). In the standard model run, which includes only $POC_{E.hux}$ (Figure 5.2a-c), ammonia accumulates (Figure 5.2b), while in the model run which includes cyanobacteria (Figure 5.2d-f), ammonia is used to produce secondary growth of POC_{cyano} (Figure 5.2e).

Stage 2) At the end of the growth stage, when $POC_{E.hux}$ growth becomes nutrient-limited, $CaCO_3$ production continues for another two days, until the dissolution of $CaCO_3$ becomes

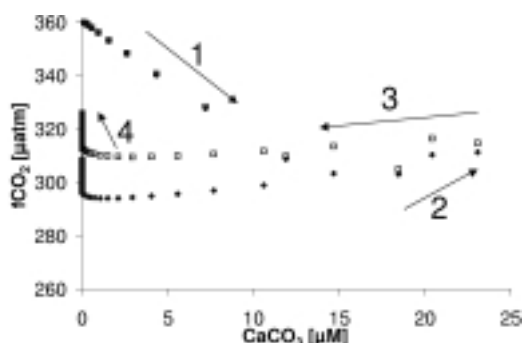


Figure 5.3 The fugacity of CO_2 ($f\text{CO}_2$) as a function of the CaCO_3 standing stock. Arrows indicate the direction of time. The successive stages of the bloom, marked 1-4 are the same as in Figure 5.2. \square $\text{POC}_{\text{cyano}} = 0 \mu\text{M}$ as in Figure 5.2a-c, \blacklozenge $\text{POC}_{\text{cyano, start}} = 0.1 \mu\text{M}$ as in Figure 5.2d-f.

higher than its production, and CaCO_3 goes through a maximum (Figure 5.2a, d). At this point $f\text{CO}_2$ goes through a (local) maximum. The DOC production rate decreases with the decrease in $\text{POC}_{E,\text{hux}}$.

Stages 3 & 4) During the declining phase of the bloom $\text{POC}_{E,\text{hux}}$, CaCO_3 and DOC are mineralised. Mineralisation of $\text{POC}_{E,\text{hux}}$ and DOC increases DIC more than alkalinity. In contrast, dissolution of CaCO_3 increases alkalinity more than DIC (Figure 5.2b,e).

Stage 3) During the early part of the declining phase the dominant process is dissolution of CaCO_3 , and $f\text{CO}_2$ decreases.

Stage 4) During the final stage air-sea exchange of CO_2 and mineralisation of DOC increase the $f\text{CO}_2$. Although depletion of nitrate in the upper mixed layer due to growth (Figure 5.2b, e) and an increase of nitrate in the deep layer by sedimentation (Figure 5.2c, f) create a gradient by which nitrate diffuses upward, this supports only an insignificant amount of $\text{POC}_{E,\text{hux}}$ during the final stage (Figure 5.2a, d). The ammonia that is produced by remineralisation of DOC gives rise to an increase in $\text{POC}_{\text{cyano}}$.

$f\text{CO}_2$ as a function of CaCO_3

Figure 5.3 shows $f\text{CO}_2$ as a function of CaCO_3 . This shows in a different way from Figure 5.2 how the $f\text{CO}_2$ decreases when production of CaCO_3 is coupled to production of $\text{POC}_{E,\text{hux}}$ (stage 1), but increases when production of CaCO_3 takes place at the same time as degradation of $\text{POC}_{E,\text{hux}}$ (stage 2). During the early part of the declining phase the increase in alkalinity outweighs the increase in DIC and therefore $f\text{CO}_2$ decreases (stage 3), while in the final stage $f\text{CO}_2$ increases, primarily due to air-sea gas exchange.

Sensitivity analysis

In Table 5.1 and Figure 5.4 a sensitivity analysis is given of the model parameters. Two air-sea CO_2 exchange values are given: a short-term flux that occurs during the bloom and a long term potential flux that is the ultimate effect of the net transport into the deep layer. The short-term flux is the cumulative flux of air-sea exchange during the model run, and thus takes into consideration all processes that sequester carbon, and is dependent on the time that the model is run. The potential flux is the flux after mineralisation of all the particulate and organic carbon in the upper mixed layer and equilibration of the upper mixed layer with the atmosphere. In other words, the potential flux excludes the effect of increased sequestration of carbon (predominantly in DOC and $\text{POC}_{\text{cyano}}$) that is degraded in the course of the year, and calculates the effective impact of the net transport of DIC, alkalinity and DOC by sedimentation and diffusion to the deep layer (see the POTFLUX function in Materials & Methods for details).

In the parameters that affect $\text{POC}_{E,\text{hux}}$ a clear feedback can be seen between degradation, solubilisation and sedimentation (the latter is controlled by the parameter power, see the SEDIMENTATION function in Materials & Methods). If one of these three rates is increased this decreases the amount of $\text{POC}_{E,\text{hux}}$ that will be passed to the other two processes.

Table 5.1 Sensitivity analysis. PotFlux, potential flux to the deep layer. AirSea, cumulative air-sea gas exchange during the model run. sedCa and sedPOC, cumulative amounts of CaCO₃ and POC, sedimented to the deep layer. DOC amount of DOC in the upper mixed layer at the end of the model run. Output in mol·m⁻².

Parameter*	Value	air-sea flux	potential flux	CaCO ₃ sedimented	POC _{<i>E.hux</i>} sedimented	DOC
Standard run	*	0.29	0.42	0.37	0.51	0.61
Degradation (0.06)	0.03	0.33	0.47	0.38	0.55	0.76
POC _{<i>E.hux</i>} → DIC	0.12	0.22	0.34	0.35	0.43	0.43
delay (2)	0	0.17	0.45	0.08	0.22	0.74
	3	0.26	0.38	0.57	0.61	0.56
Diffusion (0.0216)	0	0.30	0.41	0.37	0.50	0.60
	0.216	0.20	0.43	0.37	0.52	0.67
Dissolution (0/0.17)	0/0	0.18	0.34	0.84	0.70	0.51
	CaCO ₃ → DIC	0.17/0.17	0.26	0.44	0.19	0.36
loss (0.75)	0.44	0.30	0.40	0.48	0.58	0.57
POC _{cyano, start} (0)	0.1	0.29	0.56	0.37	0.51	0.61
NO ₃ (6 μM)	10 μM	0.48	0.65	0.62	0.85	1.01
power (-1.2)	-1.08	0.54	0.42	0.51	0.82	0.46
	-1.32	0.10	0.42	0.17	0.21	0.74
rem mineralisation (0.003)	0.03	0.28	0.34	0.37	0.51	0.19
DOC → DIC						
solubilisation (0.07)	0.03	0.34	0.37	0.38	0.56	0.36
	POC _{<i>E.hux</i>} → DOC	0.14	0.22	0.45	0.34	0.42

* values for standard run in parentheses. For dissolution the two values designate the rates before and after the peak of POC_{*E.hux*}.

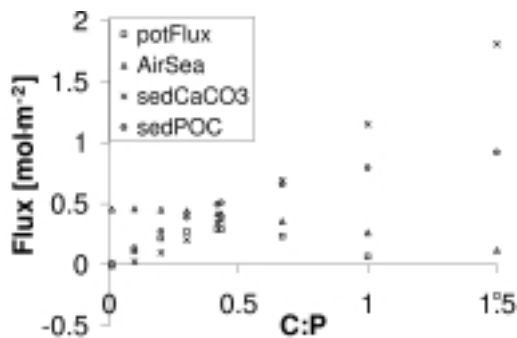


Figure 5.4 Fluxes in the modelled bloom as a function of the C:P ratio of the nitrate-using phytoplankton (POC_{*E.hux*} box). Ammonia is not used (POC_{cyano} = 0 μM). PotFlux is the flux of CO₂ from the atmosphere due to transport of DIC, alkalinity, DOC and NO₃⁻ to the deep layer. AirSea is the flux of CO₂ from the atmosphere during the model run (60 days). SedCaCO₃ and sedPOC are the amounts of CaCO₃ and POC_{*E.hux*} that are sedimented to the deep layer during the model run. Please note that the C:P parameter on the x-axis is not the C:P production ratio, as is explained in the Materials and Methods section.

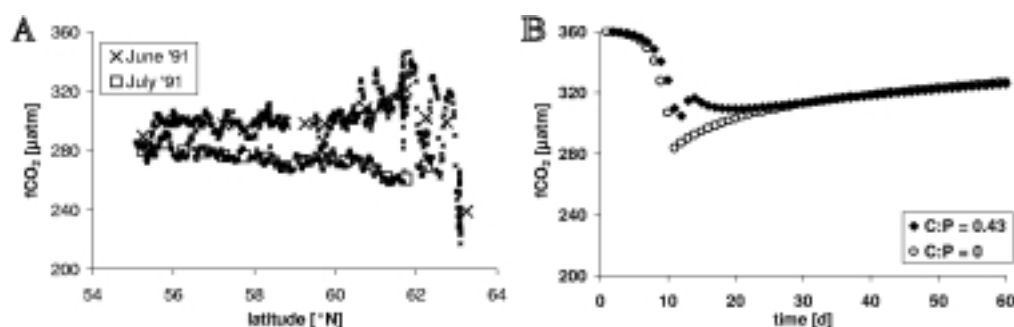


Figure 5.5 a) $f\text{CO}_2$ along the 20°W meridian. \times Transect from 16 – 21 June 1991 during a bloom of *Emiliania huxleyi*. Transect was sampled from South to North. \square Transect from 24 – 26 July 1991. Transect was sampled from North to South. b) Model output of $f\text{CO}_2$ for calcifying (\blacklozenge) and non-calcifying (\diamond) nitrate-using algae.

In Table 5.1 it can be seen that if the rates of degradation or sedimentation are increased the amount of DOC formed is decreased. Likewise, if the rates of degradation or solubilisation are increased the amount of $\text{POC}_{E.hux}$ that is sedimented is decreased. The effect on the amount of $\text{POC}_{E.hux}$ that is degraded is not shown.

The parameters that affect DOC have an opposite effect on the potential flux and the air-sea flux because DOC temporarily sequesters carbon in the upper mixed layer. This DOC will be degraded after the end of the bloom, while the fraction of DOC that is transported to the deep layer by turbulent diffusion is rather limited (Figure 5.2c).

The effect of the changes in CaCO_3 cycling on the potential flux and the air-sea flux is less straightforward. On the one hand the chemical effect of production of CaCO_3 increases $f\text{CO}_2$ and thus decreases the air to sea exchange of CO_2 . On the other hand the physical effect of inclusion of CaCO_3 in fecal pellets increases the sedimentation rate and thus increases the air to sea exchange of CO_2 . The relative importance of these two effects was tested by varying the C:P parameter in the model to simulate a varying proportion of *E. huxleyi* in the nitrate-using phytoplankton or a different C:P production ratio by *E. huxleyi*. Variation of the C:P parameter gives rise to a weak optimum for the air-sea exchange and a sharper optimum for the potential flux (Figure 5.4). The amount of CaCO_3 that is sedimented increases quadratically with the C:P parameter, since there is an increase in both the amount of CaCO_3 and the fraction of CaCO_3 that is sedimented due to the higher density of the sedimented material. The amount of POC that is sedimented increases asymptotically, since the fraction of POC that is sedimented increases to the same extent as CaCO_3 , but the total amount of POC that is produced from a fixed amount of nitrate stays the same. Thus, the amount of atmospheric CO_2 that is drawn down into the sea goes through a maximum. For the short-term flux the maximum lies at a contribution of 23% *E. huxleyi* of the total POC (C:P = 0.1). For the potential flux the maximum lies at a contribution of 97% of the total POC (C:P = 0.42). The difference between these two is primarily caused by the contribution of DOC to the short-term flux: half of the POC that is not sedimented is converted into DOC, and DOC production increases the air-sea flux, but does not affect the potential flux.

Model validation

The model is based on the results of a field expedition in the North Sea in 1993 and a mesocosm study near Bergen, Norway in 1992. In an attempt to verify the validity of the model results with independent data the model output was compared to data from two field

expeditions in the North Atlantic in 1991 that were collected by J. Robertson (Lowry et al. 1994).

In 1991 two cruises with the RRS Charles Darwin took samples along the 20°W meridian. During the first cruise, in June, a bloom of *E. huxleyi* occurred south of Iceland. The results of this cruise are described by Robertson et al. (1994). The 0.5° averages show that fCO₂ was 10 µatm. higher between 61 and 63 °N, where the bloom of *E. huxleyi* was densest, than between 58 and 60 °N (Figure 5.5a). The data between 61 and 63 °N were collected on 20 June, which was in the week when the bloom was at its maximum extent (Robertson et al. 1994). The data of the second cruise were collected one month later. At this time the fCO₂ was 9 µatm. lower in the region where the bloom had been (61 - 63 °N compared to 58 - 60 °N, Figure 5.5a).

For comparison the model output of fCO₂ are shown for the standard model and the model without calcification (C:P = 0). The fCO₂ is 16 µatm. higher in the calcifying bloom during the week after the CaCO₃ peak (Figure 5.5b), when blooms are most visible on satellite images due to shedding of coccoliths by *E. huxleyi*. Thirty days after the CaCO₃ peak fCO₂ is 0.4 µatm. lower in the calcifying bloom. Thus, the model shows the same trends as the field observations (Figure 5.5a, and Buitenhuis et al. 1996), but with a smaller amplitude.

Discussion

Comparison of the model output to the mesocosm and North Sea blooms

Although the gross CaCO₃ production rate of 0.433 is lower than that found for some other strains, it is consistent with the results for strain CH24 (Buitenhuis et al. 1999), which was isolated from the North Sea in 1991 (Bleijswijk et al. 1991). The model outputs are consistent with measurement in the mesocosms of a peak of CaCO₃ that is about ¾ of the POC peak (Bleijswijk et al. 1994a) and in the North Sea of an average CaCO₃:POC sedimentation ratio of 0.7 (Wal et al. 1995).

Comparing the model results to the carbon fluxes that were estimated directly from measurements in the North Sea bloom (1.3 mol C·m⁻² for air-to-sea CO₂-exchange, and 2.4 mol C·m⁻² of sedimentation, Buitenhuis et al. 1996), it can be seen that both the air-sea flux and the sedimented flux in the model are about three times lower. First of all it can be seen from the sensitivity analysis (Table 5.1 and Figure 5.4) that the ranges for the parameter values give a range of model outputs. More importantly, however, there are at least three elements of bias in the model to explain this about threefold difference:

- 1) the contribution of other organisms to the carbon sink has been purposely ignored in the standard run in order to extract the contribution of *E. huxleyi* alone to the fluxes. The inclusion of a box for the cyanobacteria gives a first approximation of the effect of secondary growth on ammonia, but via microzooplankton some of this carbon will also be grazed by mesozooplankton or otherwise be transported out of the upper mixed layer (Koshikawa et al. 1999).

- 2) for the same reason the effects of seasonal warming on fCO₂ and of the wind speed on the surface mixed layer depth have been ignored. The finding that there was a very small correlation between CaCO₃ standing stock and water temperature in the 1993 North Sea bloom (Buitenhuis et al. 1996) in the presence of salinity stratification (Veldhuis 1993) suggests that the correlation of water reflectance and water temperature as found by Ackleson et al. (1988) may be primarily due to a correlation between high stratification and *E. huxleyi* abundance and not to coccolith reflectance causing warming of the upper mixed layer. The influence of (the variability of) the wind speed on the magnitude of the carbon sink during a bloom depends on the relative importance of three processes with opposing effects: a shallow upper mixed layer during low wind speeds increases light availability for photosynthesis while high wind speeds increase air-sea gas exchange and increasing wind speeds deepen the wind mixed layer and thereby entrain nutrient-rich deep waters (Hannon et al. 2000).

3) The C:N ratio of the dissolved organic matter (DOM) and the heterotrophic bacteria (which are not included in the model) is usually found to be higher than the 7.4 of the DOM or the 6.625 of the cyanobacteria ($\text{POM}_{\text{cyano}}$) that is used in the model. This effect was observed as an increase of the particulate POC:PON ratio during the mesocosm bloom (Bleijswijk et al. 1994a). Unfortunately, not enough data are available to include this mechanism in the model.

Another effect of including $\text{POC}_{\text{cyano}}$ in the model is to further uncouple the dissolution of CaCO_3 from the mineralisation of POC. The other mechanism that uncouples these processes is the delay between the peaks of CaCO_3 and $\text{POC}_{E.hux}$. This uncoupling gives rise to a decrease in $f\text{CO}_2$ during dissolution of CaCO_3 (stage 3 in Figure 5.3). By including $\text{POC}_{\text{cyano}}$ the slope of this part of the plot increases from 0.4 to 0.9 $\mu\text{atm} \cdot (\mu\text{M CaCO}_3)^{-1}$. The slope that was found during the North Sea bloom was 3.5 $\mu\text{atm} \cdot \mu\text{M}^{-1}$, indicating that CaCO_3 dissolution, POC remineralisation and secondary growth were even further uncoupled, as indicated by the inverse trends between CaCO_3 and POC in this bloom (Buitenhuis et al. 1996).

Influence of CaCO_3 on air-sea exchange of CO_2

Robertson et al. (1994) found an average increase in $p\text{CO}_2$ (a reduction of the sea-to-air gradient) of 15 μatm . in a bloom of *E. huxleyi*. This was shown by comparing samples in which CaCO_3 was greater than 18 μM with samples in which CaCO_3 was smaller than 5.5 μM . Buitenhuis et al. (1996) found an increase in $f\text{CO}_2$ of 3.5 $\mu\text{atm} \cdot (\mu\text{M CaCO}_3)^{-1}$. Wal et al. (1995) found an enhanced sedimentation of both POC and CaCO_3 in the latter of these blooms due to the increased density of fecal pellets, loaded with coccoliths, with an inferred increased sinking rate of the fecal pellets. Buitenhuis et al. (1996) noted the inconsistency between this increase in $f\text{CO}_2$ and an enhanced sedimentation, and also calculated a carbon sink of 1.3 $\text{mol C} \cdot \text{m}^{-2}$ for this bloom. With the described model these data can be reinterpreted into a consistent explanation. This was possible because the model adds a direction of time to the observations that were collected at different locations in the field studies. The results of the model indicate that the correlation between CaCO_3 and $f\text{CO}_2$ (stage 3 in Figure 5.3) does not represent an increase in $f\text{CO}_2$ as CaCO_3 is produced, but a decrease in $f\text{CO}_2$ as CaCO_3 is dissolved. This is consistent with the fact that both field studies were conducted during the end phase of the blooms, that is, when they were visible on satellite images due to light scattering of coccoliths (Robertson et al. 1994, Buitenhuis et al. 1996).

Thus, it cannot be concluded from the field data that there is a negative correlation between the amount of CaCO_3 that is produced and the air to sea flux of CO_2 . Therefore, we have addressed this question anew with the model, by performing a sensitivity analysis of the short-term and long-term air-sea CO_2 fluxes as a function of the C:P parameter (Figure 5.4). The most significant feature of this correlation is that the air-sea flux is highest at a C:P parameter value greater than 0, in other words, calcification stimulates the air-sea flux up to a certain point, after which it decreases again. The magnitude of the optimum C:P parameter value is subject to our choice of parameters (such as the change in porosity of the fecal pellets by inclusion of CaCO_3 , which was estimated by an indirect method, see SEDIMENTATION function in Materials & Methods. However, with recent improvements of the sensitivity in chemical analytical methods it should now be possible to derive the correlation between the POC and CaCO_3 contents in individual fecal pellets (POC: Ulrich-Rich et al 1998, CaCO_3 : within the detection range of graphite furnace AAS) and their densities (Urban et al. 1993) and sinking rates (Harris 1994). Together with the degradation rate (Plouf et al. 1999) this would give the correlation between the CaCO_3 :POC ratio in the water column and sedimentation rate in a more direct way.

The density excess of diatom frustules, like that of coccoliths, is much higher than that of organic material. Therefore it might be expected that the same mechanism that was found in a bloom of *E. huxleyi* (Wal et al. 1995) would function in blooms of diatoms. However, the

results of Urban et al. (1993) indicate that this may not be the case, due to a lower packing index when the dominant food source was diatoms. The density of fecal pellets changed with the diet of the zooplankton, increasing in the order of diatoms, nanoflagellates and a mixed population including coccolithophores.

Implication for paleoreconstruction and effect of enhanced sedimentation on geological time scales

Our results indicate that even at a modest nitrate concentration of 6 μM at the start of the bloom approximately half of the biomass is produced at an $f\text{CO}_2$ that is more than 32 μatm lower than at the start of the bloom. This implies that the paleoreconstruction of Jasper et al. (1994) may underestimate the oversaturation of upwelling water, because their reconstruction of the $f\text{CO}_2$ of upwelled equatorial Pacific waters over the past 225,000 years was based on the $^{13}\text{C}/^{12}\text{C}$ ratio of alkenones in the sediment that were produced by prymnesiophyte algae (of which *E. huxleyi* is a member). Thus, most of the signal would be produced during periods when algal growth is high and $f\text{CO}_2$ is relatively low. Moreover, this underestimation could have been larger if production during glacial periods would have been higher, so that the glacial to interglacial difference in oversaturation would have been even larger than the presented 50 μatm (Jasper et al. 1994).

When the effect of CaCO_3 to stimulate the co-sedimentation of POC is extrapolated to geological time scales, the control of the alkalinity budget of the ocean on the cycling of CaCO_3 becomes important. The cycling of CaCO_3 is not controlled by production. Rather, export of Ca /alkalinity from the upper ocean exceeds import, mostly by rivers, and the excess dissolves in the deep sea. The balance between these processes is maintained by the depth of the saturation horizon of calcite (Milliman et al. 1999). Since atmospheric CO_2 is not controlled by CaCO_3 production in the surface ocean, we suggest that the effect of CaCO_3 to stimulate sedimentation of POC may enhance drawdown of CO_2 from the atmosphere even more clearly on long time scales than the presented model results for a seasonal bloom suggest.

Summary

Integrating an extensive data set on the cycling of carbon within blooms of *Emiliania huxleyi* into a model it was shown how a positive correlation of $f\text{CO}_2$ and CaCO_3 within blooms can be consistent with an enhanced carbon sink for coccolithophorid blooms. It was found that the air to sea CO_2 flux as a function of the C:P parameter shows an optimum C:P parameter value. While the exact value of the optimum C:P parameter value is influenced by many assumptions in the model, the basic form of this function is due to three assumptions:

- 1) there is a positive correlation between the CaCO_3 :POC standing stock ratio in the medium and in the fecal pellets. In the model this correlation is 1:1 as found by Harris (1994);
- 2) there is a positive correlation between CaCO_3 content of fecal pellets and sinking rate. This is predicted by Stokes' law;
- 3) there is a positive correlation between sinking rate and sedimentation rate.

Additionally, a shortage of data was identified in the following areas:

- 1) the rates of production and degradation of DOC;
- 2) the degradation of POC to DIC;
- 3) the role of cyanobacteria in using regenerated ammonia, and maintaining low $f\text{CO}_2$ pressures during the collapse of the blooms of *E. huxleyi*, and the importance of the coupling between the microbial loop and the classical food chain by micro- and mesozooplankton grazing;
- 4) the importance of changes in the C:N ratio from new production to DOC and bacterial production to increase the carbon sink per unit of nutrient; and
- 5) the relationship between the CaCO_3 content of fecal pellets and the sedimentation rate.

More generally speaking, the processes of production are much better documented than the processes of decline. Rather than claiming to have provided any definitive carbon budget, we hope to have provided some new insights, as a guide towards obtaining a more accurate budget in the future.

Acknowledgements

We would like to thank all the people who were involved in the field cruise and mesocosm experiments that were the basis for the presented model, with special thanks to Judith van Bleijswijk, Rob Kempers, Marcel Veldhuis and Jorun Egge. We would like to thank Judith van Bleijswijk and Wil Buitenhuis for their helpful comments on the manuscript.

References

- Ackleson S, W M Balch, P M Holligan (1988) White waters of the Gulf of Maine. *Oceanography* **1** (20) 18-22
- Allredge A L, C Gotschalk (1988) In situ settling behavior of marine snow. *Limnol. Oceanogr.* **33** (3) 339-351
- Anning T, N Nimer, M J Merrett, C Brownlee (1996) Costs and benefits of calcification in coccolithophorids. *J. mar. syst.* **9** 45-56
- Bakker D C E, H J W de Baar, U V Bathmann (1997) Changes of carbon dioxide in surface waters during spring in the Southern Ocean. *Deep Sea Res. II* **44** (1-2) 91-128
- Bakker D C E (1998) Process studies of the air-sea exchange of carbon dioxide in the Atlantic Ocean. PhD thesis, Rijksuniversiteit Groningen, The Netherlands
- Balch W, R Evans, J Broewen, G Feldman, c McClain, W Esaias (1992) The remote sensing of ocean primary productivity: use of a new data compilation to test satellite algorithms. *J. Geophys. Res.* **97** (C2) 2279-2293
- Bates R G (1975) pH scales for sea water. *In: Dahlem workshop on the nature of seawater. Phys. Chem. Sci. Res. Rep.* **1**, p 313-331
- Berger W H, V S Smetacek, G Wefer (1989) Ocean productivity and paleoproductivity - an overview. *In: Productivity in the ocean: present and past.* Berger W H, V S Smetacek, G Wefer (eds.) John Wiley & Sons Ltd, p 1-34
- Bleijswijk J D L van (1996) Ecophysiology of the calcifying marine alga *Emiliana huxleyi*. PhD thesis, Rijksuniversiteit Groningen, The Netherlands, 71 p., ISBN 90-367-0575-4
- Bleijswijk J D L van, M J W Veldhuis (1995) In situ gross growth rates of *Emiliana huxleyi* in enclosures with different phosphate loadings revealed by diel changes in DNA content. *Mar. Ecol. Progr. Ser.* **121** 271-277
- Bleijswijk J van , P van der Wal, R Kempers, M Veldhuis (1991) Distribution of two types of *Emiliana huxleyi* (Prymnesiophyceae) in the northeast Atlantic region as determined by immunofluorescence and coccolith morphology. *J. Phycol.* **27** 566-570
- Bleijswijk J D L van , R S Kempers, M J Veldhuis (1994a) Cell and growth characteristics of types A and B of *Emiliana huxleyi* (Prymnesiophyceae) as determined by flow cytometry and chemical analyses. *J. Phycol.* **30** 230-241
- Bleijswijk J D L van, E S Kempers, P van der Wal, P , J K Egge, T Lukk (1994b) Standing stocks of PIC, POC, PON and *Emiliana huxleyi* coccospheres and liths in seawater enclosures with different phosphate loadings. *Sarsia* **79** 307-317
- Boden T A, D P Kaiser, R J Sepanski, F W Stoss (1994) Trends '93: A compendium of data on global change. Carbon dioxide information analysis centre, Oak Ridge national laboratory, Oak Ridge, Tennessee
- Bolin B, E T Degens, S Kempe, P Ketner (1979) The global carbon cycle. Wiley & sons, Chichester, UK
- Brewer P G, J C Goldman (1976) Alkalinity changes generated by phytoplankton growth. *Limnol. Oceanogr.* **21** (1) 108-117
- Broecker W S (1981) Geochemical tracers and ocean circulation. *In: BA Warren & C Wunsch* (eds.) Evolution of physical oceanography, MIT press, Cambridge, USA, p 434-460
- Broecker W S, T H Peng (1982) Tracers in the sea. Lamont-Doherty geological observatory, Columbia university, Palisades, New York 10964, USA
- Broecker W S, A Sanyal (1998) Does atmospheric CO₂ police the rate of chemical weathering? *Glob biogeochem cycles* **12** (3) 403-408
- Brown C W, J A Yoder (1994) Coccolithophorid blooms in the global ocean. *J. Geoph. Res.* **99** (C4) 7467-7482

- Brownlee C, M Davies, N Nimer, L F Dong, M J Merrett (1995) Calcification, photosynthesis and intracellular regulation in *Emiliana huxleyi*. *Bull inst. oceanogr Monaco* **14** (2) 19-35
- Bruland K W (1989) Complexation of zinc by natural organic ligands in the central North Pacific. *Limn. Oceanogr.* **34** (2) 269-285
- Buitenhuis E, J van Bleijswijk, D Bakker, M Veldhuis (1996) Trends in inorganic and organic carbon in a bloom of *Emiliana huxleyi* in the North Sea. *Mar. Ecol. Progr. Ser.* **143** 271-282
- Buitenhuis E T, H J W de Baar, M J W Veldhuis (1999) Photosynthesis and calcification by *Emiliana huxleyi* (Prymnesiophyceae) as a function of inorganic carbon species. *J. Phycol.* **35** (5) 949-959
- Butcher S S, R J Charlson, G H Orians, G V Wolfe (eds.) (1992) Global biogeochemical cycles. Academic Press, London, UK
- Campbell L, D Vaultot (1993) Photosynthetic picoplankton community structure in the subtropical North Pacific Ocean near Hawaii (station ALOHA). *Deep Sea Res.* **40** (10) 2043-2060
- Chamberlin T C (1898) Influence of great epochs of limestone formation on the constitution of the atmosphere. *J. Geol.* **6** 609-621
- Chipman D W, J Marra, T Takahashi (1993) Primary production at 47°N and 20°W in the North Atlantic Ocean: a comparison between the ¹⁴C incubation method and the mixed layer carbon budget. *Deep Sea Res. II* **40** (1/2) 151-169
- Ciais P, P P Tans, M Trolier, J W C White, R J Francey (1995) A large northern hemisphere terrestrial CO₂ sink indicated by the ¹³C/¹²C ratio of atmospheric CO₂. *Science* **269** 1098-1102
- Clercq M le (1997) Radiocarbon in marine dissolved organic carbon. PhD thesis, Rijksuniversiteit Groningen, The Netherlands, 118 p.
- Crawford D W, Purdie D A (1997) Increase of PCO₂ during blooms of *Emiliana huxleyi*: theoretical considerations on the asymmetry between acquisition of HCO₃⁻ and respiration of free CO₂. *Limnol. Oceanogr.* **42** (2) 365-372
- Dickson A G (1981) An exact definition of total alkalinity and a procedure for the estimation of alkalinity and total inorganic carbon from titration data. *Deep sea res.* **28A** (6) 609-623
- DOE (1991) Handbook of methods for the analysis of the various parameters of the carbon dioxide system in sea water. Dickson A G, C Goyet (eds.) version 1.0
- DOE (1994) Handbook of methods for the analysis of the various parameters of the carbon dioxide system in sea water. Dickson A G, C Goyet (eds.) version 2
- Dong L F, N A Nimer, E Okus, M J Merrett (1993) Dissolved inorganic carbon utilization in relation to calcite production in *Emiliana huxleyi* (Lohmann) Kamptner. *New Phytologist* **123** 679-684
- Droop M R (1983) 25 Years of algal growth kinetics. *Botanica Marina* **26** 99-112
- Egge J K (1993) Nutrient control of phytoplankton growth: effects of macronutrient composition (N, P, Si) on species succession. PhD thesis, University of Bergen, Norway
- Egge J K, B R Heimdal (1994) Blooms of phytoplankton including *Emiliana huxleyi* (Haptophyta). Effects of nutrient supply in different N:P ratios. *Sarsia* **79** (4) 333-348
- Faústro da Silva J J R, Williams R J P (1991) The biological chemistry of elements: The inorganic chemistry of life. Clarendon Press, Oxford
- Goyet C, A Poisson (1989) New determination of carbonic acid dissociation constants in seawater as a function of temperature and salinity. *Deep Sea Res.* **36** (11) 1635-1654
- Goyet C, F J Millero, A Poisson, D K Shafer (1993) Temperature dependence of CO₂ fugacity in seawater. *Mar. Chem.* **44** 205-219
- Graham D, M L Reed, B D Patterson, D G Hockley (1984) Chemical properties, distribution, and physiology of plant and algal carbonic anhydrases. *Annls. NY. Acad. Sci.* **429** 222-237

- Guillard R R L (1975) Culture of phytoplankton for feeding marine invertebrates. *In: Smith W L & M H Chanley (Eds.) Culture of marine invertebrate animals*. Plenum press, New York, p 29-60
- Hannon E, M Stoll, H J W de Baar, C Veth, C Lancelot (2000) Control of CO₂ drawdown in the Southern Ocean by iron and wind: a modelling study. In preparation.
- Harris R P (1994) Zooplankton grazing on the coccolithophore *Emiliana huxleyi* and its role in inorganic carbon flux. *Mar. Biol.* **119** 431-439
- Hay W W (1985) Potential errors in estimates of carbonate rock accumulating through geologic time. *In: The carbon cycle and atmospheric CO₂: natural variations archaic to present*. E T Sundquist & W S Broecker (eds.) American geophysical union, Washington D.C., USA
- Hay W W, E Zakevich (1999) Cesare Emiliani (1922-1995): the founder of paleoceanography *Internatl. Microbiol.* **2** 52-54
- Hayes J M, B N Popp, R Takigiku, M W Johnson (1989) An isotopic study of biogeochemical relationships between carbonates and organic carbon in the Greenhorn Formation. *Geochim. Cosmochim. Acta* **53** 2961-2972
- Herbert F (1985) Eye. Ace, New York, USA
- Holligan P M, W M Balch (1991) From the ocean to cells: coccolithophore optics and biogeochemistry. *In: Particulate analysis in oceanography*, NATO ASI **27** S Demers (ed) Springer Verlag, New York, p 301-324
- Holligan P M, E Fernandez, J Aiken, W M Balch, P Boyd, P H Burkill, M Finch, S B Groom, G Malin, K Muller, D A Purdie, C Robinson, C C Trees, S M Turner, P van der Wal (1993) A biogeochemical study of the coccolithophore, *Emiliana huxleyi*, in the North Atlantic. *Glob. Biogeochem. Cycl.* **7** (4) 879-900
- Huxley T H (1868) On some organisms living at great depths in the North Atlantic Ocean. *Quart. J. Microscopical Soc.* New Ser. **8** 203-212
- IPCC (1990) Climate change. Cambridge university press, Cambridge, UK
- IPCC (1996) Climate change 1995. Cambridge university press, Cambridge, UK
- Jasper J P, J M Hayes, A C Mix, F G Prahl (1994) Photosynthetic fractionation of ¹³C and concentrations of dissolved CO₂ in the central equatorial Pacific during the last 255,000 years. *Paleocean.* **9** (6) 781-798
- Jordan R, J C Green (1994) A checklist of extant Haptophyta of the world. *J. Mar. Biol. Ass.* **74** 149-174
- Keeling C D, J F S Chin, T P Whorf (1996) Increased activity of northern vegetation inferred from atmospheric CO₂ measurements. *Nature* **382** 146-149
- Koshikawa H, S Harada, M Watanabe, K Kogure, T Ioriya, K Kohata, T Kimura, K Sato, T Akehata (1999) Influence of plankton community structure on the contribution of bacterial production to metazooplankton in a coastal mesocosm. *Mar. Ecol. Progr. Ser.* **186** 31-42
- Kump L R, M A Arthur (1999) Interpreting carbon-isotope excursions: carbonates and organic matter. *Chem. Geol.* **161** 181-198
- Lalli C M, T R Parsons (1993) Biological oceanography: an introduction. Pergamon press, Oxford.
- Laws E A, B N Popp, R R Bidigare, M C Kennicutt, S A Macko (1995) Dependence of phytoplankton carbon isotopic composition on growth rate and [CO₂]_{aq}: theoretical considerations and experimental results. *Geochim. Cosmochim. Acta* **59** (6) 1131-1138
- Lowry R K, P Machin, R N Cramer (1994) The Biogeochemical Ocean Flux Study North Atlantic Data Set CD-ROM. British Oceanographic Data Centre, Birkenhead, UK. <http://www.pol.ac.uk/bodc/bofs.html>
- MacArthur R H, E O Wilson (1967) The theory of island biogeography. Princeton university press, Princeton, N.J., USA

- McConnaughey T (1989a) ^{13}C and ^{18}O isotopic disequilibrium in biological carbonates: I. Patterns. *Geochim. Cosmochim. Acta* **53** 151-162
- McConnaughey T (1989b) ^{13}C and ^{18}O isotopic disequilibrium in biological carbonates: II. In vitro simulation of kinetic isotope effects. *Geochim. Cosmochim. Acta* **53** 163-171
- McConnaughey T (1994) Calcification, photosynthesis, and global carbon cycles. *Bull. Inst. Oceanogr. Monaco* **13** (special) 137-156
- McIntyre A (1970) *Gephyrocapsa protohuxleyi* sp. n. a possible phyletic link and index fossil for the Pleistocene. *Deep Sea Res.* **17** 187-190
- McIntyre A, A W H Bé (1967) Modern coccolithophorids of the Atlantic Ocean – I. Placoliths and cyrtoliths. *Deep Sea Res.* **14** 561-597
- Medlin L K, G L A Barker, L Campbell, J C Green, P K Hayes, D Marie, S Wrieden, D Vault (1996) Genetic characterisation of *Emiliana huxleyi* (Haptophyta). *J. Mar. Syst.* **9** (1/2) 13-31
- Menard H W, S M Smith (1966) Hypsometry of ocean basin provinces. *J. Geophys. Res.* **71** (18) 4305-4325
- Michaelis M, M L Menten (1913) Kinetics of invertase action. *Zeitschrift für Biochemie* **49** 333
- Millero F J (1995) Thermodynamics of the carbon dioxide system in the oceans. *Geochim. Cosmochim. Acta* **59** (4) 661-677
- Milliman J D, P J Troy, W M Balch, A K Adams, Y-H Li, F T Mackenzie (1999) Biologically mediated dissolution of calcium carbonate above the chemical lysocline? *Deep Sea Res. I* **46** 1653-1669
- Mills E (1989) Biological oceanography. An early history, 1870-1960. Cornell University Press, Ithaca, USA
- Mook W G, J C Bommerson, W H Staverman (1974) Carbon isotope fractionation between dissolved bicarbonate and gaseous carbon dioxide. *Earth Planet. Sci. Letters* **22** 169-176
- Morel F M M (1987) Kinetics of nutrient uptake and growth in phytoplankton. *J. Phycol.* **23** 137-150
- Morel F M M, J G Reinfelder, S B Roberts, C P Chamberlain, J G Lee, D Yee (1994) Zinc and carbon colimitation of marine phytoplankton. *Nature* **369** 740-742
- Morse J W, F T Mackenzie (1990) Geochemistry of sedimentary carbonates. Elsevier, Amsterdam, The Netherlands ISBN 0-444-88781-4
- Mucci A (1983) The solubility of calcite and aragonite in seawater at various salinities, temperatures and one atmosphere total pressure. *Am. J. Sci.* **283** (7) 780-799
- Muggli, Harrison (1996) EDTA suppresses the growth of oceanic phytoplankton from the Northeast Subarctic Pacific. *J. Exp. Biol. Ecol.* **205** 221-227
- Nimer N A, Q Guan, M J Merrett (1994a) Extra and intra-cellular carbonic anhydrase in relation to culture age in a high-calcifying strain of *Emiliana huxleyi* Lohmann. *New Phytol.* **126** 601-607
- Nimer N A, C Brownlee, M J Merrett (1994b) Carbon dioxide availability, intracellular pH and growth rate of the coccolithophore *Emiliana huxleyi*. *Mar. Ecol. Progr. Ser.* **109** 257-262
- Nimer N A, L F Dong, Q Guan, M J Merrett (1995) Calcification rate, dissolved inorganic carbon utilization and carbonic anhydrase activity in *Emiliana huxleyi*. *Bull. Inst. Oceanogr. Monaco* **14** (2) 43-49
- Paasche E (1962) Coccolith formation. *Nature* **193** 1094-1095
- Paasche E (1964) A tracer study of the inorganic carbon uptake during coccolith formation and photosynthesis in the coccolithophorid *Coccolithus huxleyi*. *Physiologia Plantarum suppl.* **III** 1-82
- Paasche E (1998) Roles of nitrogen and phosphorus in coccolith formation in *Emiliana huxleyi* (Prymnesiophyceae). *Eur. J. Phycol.* **33** 324-330

- Paasche E, S Brubak (1994) Enhanced calcification in the coccolithophorid *Emiliania huxleyi* (Haptophyceae) under phosphorus limitation. *Phycologia* **33** 324-330
- Pienaar R N (1994) Ultrastructure and calcification of coccolithophores. *In: Coccolithophores*, A Winter & W G Siesser (eds.) p 63-82
- Pilson M E Q (1998) An introduction to the chemistry of the sea. Prentice Hall, Upper Saddle River, NJ, USA
- Ploug H, H-P Grossart, F Azam, B B Jorgenson (1999) Photosynthesis, respiration, and carbon turnover in sinking marine snow from surface waters of Southern California Bight: implications for the carbon cycle in the ocean. *Mar. Ecol. Progr. Ser.* **179** 1-11
- Price G D, M R Badger (1989) Ethoxzolamide inhibition of CO₂ uptake in the cyanobacterium *Synechococcus* PCC7942 without apparent inhibition of internal carbonic anhydrase activity. *Plant. Physiol.* **89** 37-43
- Purdie D A, M S Finch (1994) Impact of a coccolithophorid on dissolved carbon dioxide in sea water enclosures in a Norwegian fjord. *Sarsia* **79** (4) 28-425
- Raven J A, A M Johnston (1991) Mechanisms of inorganic carbon acquisition in marine phytoplankton and their implications for the use of other resources. *Limnol. Oceanogr.* **36** (8) 1701-1714
- Raven J A, W J Lucas (1985) Energy costs of carbon acquisition. *In: Inorganic carbon uptake by aquatic photosynthetic organisms*. W J Lucas & J A Berry (eds.) Am. Soc. Plant Physiol. p 305-324
- Raven J A, A M Johnston, D H Turnpin (1993) The influence of changes in CO₂ concentration and temperature on marine phytoplankton ¹³C/¹²C ratios: an analysis of possible mechanisms. *Glob. Plan. Change* **8** (1/2) 1-12
- Redfield A C, B H Ketchum, F A Richards (1963) The influence of organisms on the composition of sea-water. *In: The sea*, vol. 2. M N Hill (ed.) Interscience, New York, USA, 26-77
- Riebesell U Pathways of carbon acquisition in marine phytoplankton: I. Carbonic anhydrase. Unpublished.
- Riegman R, A A M Noordeloos, G C Cadée (1992) Phaeocystis blooms and eutrophication of the continental coastal zones of the North Sea. *Mar. Biol.* **112** 479-484
- Riegman R, W Stolte, A A M Noordeloos (1998) A model system approach to biological climate forcing: the example of *Emiliania huxleyi*. (b) Physiology. NIOZ rapport 1998-8, P.O.box 59, 1790 AB Texel, The Netherlands
- Robertson J E , A J Watson, C Langdon, R D Ling, J W Wood (1993) Diurnal variation in surface pCO₂ and O₂ at 60°N, 20°W in the North Atlantic. *Deep Sea Res.* **40** (1/2) 409-422
- Robertson J E, C Robinson, D R Turner, P Holligan, A J Watson, P Boyd, E Fernandez, M Finch (1994) The impact of a coccolithophore bloom on oceanic carbon uptake in the northeast Atlantic during summer 1991. *Deep Sea Res.* **41** (2) 297-314
- Ronov (1980) Sedimentary cover of the earth. Nauka, Moscow, (in Russian)
- Roy R N , L N Roy, K M Vogel, C Porter-Moore, T Pearson, C E Good, F J Millero, D M Campbell (1993) The dissociation constants of carbonic acid in seawater at salinities 5 to 45 and temperatures 0 to 45 °C. *Mar. Chem.* **44** 249-267
- Siesser W G (1994) Historical background of coccolithophore studies. *In: Coccolithophores*, A Winter & W G Siesser (eds.) p 1-11
- Sikes C S , R D Roer, K M Wilbur (1980) Photosynthesis and coccolith formation: Inorganic carbon sources and net inorganic reaction of deposition. *Limnol. Oceanogr.* **25** (2) 248-261
- Sikes C S , K M Wilbur (1982) Functions of coccolith formation. *Limnol. Oceanogr.* **27** (1) 18-26
- Spero H J, J Bijma, D W Lea, B E Bemis (1997) Effect of seawater carbonate chemistry on planktonic foraminiferal carbon and oxygen isotope values. *Nature* **390** 497-500

- Stoll M H C (1994) Inorganic carbon behaviour in the North Atlantic Ocean. PhD thesis, Rijksuniversiteit Groningen, The Netherlands
- Stolte W (1996) Size-dependent restrictions on competition for nutrients by marine phytoplankton. PhD thesis Rijksuniversiteit Groningen, The Netherlands
- Strathmann R R (1967) Estimating the organic carbon content of phytoplankton from cell volume or plasma volume. *Limnol. Oceanogr.* **12** 411-418
- Sunda W G, S A Huntsman (1992) Feedback interactions between zinc and phytoplankton in seawater. *Limnol. Oceanogr.* **37** (1) 25-40
- Sunda W G, S A Huntsman (1995) Co and Zn interreplacement in marine phytoplankton: Evolutionary and ecological implications. *Limnol. Oceanogr.* **40** 1404-1417
- Takahashi M, K Kikuchi, Y Hara (1985) Importance of picocyanobacteria biomass (unicellular, blue-green algae) in the phytoplankton population of the coastal waters of Japan. *Mar. Biol.* **89** 63-69
- Thode H G, M Shima, C F Rees, K V Krishnamurty (1965) Carbon-13 isotope effects in systems containing carbon dioxide, bicarbonate and metal ions. *Canad. J. Chem.* **43** 582
- Tortell, Morel (1999) Phytoplankton / CO₂ studies in the North Pacific Ocean. *EOS* **40** (49) 212
- Trilling L, H Bloom (1973) T. H. Huxley (1825-1895) In: The Oxford anthology of English literature, victorian prose and poetry. Oxford university press, New York, USA. p. 269-272.
- Tsuzuki M, S Miyachi (1989) The function of carbonic anhydrase in aquatic photosynthesis. *Aquatic botany* **34** 85-104
- Ulrich-Rich J, D A Hansell, M R Roman (1998) Analysis of copepod fecal pellet carbon using a high temperature combustion method. *Mar. Ecol. Progr. Ser.* **171** 199-208
- Urban J L, D Deibel, P Schwinghamer (1993) Seasonal variation in the densities of fecal pellets produced by *Oikopleura vanhoeffeni* (C. Larvacea) and *Calanus finmarchicus* (C. Copepoda). *Mar. Biol.* **117** 607-613
- Veldhuis M J W (1993) Bloom93 vaarverslag. Unpublished
- Veldhuis M J W, G W Kraay, J D L van Bleijswijk (1997) Seasonal and spatial variability in phytoplankton biomass, productivity and growth in the northwestern Indian Ocean: the southwest and northeast monsoon, 1992-1993. *Deep Sea Res. I* **40** (3) 425-449
- Verardo D J, P N Froelich, A McIntyre (1990) Determination of organic carbon and nitrogen in marine sediments using the Carlo Erba NA-1500 analyzer. *Deep Sea Res.* **37** (1) 157-165
- Verkoren (2000) De atlas van de toekomst. *Trouw* 29-1-2000
- Vogel J C, P M Grootes, W G Mook (1970) Isotope fractionation between gaseous and dissolved carbon dioxide. *Z. Phys.* **230** 225-238
- Wal P van der, J D L van Bleijswijk, J K Egge (1994) Primary productivity and calcification rate in blooms of the coccolithophorid *Emiliania huxleyi* (Lohmann) Hay et Mohler developing in mesocosms. *Sarsia* **79** (4) 401-408
- Wal P van der, R S Kempers, M J W Veldhuis (1995) Production and downward flux of organic matter and calcite in a North Sea bloom of the coccolithophore *Emiliania huxleyi*. *Mar. Ecol. Progr. Ser.* **126** 247-265
- Wanninkhof R (1992) Relationship between wind speed and gas exchange over the ocean. *J. Geophys. Res.* **97** (c5) 7373-7382
- Wanninkhof R, K Thoning (1993) Measurement of fugacity of CO₂ in surface water using continuous and discrete sampling methods. *Mar. Chem.* **44** 189-204
- Weiss R F (1974) Carbon dioxide in water and seawater: the solubility of a non-ideal gas. *Mar. Chem.* **2** 203-215
- Westbroek P (1991) Life as a geological force: dynamics of the earth. Norton, New York, USA
- Westbroek P, E W de Vrind-de Jong, P van der Wal, A H Borman, J P M de Vrind (1985) Biopolymer-mediated Ca and Mn accumulation and biomineralization. *Geologie en Mijnbouw* **64** 5-15

- Westbroek P, J R Young, K Linschooten (1989) Coccolith production (biomineralization) in the marine alga *Emiliana huxleyi*. *J. Protozool.* **36** (4)368-373
- Westbroek P, B Buddemeier, M Coleman, D J Kok, D Fautin, L Stal (1994) Strategies for the study of climate forcing by calcification. *Bull. Inst. Oceanogr. Monaco* **13** (special) 37-60
- Westbroek P, C Brown, J van Bleijswijk, c Brownlee, G Brummer, M Conte, J Egge, E Fernandez, R Jordan, M Knappetsbusch, J Stefers, M Veldhuis, P van der Wal, J Young (1993) A model system approach to biological climate forcing. The example of *Emiliana huxleyi*. *Glob. Planet. Change* **8** 27-46
- Wiebinga C J (1999) Process studies of dissolved organic carbon and bacterioplankton in the ocean. PhD thesis, Rijksuniversiteit Groningen, The Netherlands ISBN 90-367-1135-5
- Wiebinga C J, M Okbamichael, H J W de Baar (2000) Dissolved organic carbon dynamics: implications for carbon cycling in coastal seas. Submitted *Mar. Chem.*
- Winter A, W G Siesser (1994) Coccolithophores. Cambridge University Press, UK
- Wolf-Gladrow D A, U Riebesell (1997) Diffusion and reactions in the vicinity of plankton: a refined model for inorganic carbon transport. *Mar. Chem.* **59** (1-2) 17-34
- Wollast R (1994) The relative importance of biomineralization and dissolution of CaCO₃ in the global carbon cycle. *Bull. Inst. Oceanogr. Monaco* **13** (special) 13-35
- Young J R 1994 Functions of coccoliths. *In: Coccolithophores, A Winter & W G Siesser (eds.)* p 63-82
- Young J R, P Westbroek (1991) Genotypic variation in the coccolithophorid species *Emiliana huxleyi*. *Mar. Micropaleontol.* **18** 5-23
- Young J R, J M Didymus, S Mann (1991) On the reported presence of vaterite and aragonite in coccoliths of *Emiliana huxleyi*. *Botanica marina* **34** 589-591
- Young J R, P R Bown, J A Burnett (1994) Paleontological perspectives. *In: The haptophyte algae, J C Green & B S C Leadbeater (eds.)* Clarendon press, Oxford, UK
- Zeebe R E, D A Wolf-Gladrow (in prep.) CO₂ in Seawater: Equilibrium, Kinetics, Isotopes. In preparation for Elsevier, Amsterdam, The Netherlands
- Zonneveld C (1996) Modelling the kinetics of non-limiting nutrients in microalgae. *J. Mar. Syst.* **9** (1/2) 121-136

Biography of Cesare Emiliani (1922-1995)

Abridged from Hay & Zakevich (1999)

Cesare Emiliani was born as a son to Luigi and Maria (Manfredidi) Emiliani on December 8, 1922 in Bologna, Italy. He studied geology at the University of Bologna, specializing in micropaleontology. He received the D.Sc. from the University of Bologna in 1945. His earliest publications concerned philately, an interest that continued throughout his life. After graduation he worked as a micropaleontologist with the Societa Idrocarburi Nationali in Florence from 1946-48. During this time he published several papers on taxonomy and stratigraphy of foraminifera of the Cretaceous argille scagliose near Bologna, and from Pliocene sections near Faenza.

In 1948 he received the Rollin D. Salisbury Fellowship in the Department of Geology at the University of Chicago and obtained the Ph.D. in 1950. It was in Chicago that he met, and on June 28, 1951, married his wife, Rosita. They had two children, Sandra and Mario. From 1950 to 1956 he was Research Associate in Harold Urey's Geochemistry Laboratory in the Enrico Fermi Institute for Nuclear Studies at the University of Chicago. It was in this laboratory that the pioneering work was being done to establish relationships between stable isotopes and environmental variables. The early work of Urey and his students had involved studies of the relation between oxygen isotopes and temperature in recent molluscs, and the application of this relationship to the determination of paleotemperatures in the Cretaceous. Emiliani initiated use of this technique to the shells of foraminifera in ancient sediments from the ocean floor and concluded that the deep waters of the ocean had been much warmer in the early Tertiary. The discovery that the deep ocean was not the constant unchanging environment that had been assumed marked the beginning of a new field of science: paleoceanography.

Further major discoveries followed rapidly. Using the piston corer developed by Kullenberg, the Swedish Deep Sea Expedition (1947-1949) and the Lamont Geological Observatory had taken long cores in the deep-sea carbonate oozes of the Pacific and Caribbean. Emiliani took on the job of applying the oxygen isotope technique to the tests of planktonic foraminifera sampled at 10 cm intervals down the length of the cores. He found a systematic periodic variation in the ratio of $^{18}\text{O}:^{16}\text{O}$ following a characteristic sawtooth pattern. It was known that the changing ratios reflected two major factors, the temperature of the seawater and the volume of glacial ice. Cooler temperatures and greater ice volumes both result in more positive $^{18}\text{O}:^{16}\text{O}$ ratios. He supposed that 60% of the signal was due to the temperature effect, 40% to the ice effect. He concluded that equatorial and tropical ocean surface temperatures had been several degrees cooler during times of glaciation. At the time he did this work, it was thought that there had been only four major glaciations during the Pleistocene. Emiliani's analysis indicated that there had been many more cycles of glaciation; he found seven, extending to the base of the Caribbean cores and fifteen in the Pacific cores. He concluded that the cyclic glaciations were related to orogenic uplift, changing insolation (Milankovitch cycles), ice-albedo feedback, and the effect of isostatic adjustments to the loading of continental crust by glacial ice sheets—all topics still being actively discussed today. His discoveries revolutionized ideas about the history of the ocean and of the glaciation.

In 1957 Emiliani moved to the University of Miami's Institute of Marine Science, later to become the Rosenstiel School of Marine and Atmospheric Sciences. There, he organized the program in marine geology and geophysics, built a major laboratory for isotope geology, and continued to develop the ideas about the nature and cause of the Quaternary glaciations. At this time, a major activity in American science was "Project Mohole", the effort to drill a hole to the Mohorovicic Discontinuity, the surface separating the Earth's crust from mantle. Cesare Emiliani, however, was convinced that much more could be learned from recovering long cores

which would record the history of the ocean. As the cost projections for "Project Mohole" escalated and the project collapsed, Emiliani submitted a proposal termed "LOCO" (for Long Cores) to the U.S. National Science Foundation. A suitable ship, the SUBMAREX, was chartered for test drilling of cores on the Nicaragua Rise. The success was such that it was immediately recognized that the recovery of drilled cores from the deep sea would provide evidence of the history of the ocean and also serve to test the hypotheses of sea-floor spreading and plate tectonics. The result was formation of JOIDES (Joint Oceanographic Institutions for Deep Earth Sampling) and its three sequential projects, the JOIDES drilling on the Atlantic continental margin off Jacksonville, Florida (1966), the Deep Sea Drilling Project (1967-1983) and the Ocean Drilling Program (1984-2003).

In 1967 he organized the Department of Geological Sciences on the main campus of the University of Miami and remained its Chairman until his retirement in 1993. He was an extraordinary, exciting teacher; he used Earth Sciences as a focus for introducing large numbers of students to the sciences as a whole.

Cesare Emiliani was a renaissance scientist in the truest sense. He was a scholar familiar with classical languages, and extraordinarily well versed in history. His interests were very broad, ranging far beyond the field of stable isotope geology to tectonics, catastrophes, extinction, evolution, human history and human impact on the planet. Among other innovative ideas, he proposed drilling to the oceanic Mohorovicic Discontinuity from land (Eleuthera Island in the Bahamas), controlling earthquakes by the use of nuclear explosions, that viruses might be responsible for extinctions, and that evolution might be more a process of niche-filling after extinctions rather than direct competition.

He worked to introduce calendar reform, in part to eliminate the BC-AD chronology hiatus caused by the lack of a zero year, but more importantly to eliminate the use of religion-based systems in a multicultural context. He was also very much concerned about the unrestrained growth of the human population and its effect on the environment of the planet.

He was very much concerned that scientists and the public in general were losing touch with the development of knowledge as a whole. To combat this he wrote *The Scientific Companion* (1988) which is a broad review of science that makes entertaining and excellent reading for specialists and laymen alike. Much of his extraordinary character and his broad interests are revealed in *Planet Earth* (1992) which is a fascinating introduction to mathematics, physics, chemistry, and biology, and as well as earth science, all set in the historical context of the development of ideas.

Cesare Emiliani was honored by having the genus *Emiliana* erected as home for the taxon *huxleyi*, which had previously been assigned to *Coccolithus*. He was further honored by receiving the Vega Medal (Sweden) in 1983, and the Agaasiz Medal of the U.S. National Academy of Sciences in 1989. He died unexpectedly of a heart attack on July 20, 1995 at his home in Palm Beach Gardens, Florida.

Biography of Thomas Henry Huxley (1825-1895)

From Trilling & Bloom (1973)

It may be thought an amusing small curiosity of Victorian intellectual history that when John Henry Newman was a pupil at the private school at Ealing where he had the decisive experience of his life, the self-evidence of God's existence, one of his masters—he is known to have held the young Newman in the highest regard—was the father of T. H. Huxley, among whose claims to fame is the fact that he coined the word "agnostic." It was a word that many Victorians found useful to describe their position as to the existence of God: while disclaiming atheism, it signifies that no predication of either the existence or the non-existence of the Deity can be made on the basis of knowledge.

As Newman dedicated his life to the defense and advancement of religion, especially those of its elements which were transcendent and supernatural, and conceived one of its chief enemies to be the animus and error of the modern scientific imagination, so Huxley was committed to the defense and advancement of science, whose leading antagonist he identified as organized religion. A scientist of great ability, Huxley in time turned from research; although his achievement in that line was considerable, he is now remembered chiefly for his effectiveness as an educator of the public, for having been in his day the pre-eminent exponent of the scientific spirit. As he says in the autobiographical essay he wrote in 1889, he subordinated his ambition for scientific fame to other ends: "to the popularisation of science; to the development and organisation of scientific education; to the endless series of battles over evolution; and to untiring opposition to that ecclesiastical spirit, that clericalism, which in England, as everywhere else, and to whatever denomination it may belong, is the deadly enemy of science."

Thomas Henry Huxley was born at Ealing in 1825. He set store by the first of his Christian names, that of the doubting disciple of Christ, as being indicative of his intellectual temper, although he records of his early childhood a strong identification with the aristocratic vicar of the parish, which led to his preaching to his mother's maids one Sunday morning, his pinafore turned wrong side forward to represent a surplice. His time of systematic education was as short as it was unpleasant. The Ealing school, excellent in Newman's day and for a time thereafter, deteriorated on the death of its headmaster. In 1835, when his son was ten, the elder Huxley gave up teaching and returned to his native Coventry to become manager of a bank. After that, Thomas had no formal instruction. But he read widely in every direction, with a special appetite for science and logical and metaphysical speculation. He held the works of Carlyle in especial admiration and under their influence began to teach himself German. He later went on to the study of French and Italian. In 1841, he undertook the study of medicine, became an assistant to a doctor in one of the poor sections of London, then apprenticed himself to one of his brothers-in-law, attended medical lectures at Sydenham College, and won a Free Scholarship to Charing Cross Hospital. (It is worth relating that the elder Huxley applied to his former pupil, Newman, to support his son's candidacy, and although Huxley's biographer does not say so, we may suppose the request was granted.) In 1845 Huxley took his Bachelor of Medicine degree at the University of London. Through his own enterprise he secured an appointment in the medical service of the navy and was posted to a naval hospital and subsequently to the *Rattlesnake*, a frigate which was being prepared for a long cruise of survey and exploration in Australian and East India waters, to the special end of bringing back an account of the geography, geology, and natural history of New Guinea. For four years the young assistant-surgeon of the ship was unremitting in his researches, carried out with inadequate equipment, chiefly into the physiology of marine animals. (His journal of the cruise was published in 1935.) He sent back numerous scientific articles, some of which were published

before his return in 1850; in 1851, on the strength of his paper on the structure of the Medusae (jellyfish), he was elected Fellow of the Royal Society, a coveted honor, and in the following year was awarded the Society's Royal Medal. Despite this signal recognition, he had difficulty in finding a salaried position, but he continued his research and began to be known as a lecturer and writer whose lucidity and charm of presentation could make any scientific subject comprehensible to virtually anyone. By 1854 his posts were numerous; he was lecturer in Natural History in the Royal School of Mines, Naturalist to the Geological Survey, and lecturer in Comparative Anatomy at St. Thomas's Hospital; the next year he married the young lady to whom he had become engaged on his visit to Australia. His researches at this period dealt with invertebrates, vertebrates, and plants, and during a visit to Switzerland he undertook the study of the action of glaciers. He was instrumental in the establishment of two important scientific journals, the *Natural History Review* and *Nature*.

In 1859 Charles Darwin published his epoch-making *Origin of Species*, which Huxley reviewed for the *London Times*. Evolution was of course not a new idea for the Victorians. In one or another formulation, the theory that the universe had not been brought into being by a special act of creation but that it and its inhabitants, including man himself, had evolved from more primitive forms, had for some time disquieted the religious imagination; the depth of the distress it could cause is classically exemplified by Tennyson's *In Memoriam*, begun in 1833 and published in 1850. But *The Origin of Species* gave a new force to the idea, partly because it specified by its theory of natural selection the means by which biological evolution proceeds, and it was greeted with a vociferous anger which had its roots in the fear that the supernatural basis of religion stood threatened as never before. Huxley, who had rejected the idea of evolution until Darwin's book convinced him of its truth, was drawn into the great national debate that followed—Darwin himself could not be drawn into controversy—and became the pre-eminent polemicist of the evolutionists.

The most famous, and certainly to him most gratifying, moment of Huxley's career as "Darwin's bulldog," came in the exchange between Bishop Wilberforce and him at the meeting of the British Association at Oxford in 1860. The bishop, who had recently attacked Darwin in an elegant but ignorant article, rose to speak in the discussion period and went on for half an hour ridiculing Darwin and Huxley, his line being that there was really no such thing as evolution. "Then, turning to his antagonist with a smiling insolence, he begged to know, was it through his grandfather or grandmother that he claimed his descent from a monkey?" At this, Huxley said to his neighbor, "The Lord hath delivered him into mine hands," rose to answer the bishop, and concluded his statement by saying that "he was not ashamed to have a monkey for his ancestor; but he would be ashamed to be connected with a man who used great gifts to obscure the truth." (There are many different versions of Huxley's precise words, but all agree as to their purport and the effect they produced in the crowded hall, of elation on the part of the pro-Darwinists, of bitterness on the part of the chiefly clerical anti-Darwinists.)

By 1863, although he continued his researches, Huxley's energies, which were inexhaustible despite his frequent ill-health, were increasingly devoted to science as a cultural issue, as the basis of intellectual and even moral virtue. Huxley became, among other things, a leading theorist of education, and one of his later lectures, *Science and Culture* (1880), was the occasion for Matthew Arnold's *Literature and Science* (see above). His insistence that science had to play a larger part in education than it did was based on intellectual rather than utilitarian grounds; the humanistic bent that had led him from Carlyle to Goethe was permanent, and, despite what might be inferred from Arnold's reply, he had no doubt that literature had to be salient in any effectual system of education. This dedicated exponent of the intellectual value of science undertook the study of Greek in his fifties and made it a first requirement in the training of a scientist that he learn to write well.

The honors that came to Huxley in the course of his life were innumerable, and the responsibilities he assumed were equally beyond count. At one time or another he was president of virtually every scientific association of importance; he served on no less than ten Royal Commissions; he was elected to the first London school board. In 1871 he published his *Manual of the Anatomy of Vertebrated Animals*, which remained a standard text at least until the end of the century. His lectures and essays on scientific subjects, which evinced an ever-growing readiness to bring scientific facts and principles to bear upon the problems of ethics and politics, appeared at frequent intervals and were eagerly read. In 1876 he visited America to give an address on university education at the newly founded Johns Hopkins University and stayed on to lecture through the next year. His health had broken down in 1872; it failed again in 1884 and he gave up his salaried posts to retire on a generous government allowance; yet he carried on the activity which he had come to think of as the one to which he had been peculiarly called, that of offering a ceaseless resistance to the ecclesiastical spirit in its continuing, if ever less sanguine, attacks upon science. He died in 1895.

His grandson Aldous Huxley, before undertaking the career as a novelist which brought him fame, intended to be a biologist but was prevented by an eye disease. Sir Julian Huxley, the elder brother of Aldous, is a biologist of great eminence. Andrew Huxley, the half-brother of Aldous and Julian, was awarded the Nobel Prize in 1963 for his work in physiology.

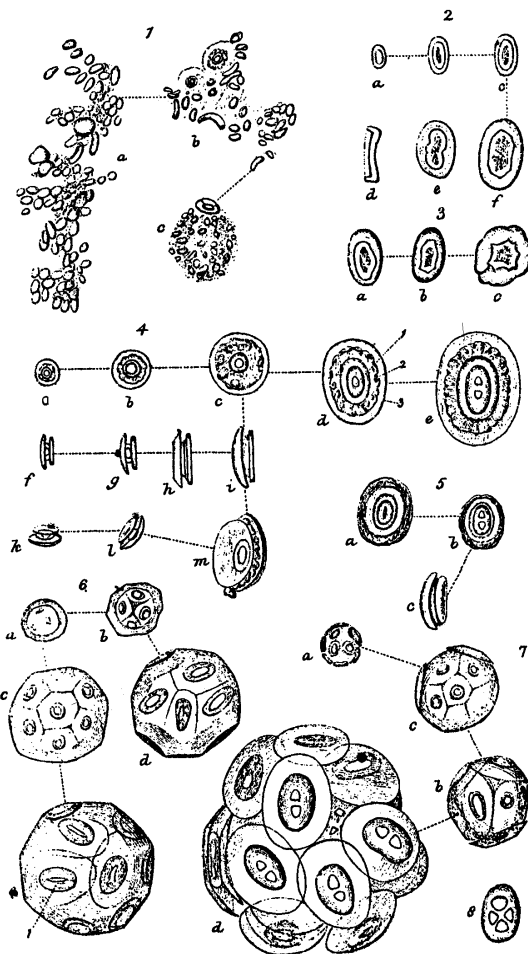


Figure 0.1 Coccospheres and coccoliths from Huxley (1868). Figure 2 in Siesser (1994). (Coccoliths of *Emiliana huxleyi* are too small to observe coccolith morphology with a light microscope.)

Samenvatting

Erik T. Buitenhuis, Hein J. W. de Baar

De oceanen bedekken 71 procent van het oppervlak van onze planeet en Oceaan zou een beter passende naam zijn dan Aarde. De buitenkant van de Aarde noemen we de biosfeer waar alle levende organismen een nauwe relatie hebben met hun omgeving: de chemische stoffen in de bodem, de lucht en het water. Het belang van de oceanen wordt duidelijk wanneer we kijken waar sommige stoffen zich bevinden in de biosfeer. Zo bevindt zich 97,2 % van het water (H_2O) in de oceanen, 2,15 % als landijs in de grote ijskappen van Groenland en Antarctica, ongeveer 0.63 % als grondwater op het land, en slechts 0,017 % als alle water in meren en rivieren.

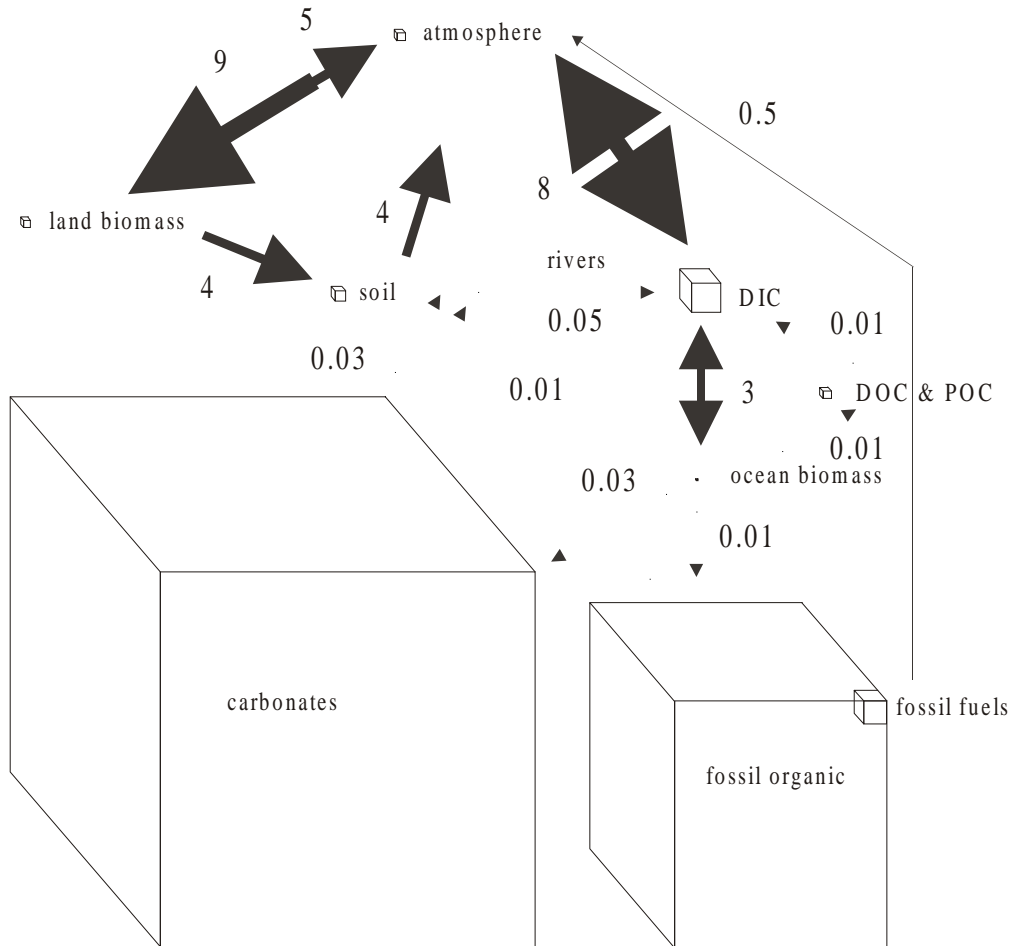
Zoals in figuur 0.2 te zien is, is welliswaar de meeste koolstof op aarde aanwezig in de sedimenten, maar de oceaan speelt een belangrijke rol in de meer actieve reservoirs. Ongeveer de helft van de uitwisseling van CO_2 met de atmosfeer vindt plaats met de oceaan. Dit CO_2 lost op in het zeewater, waar het, door chemische evenwichten met het water (H_2O) zelf, vooral voorkomt als bicarbonaat (HCO_3^-) en carbonaat (CO_3^{2-}). Deze chemische vormen (CO_2 , HCO_3^- en CO_3^{2-}) en hun onderlinge chemische evenwichten vormen het opgelost anorganisch koolstof systeem uit de titel van dit proefschrift (DIC in figuur 0.2). Er zijn twee belangrijke biologische processen waarbij dit anorganisch koolstof wordt omgezet in vaste koolstof vormen, waaruit alle planten, dieren en bacteriën ter land ter zee en in de lucht bestaan.

Het eerste proces is de fotosynthese, waarbij planten de energie van zonlicht invangen en deze energie gebruiken om CO_2 om te zetten in organisch koolstof (C) en zuurstof (O_2). De planten in de oceanen zijn vrijwel allemaal eencellig en noemen we algen of fytoplankton. Een deel van het organische algenmateriaal zinkt naar de zeebodem. Het grootste deel van dit materiaal wordt afgebroken, maar een klein deel gaat uiteindelijk het organische deel van het sediment vormen (fossil organic in figuur 0.2).

Het tweede proces is de vorming van kalk ($CaCO_3$) door samenvoeging van opgeloste calcium met opgelost anorganisch koolstof. De kalkvorming kan zijn als schelpjes van sommige dieren (zoals koralen en verschillende groepen in de open oceaan zwevende diertjes), of als kalkplaatjes die door sommige algen (fytoplankton) worden gemaakt. Ook een deel van deze kalk zinkt naar de zeebodem, en ook wordt het grootste deel van de kalk afgebroken tijdens haar reis naar of aangekomen op de zeebodem, waar het de fossiele carbonaten in het sediment gaat vormen (carbonates in figuur 0.2).

Deze twee processen zijn al miljarden jaren aan de gang en hebben tot een semi-stabiele toestand geleid, waarbij de meeste koolstof in de sedimenten aanwezig is er ongeveer 100 miljoen jaar over doet tussen gevormd worden en weer in de actieve reservoirs terecht komen, waar het dan snel even een heleboel rondjes draait tussen land, zee en lucht, om vervolgens weer een hele tijd in het sediment door te brengen. Er verandert ook wel eens wat op aarde, doordat de zon wat harder gaat schijnen of doordat er een soort plant of dier uitsterft of bijkomt, en sinds kort is daar de mens die bezig is in een nog nooit vertoond tempo fossiele brandstof te verbranden tot CO_2 (de pijl uiterst rechts in figuur 0.2 van de fossiele brandstoffen naar de atmosfeer) Sinds ongeveer 1780 is het verbranden van fossiele brandstoffen flink toegenomen, en als gevolg daarvan is het percentage CO_2 in de lucht gestegen van 0.028 % in het jaar 1780 tot 0.037 % in het jaar 2000. Met de economische groei versnelt ook de toename van CO_2 in de lucht en gecombineerde modellen van economie en klimaat voorspellen een verdubbeling van CO_2 in de lucht rond het jaar 2040. Overigens is de toename in de atmosfeer slechts ongeveer 50 % van de CO_2 uitstoot, ongeveer 30% wordt door de oceanen opgenomen, en 10% wordt door landplanten opgenomen (door onzekerheden in het koolstofbudget komt dit niet op 100% uit).

Samenvatting



Figuur 0.2 De wereldwijde koolstofcyclus. DIC = opgelost anorganisch koolstof, DOC & POC = opgelost & particeair organisch koolstof, fossil carbonates = kalk in de sedimenten, fossil organic = organisch materiaal in de sedimenten. Uitwisselingssnelheden tussen reservoirs in 10^{15} mol per jaar (overgenomen uit IPCC 1992), voor reservoirgroottes zie figuur 1.1.

In 1824 al concludeerde Fourier dat de atmosfeer als een broeikas zou werken, en in 1896 publiceerde Arrhenius nauwkeurige berekeningen van het effect van CO_2 op de warmtebalans van de planeet Aarde. (De vergelijking met een broeikas gaat overigens enigszins mank, omdat de atmosfeer van de aarde warmte vasthoudt doordat gassen (voornamelijk water en ook kooldioxide) zonlicht doorlaten en de infrarode straling van de aarde absorberen, terwijl dit effect van weinig belang is voor een broeikas, die warmte vasthoudt door menging van opgewarmde lucht met koudere omgevingslucht te belemmeren.) Arrhenius rekende aan de warmteabsorbtie van CO_2 omdat hij naar een verklaring voor de ijstijden zocht. Oorzaken en gevolgen van ijstijden, CO_2 en temperatuur zijn nog steeds onderwerp van veel discussie.

Op dit moment wordt in elk geval bijna al het sediment onder de oceanen gevormd, voor een groot deel uit de resten van mariene planten en dieren, en dus spelen de oceanen en hun biologie een sleutelrol in de wereldwijde koolstofcyclus. Algen leggen met hun fotosynthese het zonlicht vast dat het voedselweb van energie voorziet door het produceren van organische

(koolstof-)verbindingen uit anorganische voedingsstoffen (zoals CO₂). Onder de algen is een groep die naast fotosynthese ook het andere proces uitvoeren dat opgeloste koolstof omzet in vaste koolstof: de vorming van kalk. Deze groep algen zijn de coccolithophoriden, d.w.z. de makers van coccolieten, dat zijn kleine geometrisch vormgegeven plaatjes kalk. Binnen deze groep coccolithophoriden is er weer een soort die volgens recente bevindingen welliswaar niet de meeste kalk produceert, maar die numeriek althans de meeste kalkplaatjes maakt: *Emiliana huxleyi*. Deze coccolithophoride alg is vernoemd naar de geoloog Cesare Emiliani en de bioloog en voorvechter van de wetenschap Thomas Henry Huxley.

Alles bij elkaar vormt deze specificering vanaf de wereldwijde koolstofcyclus tot één algje van één tweehonderdste millimeter grootte nogal een telescoopvisie, maar dit proefschrift is een klein onderdeel van een poging om uit een hoop detail uiteindelijk weer tot generalisaties te komen en tot een nauwkeuriger beschrijving te komen van het belang van het voedselweb in de oceaan voor de wereldwijde koolstofcyclus.

Het onderwerp van dit proefschrift is de interactie tussen *Emiliana huxleyi* en opgelost anorganisch koolstof in zeewater. De twee richtingen van deze interactie vormen twee delen in dit proefschrift: de invloed van opgelost anorganisch koolstof vormen op *E. huxleyi* (hoofdstukken 1.4, 2 & 3), en de invloed van *E. huxleyi* op het opgelost anorganisch koolstof systeem (hoofdstukken 1.5, 4 & 5). In het begin van de synthese (hoofdstuk 1) worden de specifieke resultaten, zoals die in hoofdstukken 2 t/m 5 worden gepresenteerd, in een breder kader geplaatst van de mondiale koolstof kringloop (hoofdstuk 1.1), de mariene koolstof kringloop (hoofdstuk 1.2) en intracellulaire processen (hoofdstuk 1.3).

In hoofdstuk 2 zijn de resultaten van Paasche (1964) gereproduceerd, waaruit blijkt dat bicarbonaat (HCO₃⁻) het enige substraat is voor calcificatie en dat kooldioxide (CO₂) en bicarbonaat beide substraat zijn voor de fotosynthese (figuur 2.3). Verder wordt aangetoond dat er een zeer efficiënte koppeling is tussen de productie van protonen bij de calcificatie en het gebruik van deze protonen in het deel van de fotosynthese dat bicarbonaat gebruikt (figuur 2.1). Uit de resultaten blijkt ook dat de groeisnelheid van *E. huxleyi* bijna maximaal is bij typische concentraties van de opgelost anorganisch koolstof vormen (figuur 2.7). Vanwege dit laatste feit zal er normaliter geen significante terugkoppeling plaatsvinden tussen de invloed die het anorganisch koolstof op *E. huxleyi* uitoefent en de invloed die *E. huxleyi* op het anorganisch koolstof uitoefent. Daarom is er ook geen derde deel gewijdt aan deze terugkoppeling, net zomin als in het model het opgelost anorganisch koolstof invloed uitoefent op de groeisnelheid (hoofdstuk 5). In hoofdstuk 3 is de rol van het enzym carbonzuuranhydrase in de koppeling tussen calcificatie en het gebruik van bicarbonaat in de fotosynthese nader onderzocht. Dit is gedaan door middel van een zink-limitatie experiment (figuren 3.2) en een zink-bicarbonaat colimitatie experiment (figuur 3.3). De resultaten zijn in overeenstemming met de functie van carbonzuuranhydrase in het gebruik van bicarbonaat zoals die te zien is in het schema in figuur 3.1 (= figuur 2.1), maar ook dat zink-limitatie eveneens invloed heeft op het gebruik van kooldioxide, wat niet voorspeld wordt door dit schema.

Hoofdstuk 4 en 5 gaan over de invloed van *E. huxleyi* op opgelost anorganisch koolstof. In hoofdstuk 4 wordt beschreven dat de algenbloei met *E. huxleyi* die in 1993 in de Noordzee werd bemonsterd kooldioxide uit de atmosfeer naar de diepzee transporteerde (figuur 4.6a). Dit terwijl er toch een positieve correlatie werd gevonden tussen de hoeveelheid particulier kalk in het water en de activiteit van kooldioxide (figuur 4.2). In hoofdstuk 5 wordt een computersimulatie van een bloei van *E. huxleyi* gepresenteerd. Deze simulatie reproduceert de in het veld gemeten positieve correlatie tussen kalk en kooldioxide (figuur 5.3), en laat zien dat deze correlatie een afname van de activiteit van kooldioxide laat zien tijdens het oplossen van kalk. Daarmee is aangetoond dat ook deze waarnemingen passen in de hypothese dat er kooldioxide uit de atmosfeer de zee in wordt getransporteerd tijdens een bloei van *E. huxleyi*. Een gevoeligheidsanalyse van het model laat zien welke processen de grootste invloed

uitoefenen op het transport van atmosferisch kooldioxide (tabel 5.1). Met behulp van het model wordt bovendien aannemelijk gemaakt dat in een bloei van *E. huxleyi* meer kooldioxide uit de atmosfeer wordt getransporteerd dan in een bloei van een niet verkalkende alg (figuur 5.4)

Aan het eind van beide delen worden enige suggesties gedaan hoe het beschreven onderzoek voortgezet zou kunnen worden (aan het eind van de discussie in hoofdstuk 3 en in de samenvatting van hoofdstuk 5).

Het onderzoek van dit proefschrift is een onderdeel van het NWO onderzoeksprogramma Verstoring van Aardsystemen. Tevens sluit het onderzoek aan bij het vanuit Nederland gestimuleerde ‘Wereldwijde *Emiliana huxleyi* Modelerings initiatief’ (Global *E. huxleyi* Modelling initiative (GEM)). Dit beoogt de intensieve studie van deze sleutelsoort onder de zoutwater algen, op alle relevante schalen van moleculair tot en met de schaal van wereldwijde kringlopen van elementen. Het Europese project MERLIM (Marine Ecosystems Resources : trace metal and carbon dioxide LIMitations) werd opgezet om limitatie van groei van algen door tekorten aan spoor elementen ijzer en zink, en tekort aan opgelost CO₂, en interacties daartussen, te bestuderen. Het onderzoek over co-limitatie van zink en CO₂ in hoofdstuk 3 werd binnen dit MERLIM kader uitgevoerd, naast diverse andere studies van *E. huxleyi* in onder meer Liverpool en Bremerhaven.

Sinds april 2000 is een nieuw Europees project begonnen dat vanuit Nederland wordt geleid. Doelstelling is het inpassen van de biologie en ecologie van 5 sleutelgroepen van algen in simulatie modellen van CO₂ en klimaat. Voor een van de 5 sleutelsoorten is gekozen voor *E. huxleyi* en de kennis verkregen in dit proefschrift zal bijdragen aan dit volgende project IRON-AGES (Iron Resources and Oceanic Nutrients; Assessment of Global Environmental Simulations).

Come, let us continue counting the minnows.

Frogs and Scientists
In: Eye
Frank Herbert (1985)